High Resolution Future Climate Ocean Model Simulations for the Northwest Atlantic Shelf Region

D. Brickman, Z. Wang, and B. DeTracey

Ocean and Ecosystem Sciences Division
Maritimes Region
Fisheries and Oceans Canada

Bedford Institute of Oceanography
P.O. Box 1006
Dartmouth, Nova Scotia
Canada B2Y 4A2

2016

Canadian Technical Report of Hydrography and Ocean Sciences 315

Fisheries and Oceans Canada Pêches et Océans Canada

Canada

Canadian Technical Report of Hydrography and Ocean Sciences

Technical reports contain scientific and technical information of a type that represents a contribution to existing knowledge but which is not normally found in the primary literature. The subject matter is generally related to programs and interests of the Oceans and Science sectors of Fisheries and Oceans Canada.

Technical reports may be cited as full publications. The correct citation appears above the abstract of each report. Each report is abstracted in the data base *Aquatic Sciences and Fisheries Abstracts.*

Technical reports are produced regionally but are numbered nationally. Requests for individual reports will be filled by the issuing establishment listed on the front cover and title page.

Regional and headquarters establishments of Ocean Science and Surveys ceased publication of their various report series as of December 1981. A complete listing of these publications and the last number issued under each title are published in the *Canadian Journal of Fisheries and Aquatic Sciences*, Volume 38: Index to Publications 1981. The current series began with Report Number 1 in January 1982.

Rapport technique canadien sur l'hydrographie et les sciences océaniques

Les rapports techniques contiennent des renseignements scientifiques et techniques qui constituent une contribution aux connaissances actuelles mais que l'on ne trouve pas normalement dans les revues scientifiques. Le sujet est généralement rattaché aux programmes et intérêts des secteurs des Océans et des Sciences de Pêches et Océans Canada.

Les rapports techniques peuvent être cités comme des publications à part entière. Le titre exact figure au-dessus du résumé de chaque rapport. Les rapports techniques sont résumés dans la base de données *Résumés des sciences aquatiques et halieutiques*.

Les rapports techniques sont produits à l'échelon régional, mais numérotés à l'échelon national. Les demandes de rapports seront satisfaites par l'établissement auteur dont le nom figure sur la couverture et la page de titre.

Les établissements de l'ancien secteur des Sciences et Levés océaniques dans les régions et à l'administration centrale ont cessé de publier leurs diverses séries de rapports en décembre 1981. Vous trouverez dans l'index des publications du volume 38 du *Journal canadien des sciences halieutiques et aquatiques*, la liste de ces publications ainsi que le dernier numéro paru dans chaque catégorie. La nouvelle série a commencé avec la publication du rapport numéro 1 en janvier 1982.

Canadian Technical Report of
Hydrography and Ocean Sciences 315
2016

High Resolution Future Climate Ocean Model Simulations for the Northwest Atlantic Shelf Region

by

David Brickman, Zeliang Wang, and Brendan DeTracey

Ocean and Ecosystem Sciences Division
Maritimes Region
Fisheries and Oceans Canada
Bedford Institute of Oceanography
P.O. Box 1006
Dartmouth, N.S.
Canada B2Y 4A2

Cat. No. Fs 97-18/315E-PDF ISBN 978-0-660-06253-2 ISSN 1488-5417

Correct citation for this publication:

Brickman, D., Wang, Z., and B. DeTracey, 2016. High Resolution Future Climate Ocean Model Simulations for the Northwest Atlantic Shelf Region. Can. Tech. Rep. Hydrogr. Ocean Sci. 315: xiv + 143 pp.

Table of Contents

List of Figures

List of Tables

Abstract

Brickman, D., Z. Wang, and B. DeTracey 2016. High Resolution Future Climate Ocean Model Simulations for the Northwest Atlantic Shelf Region
Can. Tech. Rep. Hydrogr. Ocean Sci. 315: xiv + 143 pp.

Future climate modelling of the ocean is typically performed using a low resolution ocean model, with grid dimensions ranging from 50-200 kms. While this resolution is able to capture some large scale open ocean properties, it is not sufficient for shelf scale processes or in regions, such as Atlantic Canada, where higher resolution is known to be required to accurately simulate ocean processes. This report describes and applies a downscaling technique to force a high resolution (1/12 degree) ocean model of the entire North Atlantic ocean, which is used to assess a limited number of future climate change scenarios on the shelf seas of Atlantic Canada. Output from the future climate simulations is compared to the present climate simulation to produce predictions of climate change for the Atlantic Canada region.

Résumé

Brickman, D., Z. Wang, et B. DeTracey 2016. Simulations d'un modèle océanique du climat futur à haute résolution pour la région du plateau de l'Atlantique Nord-Ouest.
Rapp. Tech. Can. Hydrogr. Sci. Océan. 315 : xiv + 143 p.

La modélisation du climat futur de l'océan est généralement effectuée à l'aide d'un modèle océanique à faible résolution, avec des dimensions de la grille allant de 50 à 200 kilomètres. Cette résolution permet de saisir certaines propriétés de haute mer à grande échelle. Toutefois, elle est insuffisante pour les processus à l'échelle du plateau ou de régions, comme le Canada atlantique, où une résolution plus élevée est requise afin de simuler correctement les processus océaniques. Le présent rapport décrit et applique une technique de réduction d'échelle en vue de forcer un modèle océanique à haute résolution (1/12 degré) de l'ensemble de l'Atlantique Nord permettant d'évaluer un nombre limité de scénarios de changement climatique envisageables dans les mers bordières du Canada atlantique. Les résultats des simulations du climat futur sont comparés aux simulations du climat actuel afin de produire des prévisions des changements climatiques pour la région du Canada atlantique.

1 Introduction

As part of the Canadian government's Aquatic Climate Change Adaptation Services Program (ACCASP) the authors were tasked with producing a high resolution future climate prediction for the shelf seas of Atlantic Canada in order to address questions pertaining to fisheries and other human-related activities under climate change. Future climate modelling of the ocean is typically performed using a low resolution ocean model. For example ocean model horizontal resolutions in the Intergovernmental Panel on Climate Change Coupled Ocean Model Intercomparison Project 5 (IPCC CMIP5) ranged from 50-200 kms (Fox-Kemper et al., 2014). While this resolution is able to capture some of the large scale open ocean properties, it is not sufficient for shelf scale processes or in regions of the ocean where higher resolution is known to be required to accurately simulate ocean processes. One such region is the area of interest for this report – the shelf region of Atlantic Canada – where resolving the interaction between the northeastward flowing Gulf Stream and the southwestward flowing Labrador Current at the tail of the Grand Banks (south of Newfoundland) is necessary to simulate properties and variability on the Scotian Shelf and Gulf of Maine (figure 1; Petrie, 2007; Greene and Pershing, 2003). The problem of low resolution ocean climate models is being addressed by the Climate Variability and Predictability (CLIVAR) Working Group on Ocean Model Development (CLIVAR Exchanges, 2014).

To improve resolution in limited areas, techniques for regional atmosphere-ocean downscaling have been developed. For the atmosphere this technique usually entails the extraction of boundary conditions from a large scale, low resolution model which are used to force a high resolution atmospheric regional climate model. (For further details see NARCCAP and CORDEX websites, listed in references.) Surface forcing for ocean regional climate models is usually derived from the output of an atmospheric regional climate model (Somot et al., 2006; Chassé et al., 2014). Because the computational demands of these systems are still quite high, downscaling simulations are typically limited to a small number of runs based on a subset of the IPCC ensemble of Atmosphere-Ocean General Circulation Models (AOGCMs).

A limitation of regional ocean models is that their interior solutions depend on the open boundary conditions, so if the latter are not well represented then important changes in the regional domain may not be correctly simulated. For example, the common source for lateral open boundary con-

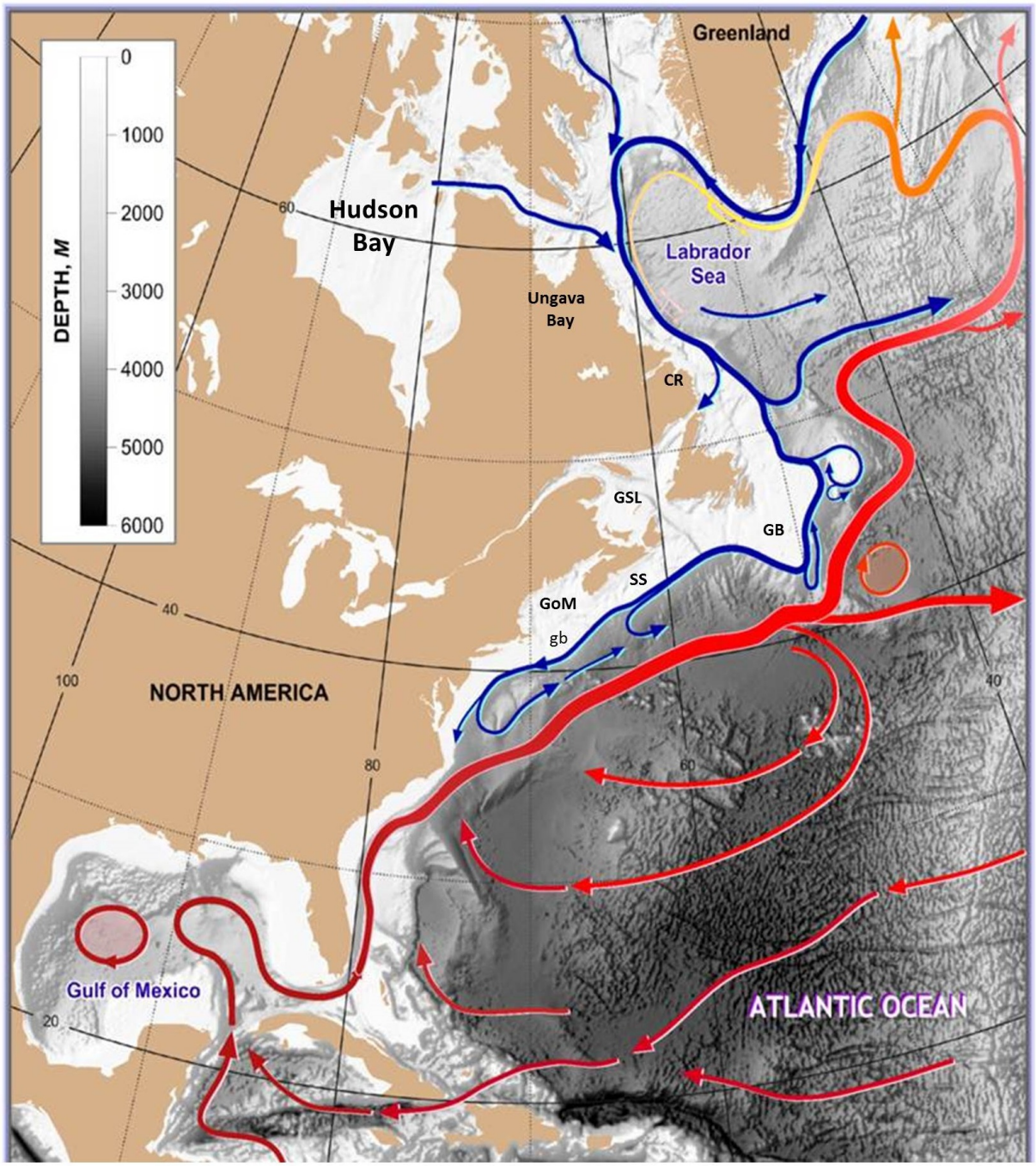

Figure 1: Schematic of circulation in northwest Atlantic Ocean, with placenames used in the text. Abbreviations are: CR = Churchill River; GB = Grand Banks; GSL = Gulf of St. Lawrence; SS = Scotian Shelf; GoM = Gulf of Maine; gb = Georges Bank.

ditions for future climate runs is output from (coupled) ocean climate models (Somot et al., 2006; Chassé et al., 2014) that do not resolve processes on the scale of the regional models. Thus if shifts

in the Gulf Stream and Labrador Current, which affect ocean properties on the Scotian Shelf and Gulf of Maine, are not adequately simulated by the ocean circulation models then open boundary forcing derived from these models would be unlikely to produce the correct solution in the regional model domain.

One way to minimize the effects of the open boundaries is to choose a model domain much larger than the area of interest. This technique, adopted in this report, requires significant computer resources for model simulations. The nature of this task, with the computational resources at hand, necessitated a strategy that minimized the number of runs that we could perform. In essence the question became: How does one produce the most representative future climate simulation if one can only do 1 run?

In this report we describe and apply a downscaling technique to force a high resolution (1/12 degree) ocean model of the entire North Atlantic ocean, which we use to assess a limited number of future climate change scenarios on the Shelf seas of Atlantic Canada. The goal of the technique is to create forcing for the ocean model that captures robust, or high confidence, features of existing future climate simulations, as presented in the IPCC 2013 report (IPCC, 2013). To do so, the technique combines a future climate scenario (the melting of the Greenland ice sheet) with atmospheric forcing anomalies derived from an ensemble of future climate AOGCMs. The present climate is simulated by forcing the ocean model with the CORE normal year (CNY) forcing dataset (Large and Yaegar, 2004). The future forcing dataset is created by adding the AOGCM anomalies to the CNY to produce a future climate normal year forcing (FCNY), which is supplemented by a representation of the Greenland glacier melt. Output from the future climate simulation is compared to the present climate simulation to produce predictions of climate change for the Atlantic Canada region.

Reading this document: Summarizing the model simulations requires a large number of figures and tables. Plots and tables considered essential to understanding the basic results are interspersed in the main body of text. Tables of interest but of lesser relevance are placed after the references. All other figures and tables are considered as supplementary material and are contained in an appendix (Appendix B). Note that due to the varied data sources and processing methods, some spatial figures are more clearly presented when plotted in model grid coordinates as opposed to

longitude/latitude coordinates. Such plots can recognized by the lack of axis labels along the ij (i.e. longitude/latitude) directions.

2 Methods

2.1 Ocean Model

The model is based on NEMO 2.3 (Nucleus for European Modelling of the Ocean) which includes an ocean component OPA (Madec et al., 2008) and the sea ice module LIM (Fichefet and Morales Maqueda, 1997). The model has a maximum of 50 levels in the vertical, with level thickness increasing from 1 m at the surface to 200 m at a depth of 1250 m and reaching the maximum value of 460 m at the bottom of the deep basins. The maximum depth represented in the model is 5730 m. The domain covered the North Atlantic ocean from 8-75°N latitude, at a resolution of 1/12° (figure 2a). In the region of interest (figure 2b), this resulted in characteristic grid cell dimensions of 5-6km, providing adequate resolution of shelf scale processes.

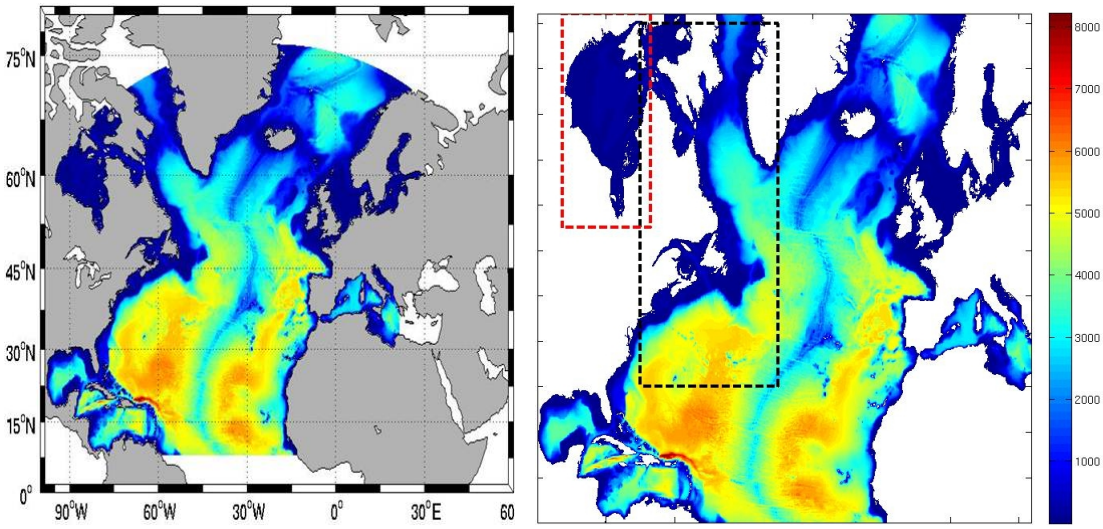

(a) (b)

Figure 2: Model domains. (a) North Atlantic domain in lon-lat coordinates. (b) Domain in grid-space showing the Atlantic Canada (black) and Hudson Bay (red) subdomains. The colorbar is model depth in meters.

2.2 Present climate forcing

The model surface forcing for the present climate (hereafter abbreviated as PC) was the CORE normal year forcing (Large and Yeagar, 2004) derived from the forcing dataset compiled for the Coordinated Ocean-ice Reference Experiments (CORE) (Griffies et al., 2009). The normal year forcing is a cyclical year climatology that resolves daily weather events. The surface momentum fluxes and the turbulent components of the heat and freshwater fluxes are calculated using the CORE bulk formulae. Monthly climatological open boundary conditions for normal velocity, temperature (T), salinity (S) and sea surface height were derived from the 18-year GLORYS reanalysis run (Ferry et al., 2010), time-interpolated to model time.

Model simulations included a representation of river inputs. The runoff of the major rivers was specified according to a monthly climatology compiled for the DRAKKAR project (Barnier et al., 2006). This dataset allows the seasonality of key freshwater sources (i.e. Hudson and Ungava Bays, Churchill River in Labrador, and the St. Lawrence Estuary) to be captured by the model. River inputs were modelled in the standard NEMO way, as precipitation applied to regions where rivers enter the ocean domain (see figure 3). This necessitated some adjustments to the precipitation "footprint" in order to achieve the desired surface flow patterns, notably in the St. Lawrence Estuary region. This method, while less realistic than desired, did capture the main freshwater flow patterns in the Atlantic Canada region.

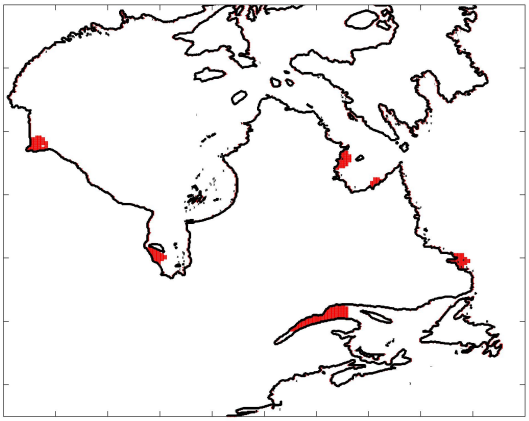

Figure 3: Precipitation footprint (red) for the major rivers in model domain.

The model simulation did not include tidal forcing, considered important for modelling tidally-

rectified flows that are known to exist around banks in the region (e.g. Georges Bank). However, because we are interested in the difference between model runs at timescales much longer than the tides, it is unlikely that this omission is relevant to our results.

To simulate the present and future climates, the model was run for 20 years to allow for equilibration. This run length should be sufficient for shallow water shelf regions but it is well known that the spin-up time for the deep ocean is longer than this. Indeed, there was evidence of lack of equilibration in deeper waters of offshelf regions – an effect that penetrated into the deep basins of the shelf. Unfortunately, longer run lengths were not possible given the computer resources available. To account for this, the data presented in this report are averages over the last 5 years of the model simulations. Aspects of model equilibration are discussed in Appendix A.

The large file sizes necessitated extraction of model data in 2 subdomains: Atlantic Canada, and Hudson Bay (figure 2b). Because Hudson Bay acts like an enclosed sea, analyses for this subdomain will, with the exception of sea ice, be reported separately.

2.3 Future climate forcing

The goal of the future climate forcing was to include the key changes expected to influence the ocean climate and circulation in the North Atlantic Ocean. Although there is considerable variability in future climate simulations, the IPCC 2013 report (and see also Diffenbaugh and Giorgi, 2012) considers that accelerated arctic warming and precipitation changes in northern latitudes will occur with high confidence. This component of the future atmospheric climate was approximated by applying spatially varying monthly surface air temperature and precipitation anomalies to the present climate CNY forcing. The atmospheric future climate monthly anomalies were calculated from ensembles of CMIP5 earth system model (ESM) climate prediction experiments. Future river runoff was also included, estimated by scaling present climate values, based on changes predicted by a hydrological model forced by three CMIP5 ESMs. Another important effect is the predicted melting of the Greenland ice sheet with its expected effect on the ocean surface layers, particularly in shelf regions. We discuss these various forcings in turn.

2.3.1 Atmospheric anomaly forcing

The future atmospheric forcing is created by adding predicted anomalies, derived from future climate simulations, to the present CNY forcing. The idea of using anomalies to force an ocean model is not new. Early examples date to the 1980's studies on the El Niño Southern Oscillation in which simplified atmosphere and ocean models were forced by anomalies in sea surface temperature (SST) and wind (see Zebiak and Cane, 1987, and references therein). Other studies have used combinations of anomalies in SST, and/or wind stress and/or ice (see for example: Miller et al., 1994; Ming and Smith, 1995; Visbeck et al., 1998; Magnusdottir et al., 2004; Schubert et al., 2009). The work of Somot et al. (2006) is an example of the use of SST anomalies derived from a low resolution future climate model to force a high resolution future climate ocean model of the Mediterrean Sea.

A subset of six CMIP5 ESMs (http://cmip-pcmdi.llnl.gov/cmip5/; Taylor et al., 2012) were selected based on their inclusion of an ocean carbon cycle, data availability, and their use in other recent DFO climate studies (Chassé et al., 2013; Lavoie et al., 2013; Lavoie and Lambert, 2013; Loder and Van der Baaren, 2013). The six ESMs are summarized in table 1. All data were taken from the r1i1p1 ensemble member. From the historical experiment, the bidecadal period 1986-2005 was taken to represent the present climate. From the long-term experiments, the two bidecadal periods 2046-2065 and 2066-2085 (referred to as 2055 and 2075 climatologies) were taken to represent future climates, using emission scenarios RCP4.5 and RCP8.5 (RCP stands for representative concentration pathway). RCP4.5 is an intermediate emission scenario in which radiative forcing increases to 4.5W/m^2 and stabilizes around 2100. RCP8.5 is high emission scenario in which radiative forcing increases to 8.5W/m^2 around 2100 but does not stabilize until it reaches 12W/m^2 in 2300 (Van Vuuren et al., 2011).

For each combination of ESM, RCP and field, monthly anomalies were calculated as the difference between a future (2046-2065 or 2066-2085) period and the historical (1986-2005) period. Anomaly values on land were corrected by recursively filling them with the average values of neighbouring sea grids (Kara et al., 2007), to prevent land contamination of sea values during spatial interpolation. The corrected monthly anomalies were bilinearly interpolated to a common $1^\circ \times 1^\circ$ grid and averaged to produce ensemble mean monthly anomalies. The ensemble mean monthly anomalies for surface air temperature and precipitation were spatially interpolated onto the CNY grid and added to their

Table 1: Summary of selected ESMs used to calculate future climate forcing. Listed grid resolutions may be approximate.

Institute	ESM Name	Reference	Atmos. grid	Ocean grid
CCCMA	CanESM2	Arora et al., 2011	2.8	1.4x1
NOAA GFDL	GFDL-ESM2M	Dunne et al., 2012	22.5	1x1
MOHC	HadGEM2-ES	Booth et al., 2012	1.875x1.25	1x1
IPSL	IPSL-CM5A-LR	Marti et al., 2010	1.9x3.8	2x2
MIROC	MIROC-ESM	Watanabe et al., 2011	2.8	1.4x1
MPI-M	MPI-ESM-LR	Brovkin et al., 2012	1.9	1.6

corresponding CNY fields. These monthly fields were subsequently linearly interpolated onto the model grid. The set of 4 scenarios (2 RCPs and 2 future time periods) will be abbreviated as: RCP8.5-2055, RCP8.5-2075, RCP4.5-2055, and RCP4.5-2075. Examples of the air temperature and precipitation anomalies are shown in figures 4 and 5.

2.3.2 River Runoff

Lambert et al. (2013) calculated estimates of annual mean future runoff, for RCPs 4.5 and 8.5, for eight sub-regions of the Atlantic watershed. The Atlantic watershed feeds the entirety of the eastern Canadian seaboard south of 60N and excludes Hudson Bay (see figure 1, Lambert et al., 2013). The mean percentage increase in runoff for the Atlantic watershed was calculated as the weighted mean of the eight sub-regions, using the sub-region annual mean runoffs as weights. Annual mean percentage changes for the Hudson Bay watershed were calculated from hydrological model results provided by Lambert (personal communication, 2013). The future annual mean percentage change in runoff for the two watersheds is summarized in table 2. The future climate runoff was calculated by scaling the present climate runoff by these percentages.

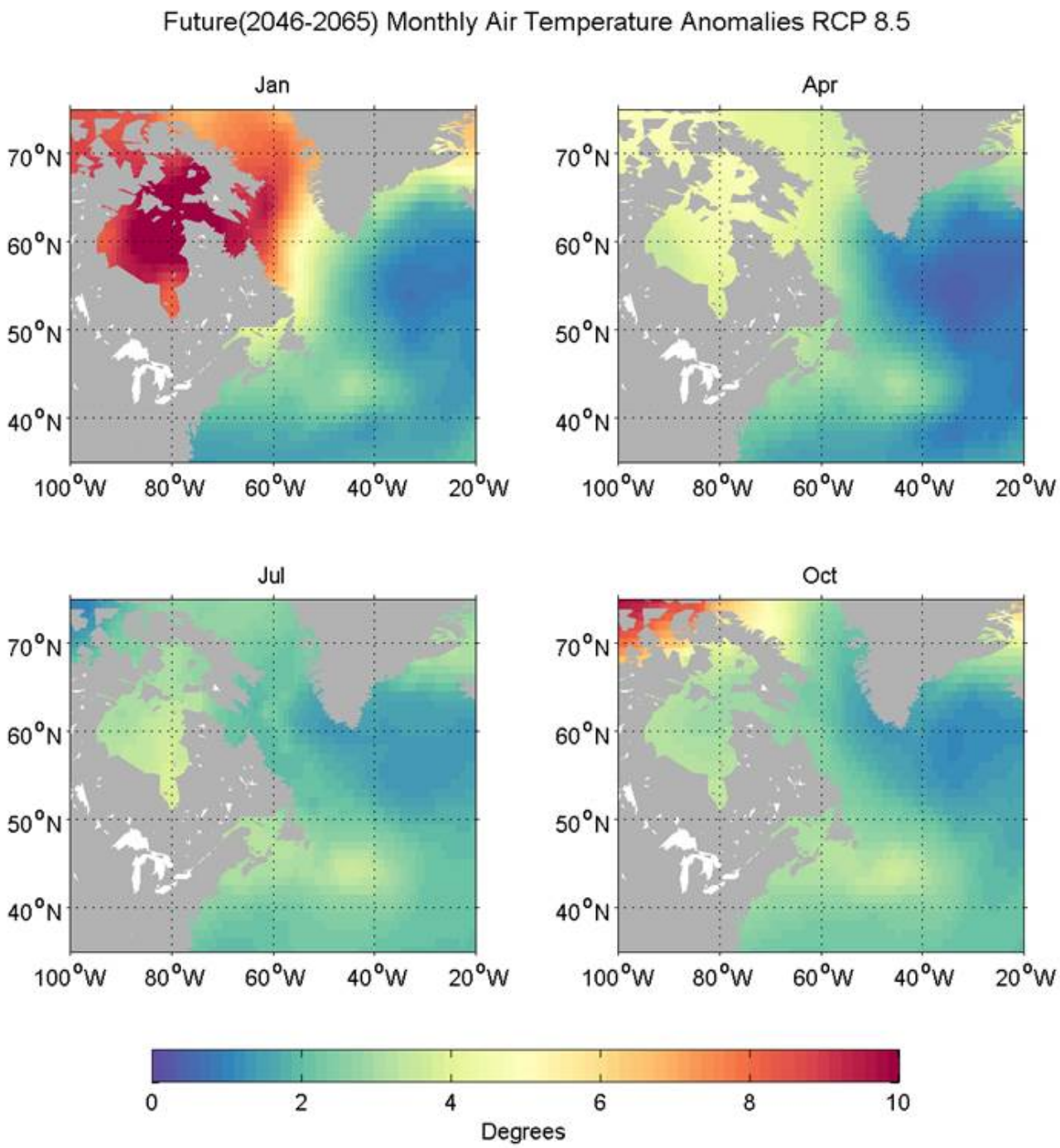

Figure 4: Surface air temperature anomalies for RCP8.5-2055, for 4 representative months.

2.3.3 Greenland ice melt

The effect of melting the Greenland ice sheet has been modelled in a series of "hosing" experiments in which a flux of freshwater is added to the surface layer of an ocean model. These experiments,

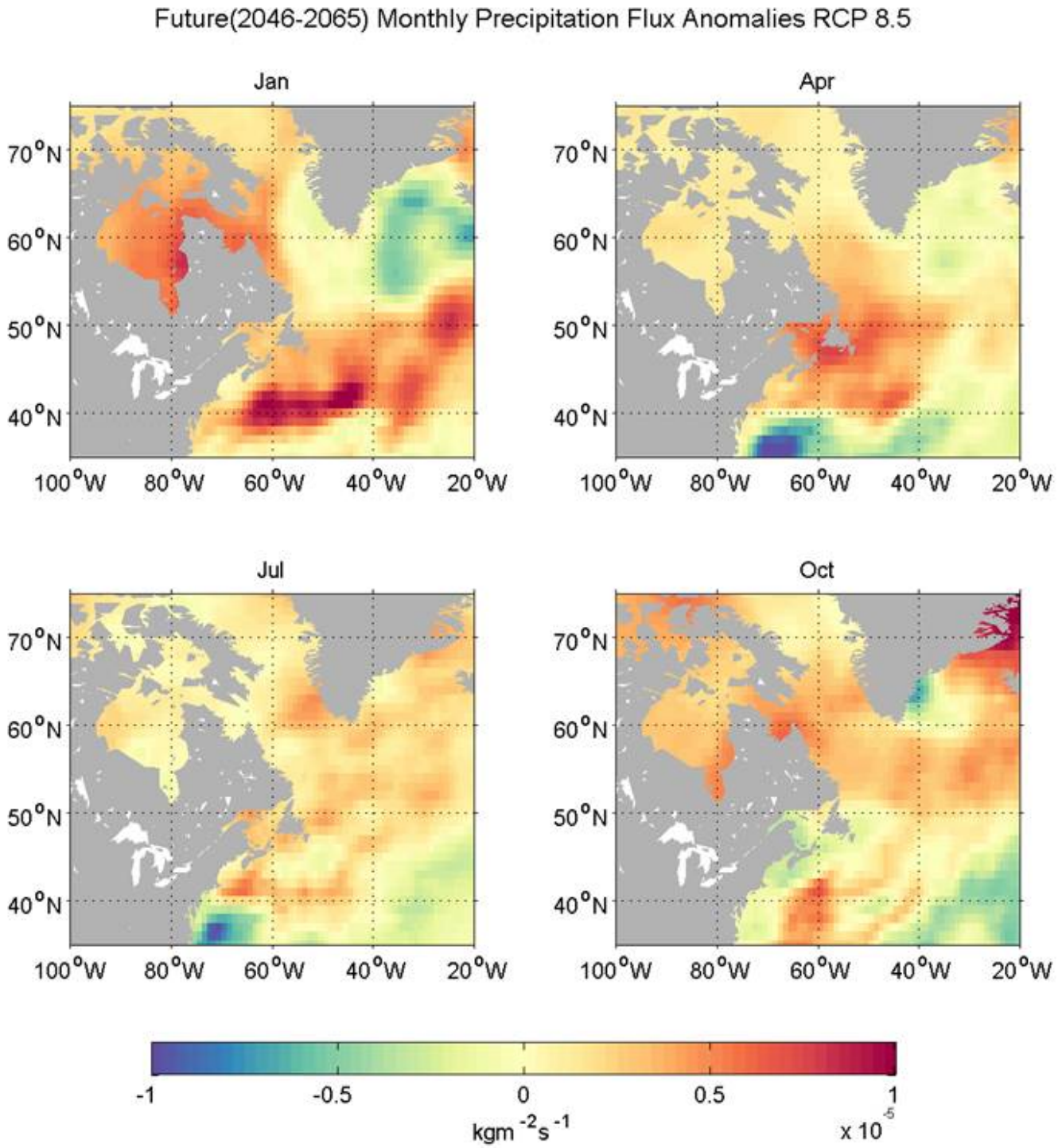

Figure 5: Precipitation flux anomalies for RCP8.5-2055, for 4 representative months.

Table 2: Estimated future percentage increase in annual mean runoff for the Atlantic and Hudson Bay watersheds, for RCPs 4.5 and 8.5, and future periods 2046-2065 and 2066-2085.

RCP	Future Period	Atlantic watershed	Hudson Bay watershed
4.5	2046-2065	2.2 %	8.4 %
	2066-2085	1.8 %	8.7 %
8.5	2046-2065	5.6 %	10 %
	2066-2085	7.8 %	15 %

originally coordinated as part of CMIP, were designed to investigate potential changes to the thermohaline circulation due to predicted increases in freshwater perturbations (Stouffer et al., 2006). The initial experiments, conducted by 14 institutes (see table 1 of Stouffer et al., 2006), "hosed" the freshwater over a region of the north Atlantic ocean. Other simulations, designed specifically to investigate melting of the Greenland ice sheet, distribute the freshwater over the shelf region surrounding Greenland (Gerdes et al., 2006; Weijer et al., 2012; Jungclaus et al., 2006).

The typical flux in these studies is 0.1Sv (i.e. $0.1 \times 10^6 \mathrm{m}^3\mathrm{s}^{-1}$). Recent estimates of the Greenland glacier melt rate and its rate of change are 12mSv and 0.76mSv/year (Rignot et al., 2011; Bamber et al., 2012) which translates to a flux of about 0.045Sv in 2055 – not entirely inconsistent with that used in the model simulations. In this report we apply a freshwater flux of 0.1 Sv to the coastal region of Greenland. This flux, applied as precipitation, includes a seasonal cycle with a maximum in the summer consistent with the DRAKKAR climatology (Barnier et al., 2006). Note that the model's response to this flux was a coastal current, part of which exited the domain at eastern Baffin Bay. To compensate for this, an equivalent freshwater flux was input at western Baffin Bay, essentially assuming that the meltwater current would follow bathymetry and become part of the Baffin Island current.

3 Results – Present Climate

It is not the goal of this report to present a detailed analysis of the model's simulation of the present climate, in part because this is done elsewhere, in part because there are questions related to the nature of the climatology produced by the CNY forcing, and finally because our interest is in *changes* in ocean climate. However, it was felt that it would be informative to present some basic results in order to provide at least a qualitative measure of model performance. In this regard, we present the model's ice and SST fields, as climatological data are readily available for comparison purposes. A similar comparison, for a suite of AOGCM simulations, is contained in the Loder and van der Baaren (2013) report, which highlights the difficulties that coarse resolution AOGCMs have in simulating present climate.

3.1 Present climate – Ice

The model present climate monthly mean sea ice field was compared to Canadian Ice Service (CIS) archived ice charts for the period 1990-2009. Two climatological products were calculated from the CIS charts: maps of monthly median ice concentration and thickness; and monthly mean ice area and volume for seven predefined areas (hereinafter ice boxes, see figure 6). The ice boxes match those used by the CIS online tool IceGraph (http://iceweb1.cis.ec.gc.ca/IceGraph20/page1.xhtml). IceGraph itself was not used because it only presents four ice categories, which is inadequate for ice volume estimates.

A qualitative comparison of the model ice concentration to the Canadian Ice Service (CIS) charts is shown in figures 7 and 8. The basic details of the development, advancement and retreat of the ice concentrationn field are captured by the model. Notable differences are the ice concentration in Hudson Bay and along the Labrador shelf, which the model underestimates in June and overestimates in November/December.

Figure 9 compares the model monthly mean ice area and volume to climatology, for the 7 ice boxes. The results quantify the above description for ice concentration, but also indicate a systematic underestimation of ice volume for all regions except the Gulf of St. Lawrence. This underestimation of ice volume is deducible from ice thickness maps (not shown) which indicate underestimation of

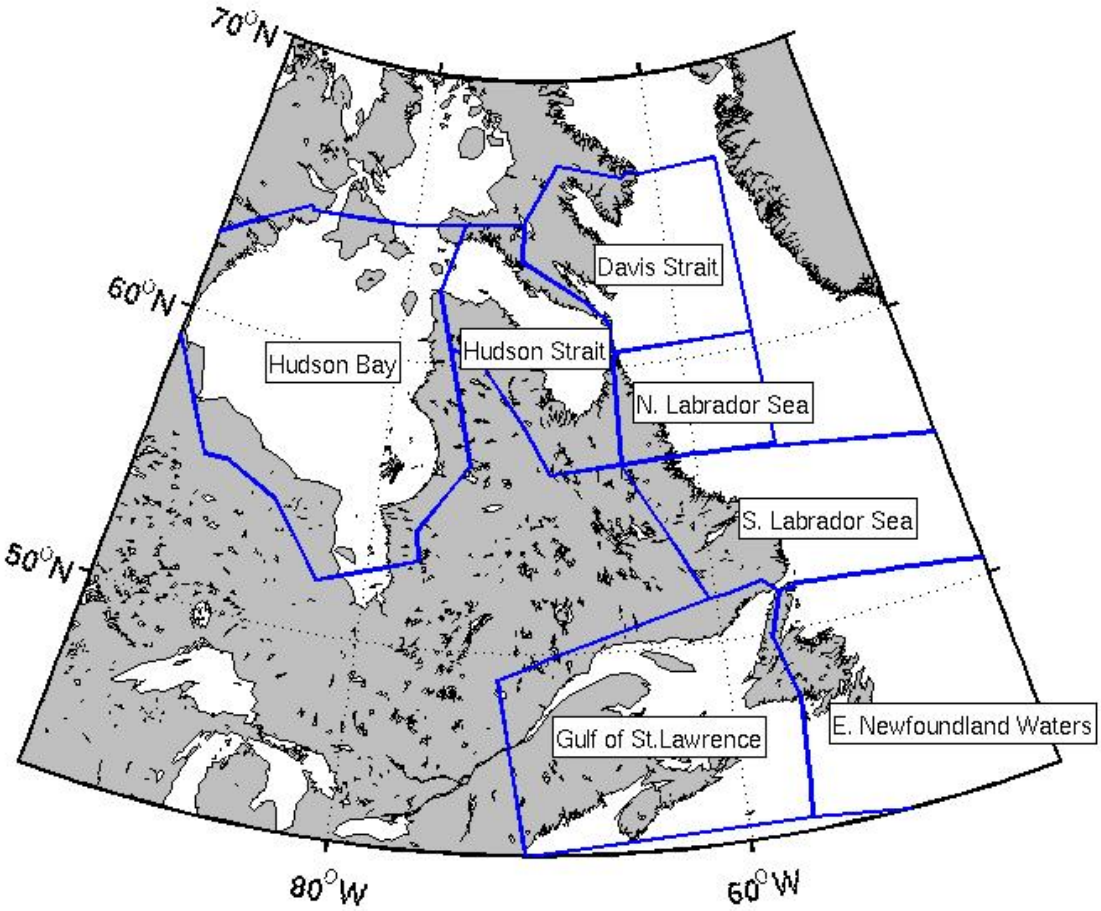

Figure 6: Ice boxes chosen for analyses. Abbreviations used in the text are: HB=Hudson Bay; HS=Hudson Strait; DS=Davis Strait; NLS= Northern Labrador Sea; SLS=Southern Labrador Sea; ENW=East Newfoundland Waters; GSL=Gulf of St.Lawrence.

that ice variable. Possible causes of this discrepancy are:

1. Problems with the (LIM) ice model as this module contains parameters that have been tuned based on previous simulations that may not be optimal for this simulation;

2. Model processes, in particular the absence of tides. The lack of tidal mixing in shelf regions can result in greater stratification which can affect the ice formation process;

3. Deficiencies in the CNY forcing. The CNY forcing is representative of a different period from which the ice data were derived (1990-2009);

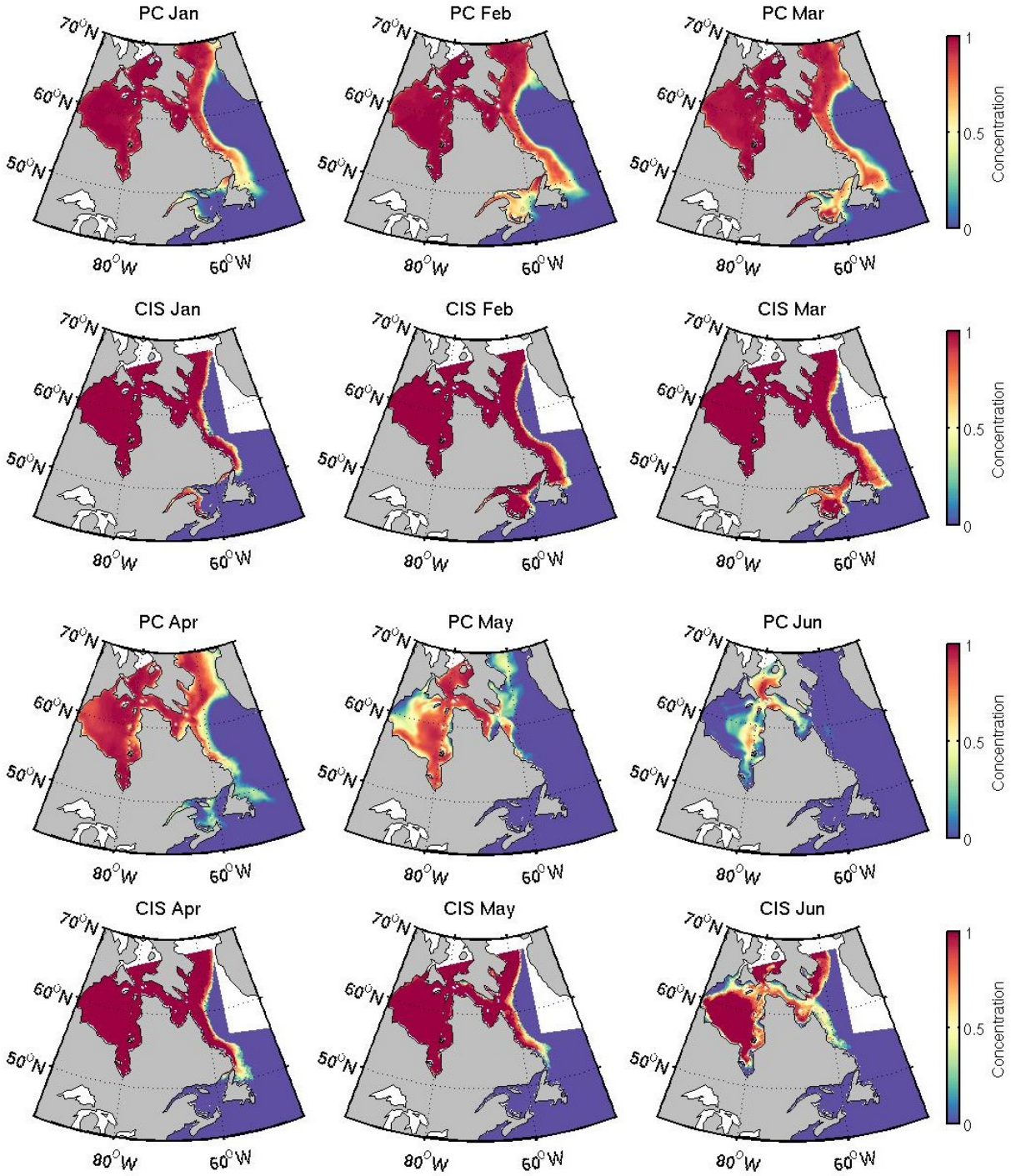

Figure 7: Comparison of PC and CIS(1990-2009) ice concentration January - June.

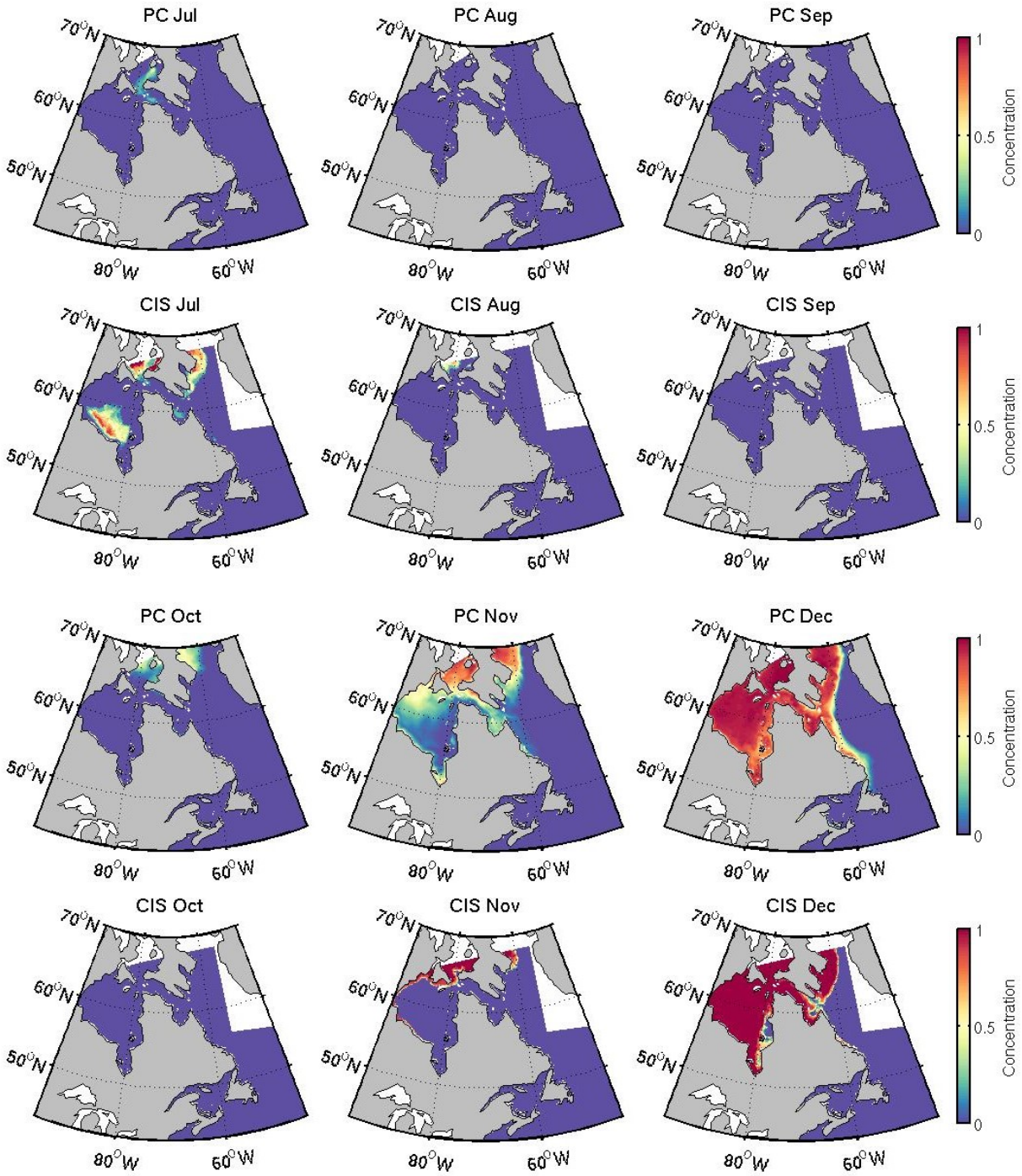

Figure 8: Comparison of PC and CIS(1990-2009) ice concentration July - December.

4. The ice data itself. The ice volume calculation uses the mean thicknesses of ice categories, which have large errors, especially for thicker ice. Since the ice category is based solely on surface observation, it does not account for possible subsurface ice processes.

The discrepancy in the simulation of the present climate ice volume is a subject for further investigation. While these estimates of ice variables need improvement, we note that the model's results are significantly better than the AOGCM results reported in Loder and van der Baaren (2013).

3.2 Present climate – SST vs satellite composites

The model's present climate SST is compared to monthly satellite composites (provided by C. Caverhill, BIO) in figure 10 a–d. (For more information on the satellite images see http://www.bio-iob.gc.ca/science/newtech-technouvelles/sensing-teledetection/index-en.php.) The colorscale in the model plots ($-2 - 30°$) is the same as the satellite images, although the colour matching is not perfect. In particular the -2 to 0 range is mauve in the satellite images and dark blue in the model plots. The white contour in the model plots is the zero-contour, which can be compared to the boundary of the mauve region in the SST images. Using this as a metric, the model is found to do an excellent job in simulating the advance and retreat of the sub-zero surface water. In particular, the fine details of the zero-contour on the Newfoundland-Labrador (NL) shelves and in the Gulf of St. Lawrence (GSL) are well simulated in January to April and November, December, with only May showing a significant mismatch. The Gulf Stream region appears too warm in the model, based on the colorscales, but the degree to which this is true is difficult to determine.

4 Results – Climate Change Scenarios

The analysis of the atmospheric climate model data produces 4 future climate scenarios (2 future periods × 2 RCPs). Each scenario consists of a FCNY, with associated change in river runoff (table 2). Glacial melt was the same for all 4 scenarios. As mentioned above, to simulate the future climates, the model was run for 20 years with one of the 4 scenarios, and the results presented here are averages over the last 5 years of the simulations (see also Appendix A). Model output was

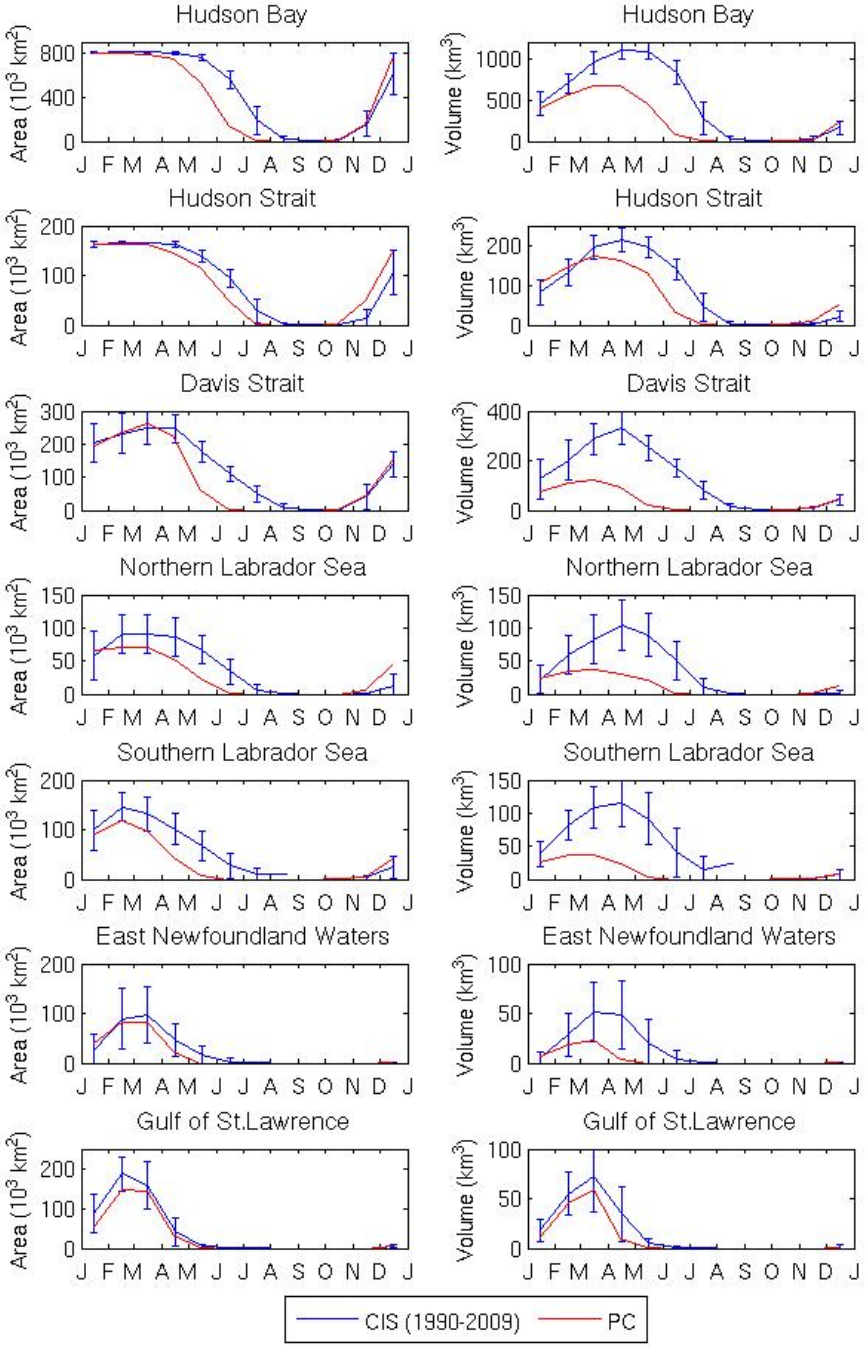

Figure 9: Ice box monthly mean ice area and volume for model PC and 1990-2009 climatology. The climatology error bars indicate ± one STD.

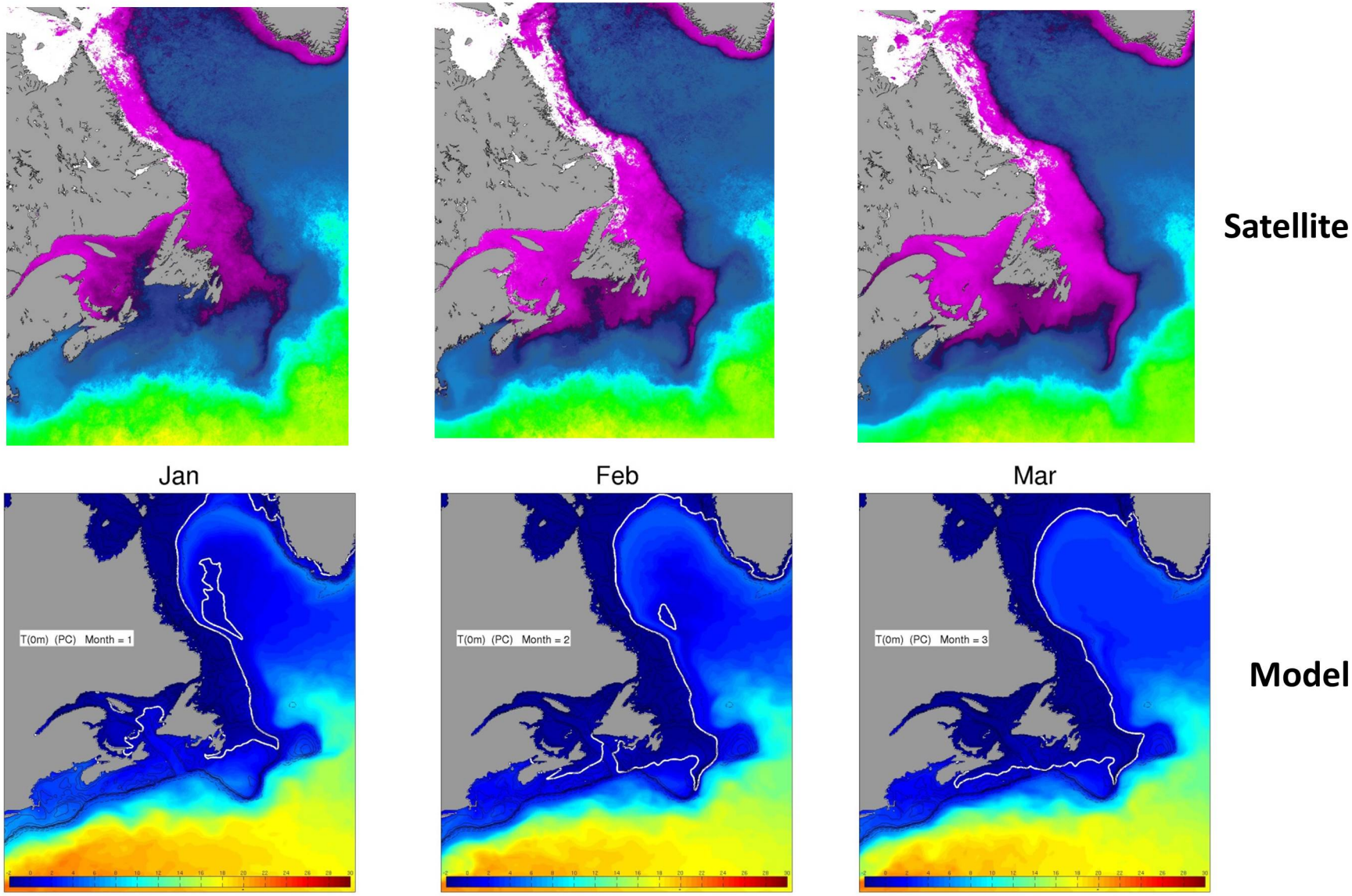

Figure 10: (a) Present climate sea surface temperature: model versus satellite climatology – January-March. The white contour in the model plot is the zero-contour, which can be compared to the mauve region in the satellite images.

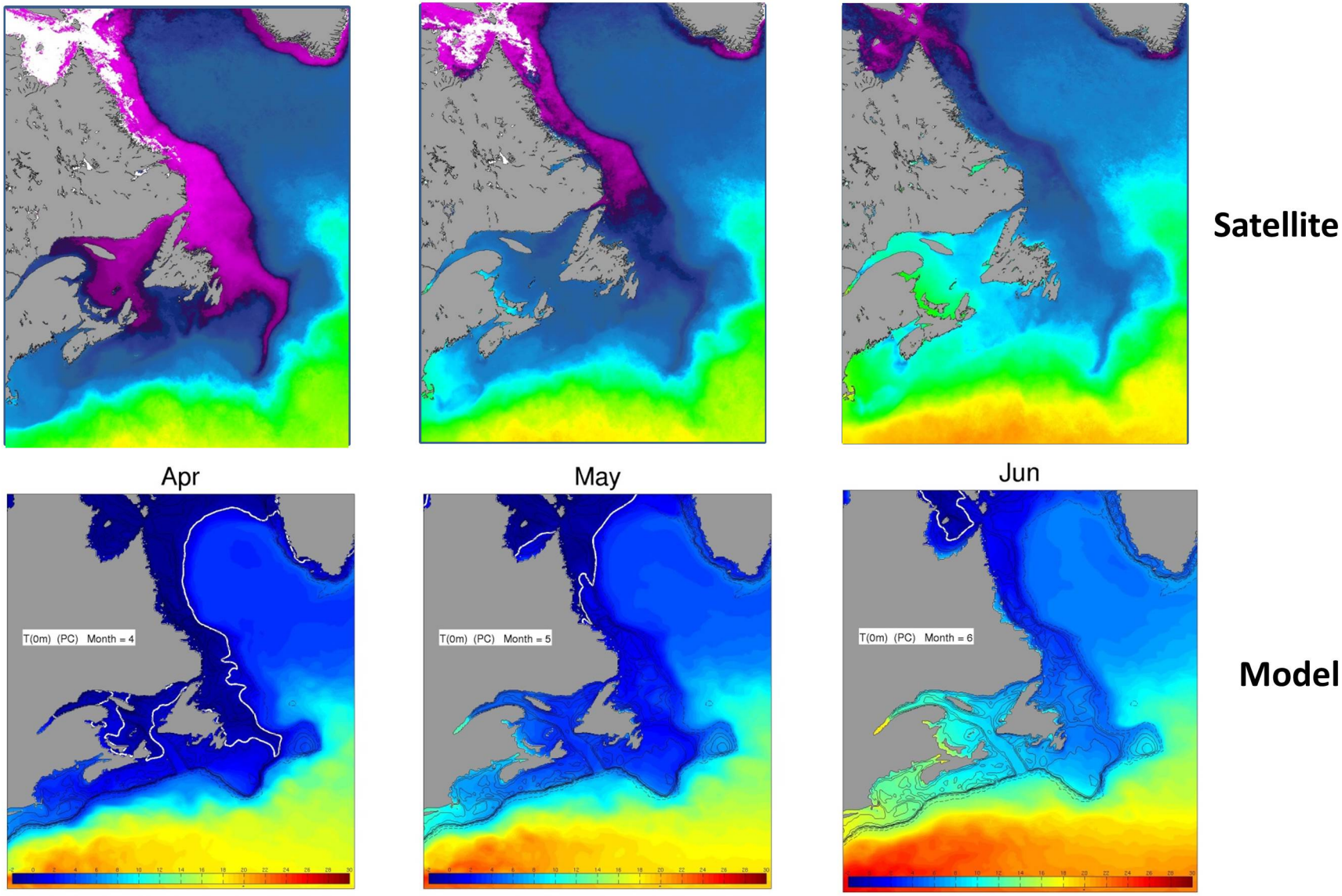

Figure 10: (b) Present climate sea surface temperature: model versus satellite climatology – Apr-Jun. The white contour in the model plot is the zero-contour, which can be compared to the mauve region in the satellite images.

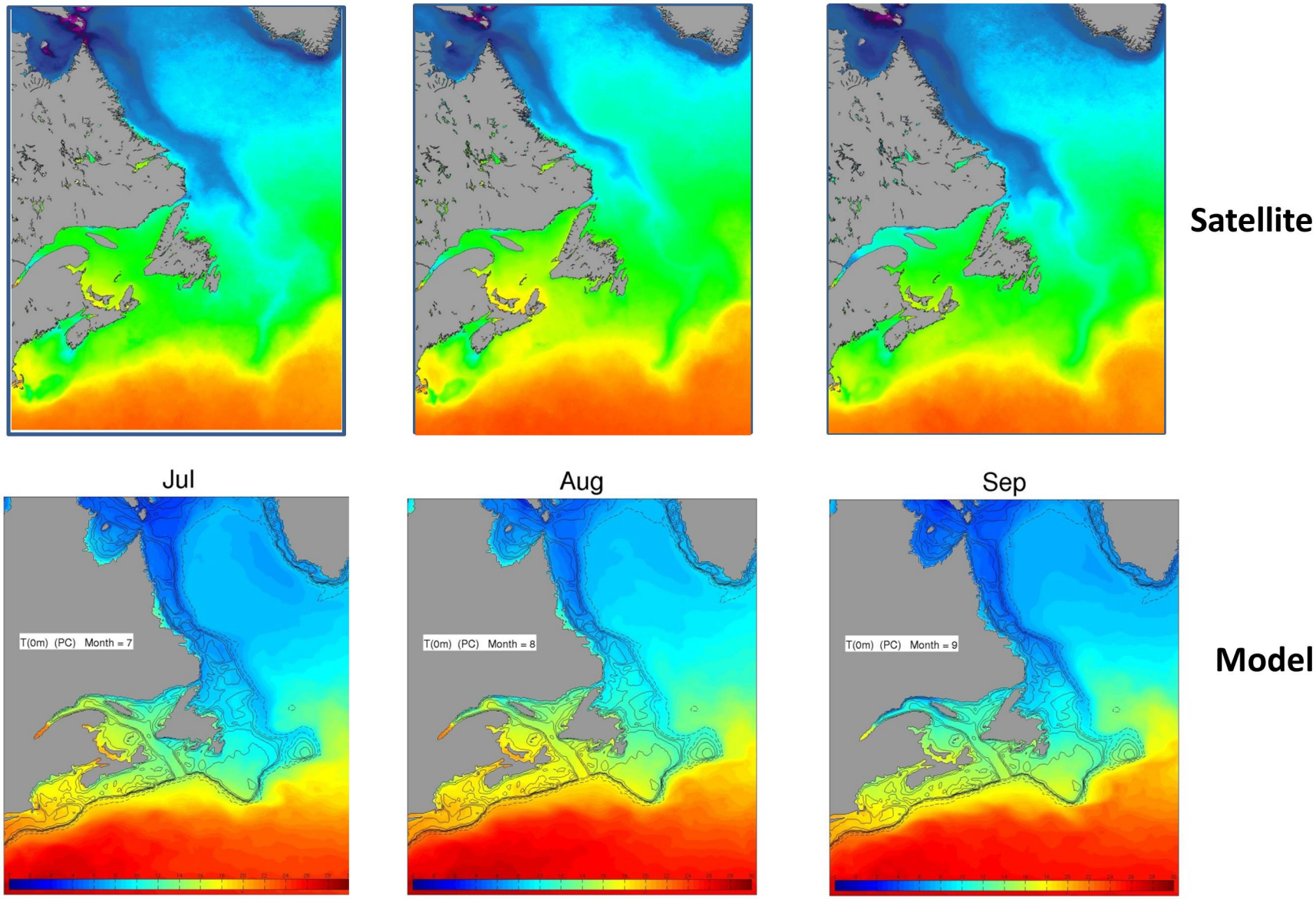

Figure 10: (c) Present climate sea surface temperature: model versus satellite climatology – Jul-Sep. The white contour in the model plot is the zero-contour, which can be compared to the mauve region in the satellite images.

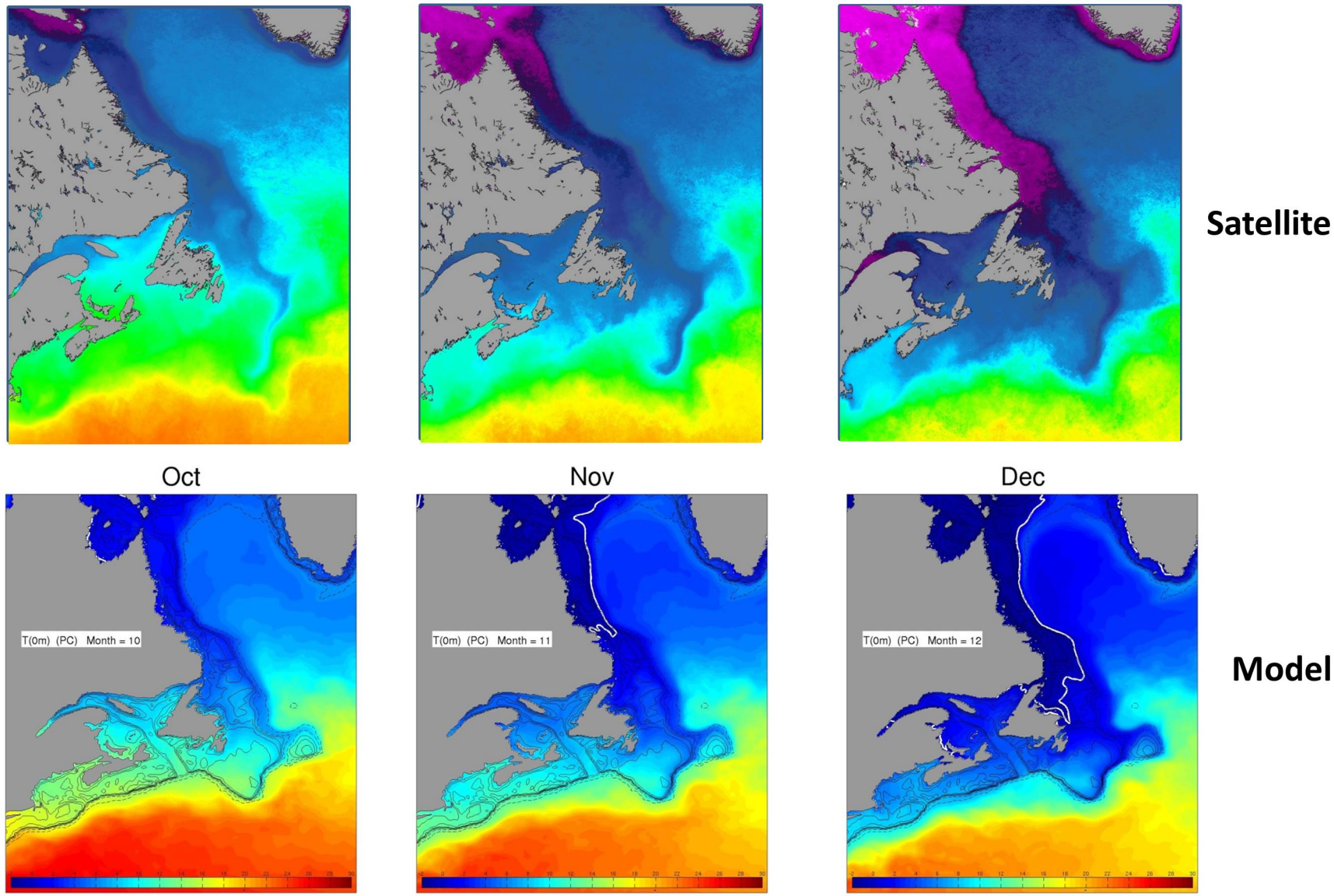

Figure 10: (d) Present climate sea surface temperature: model versus satellite climatology – Oct-Dec. The white contour in the model plot is the zero-contour, which can be compared to the mauve region in the satellite images.

monthly averages, which we use to create climate change predictions as seasonally averaged and annually averaged differences (hereafter called "seasonal" and "annual" differences). The region of interest ranges from Davis Strait in the north to the Gulf of Maine in the south, and includes the Gulf Stream and the recirculation zone south of the Scotian Shelf. To facilitate discussion of results, the domain was divided into 19 regions for analysis, with average quantities computed for each region (figure 11, table 4). The choice of regions was based on historic reference and knowledge of the circulation. Results for the regions will, for the most part, be presented in tabular form. Average quantities were also computed for Hudson Bay, which is treated as region 20 in the various tables.

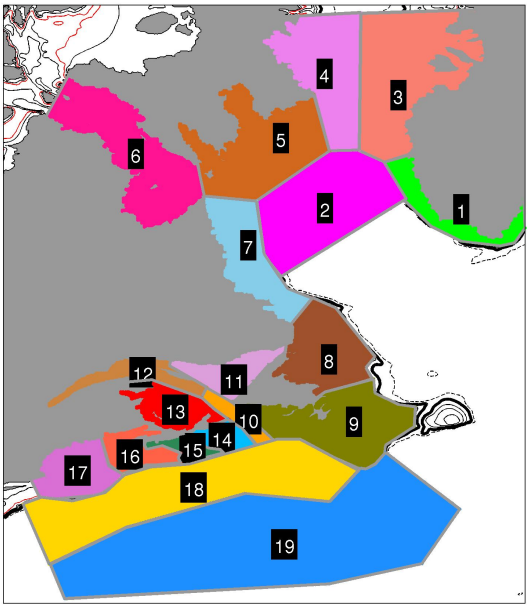

Figure 11: Regions used for various analyses. For region names see table 4

The variables presented are basic model output (T and S at various levels, ice, transports), chosen with an emphasis on those of relevance to potential ecosystem changes (e.g. changes in stratification, and surface and bottom T and S). The transports are computed for subsections of the AZMP sections as reported by Brickman et al. (2015) (see subsection 4.8 and figure 25 for more details). Standard units for T (degrees Celcius), S (PSU), and density (kg/m^3) are implied if not stated directly. In figures, the model surface layer is referred to as 0m, and future minus present climate changes in a variable "X" are denoted by dX.

4.1 General result and explanation

The model was found to have a characteristic response to the anomalous forcing which can be summarized by investigating changes in surface T and S, and density and stratification (figures 12, and 13). The response can be characterized by: cooler/fresher water on the west Greenland shelf region, warmer/fresher water on (most of) the remaining shelf area, warmer/saltier water in the northern Labrador Sea, and a chaotic pattern of variability in the Gulf Stream and slope recirculation area (figure 12).

We interpret these patterns in the following way: Changes in air temperature are uniformly positive in the north Atlantic, and changes in precipitation are positive across most of the region (see figures 4 and 5). Both of these changes tend to produce warmer and fresher (less dense) water throughout the region of interest, particularly in the surface layers. The Greenland glacier melt reinforces the freshwater tendency, especially along the Greenland shelf but also downstream on the Atlantic Canadian shelf areas. The glacier melt results in a buoyancy-driven increase in the Greenland coastal current (subsection 4.8) which advects colder water from the eastern Greenland shelf around to the western Greenland shelf. This produces a region of decreased water temperatures in the Baffin Bay area, and downstream toward the northern Labrador shelf. This signal decreases with depth but persists to the bottom in most of this region (subsection 4.5). The fresher water along the west Greenland shelf results in increased ice production in the region (subsection 4.7). Therefore, despite generally warmer air temperatures in northerly regions, ocean processes can, locally, produce effects more consistent with a cooler climate.

Density is predicted to decrease at both the surface and 50m levels, except for the Labrador Sea where increases are predicted (figure 13b). Stratification (defined as $\rho(50m) - \rho(0m)$) increases over the shelf regions (except for parts of Hudson Strait) and decreases in the northern Labrador Sea (figure 13a). The increases in stratification can be attributed to a greater decrease in the surface versus the 50m densities. In the Labrador Sea, salinity is found to increase in the surface layers ($<$ 50m; figure 12), due to the large scale circulation which recirculates saltier water from the Gulf Stream to the northeast and northwest Atlantic. This leads to a surface intensified *increase* in upper layer density, resulting in a *decrease* in stratification. This salinification of the Labrador Sea is not found in the coarse resolution AOGCM results (see Loder and van der Baaren, 2013) and highlights

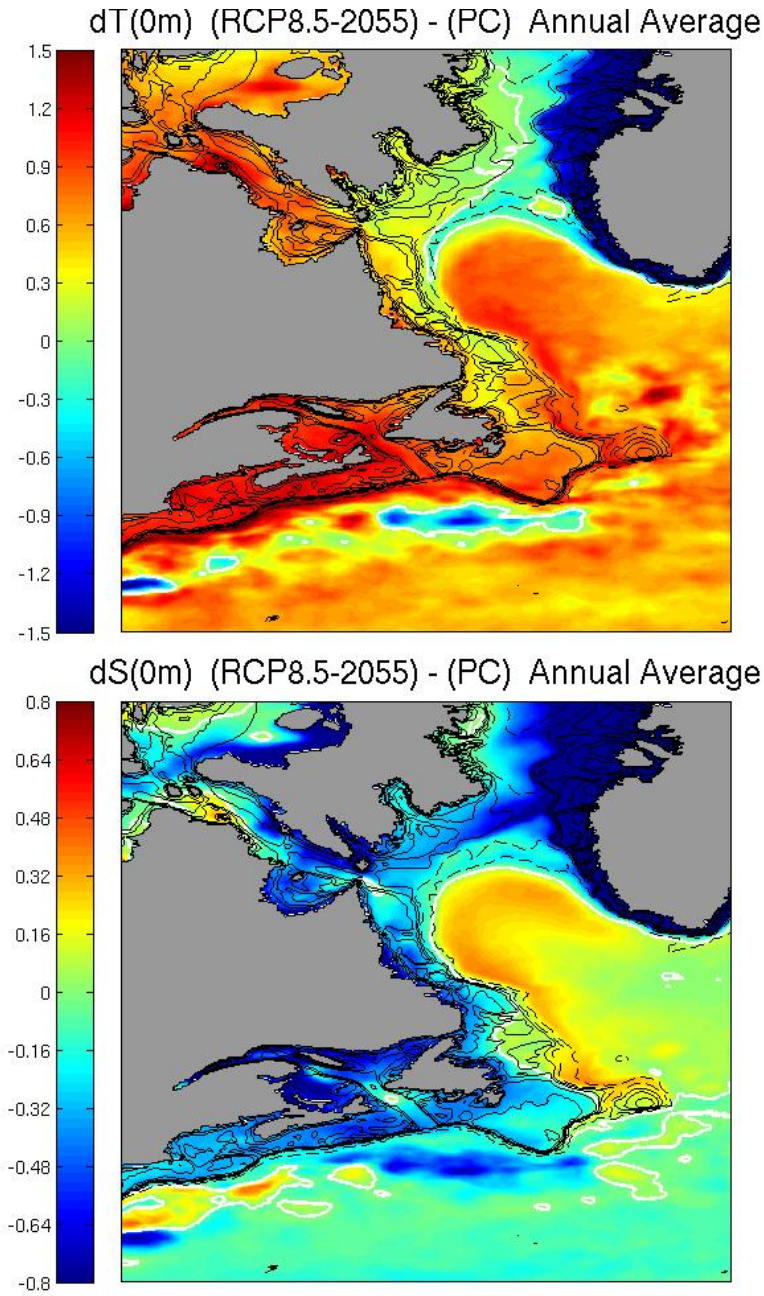

Figure 12: Predicted annual change in T and S at 0m for RCP8.5-2055. The zero contour in this and subsequent plots is drawn in white. Units for T and S are degrees C and PSU respectively.

possible differences in results when a high resolution ocean model, which properly resolves the Gulf Stream, is used for future climate simulations. The complicated stratification change in Hudson Strait can be attributed to the interaction between high surface air temperatures, that tend to increase SST and SSS (due to increased evaporation) locally and in the outflow from Hudson Bay, ice formation effects, and the colder/fresher water that enters the Strait from west Greenland.

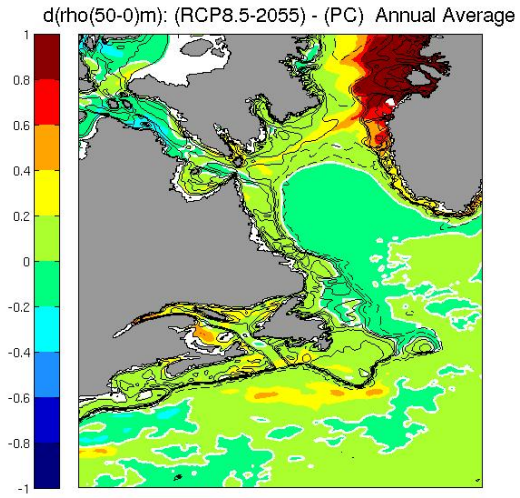

(a)

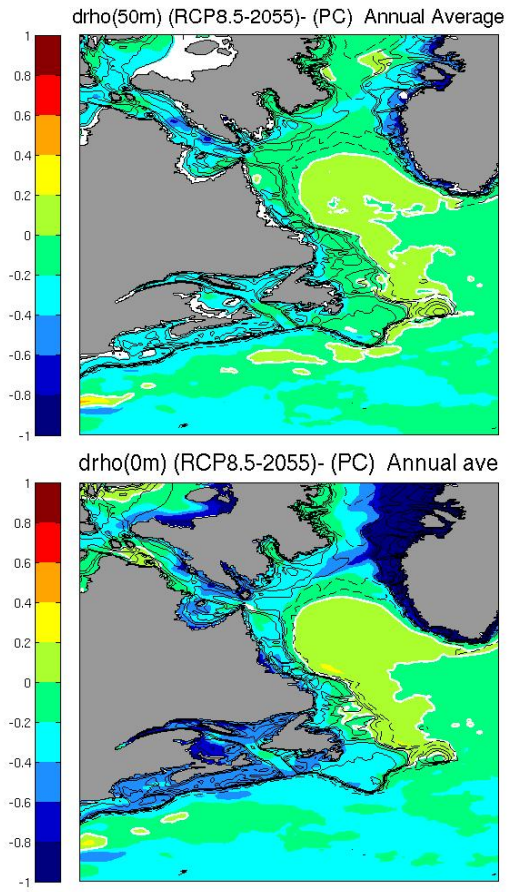

(b)

Figure 13: (a) Predicted annual change in 50m-0m stratification for RCP8.5-2055 (b) Predicted annual change in 50m and 0m density for RCP8.5-2055. The units for density are kg/m^3.

4.2 Presentation of results

A large set of plots is required to illustrate the results at various levels and for the 4 scenarios. However, it was found that there are characteristic patterns which are qualitatively similar across periods and RCPs. This is illustrated, for changes in surface T and S, in figures 14 and 15. For a given RCP (figure 14) the 2075 climatology resembles a spatially intensified version of the 2055 climatology. The same basic similarity in pattern pertains to the comparison between the two RCPs for the 2055 climatology (figure 15), with RCP8.5 resembling an intensified version of the RCP4.5 scenario.

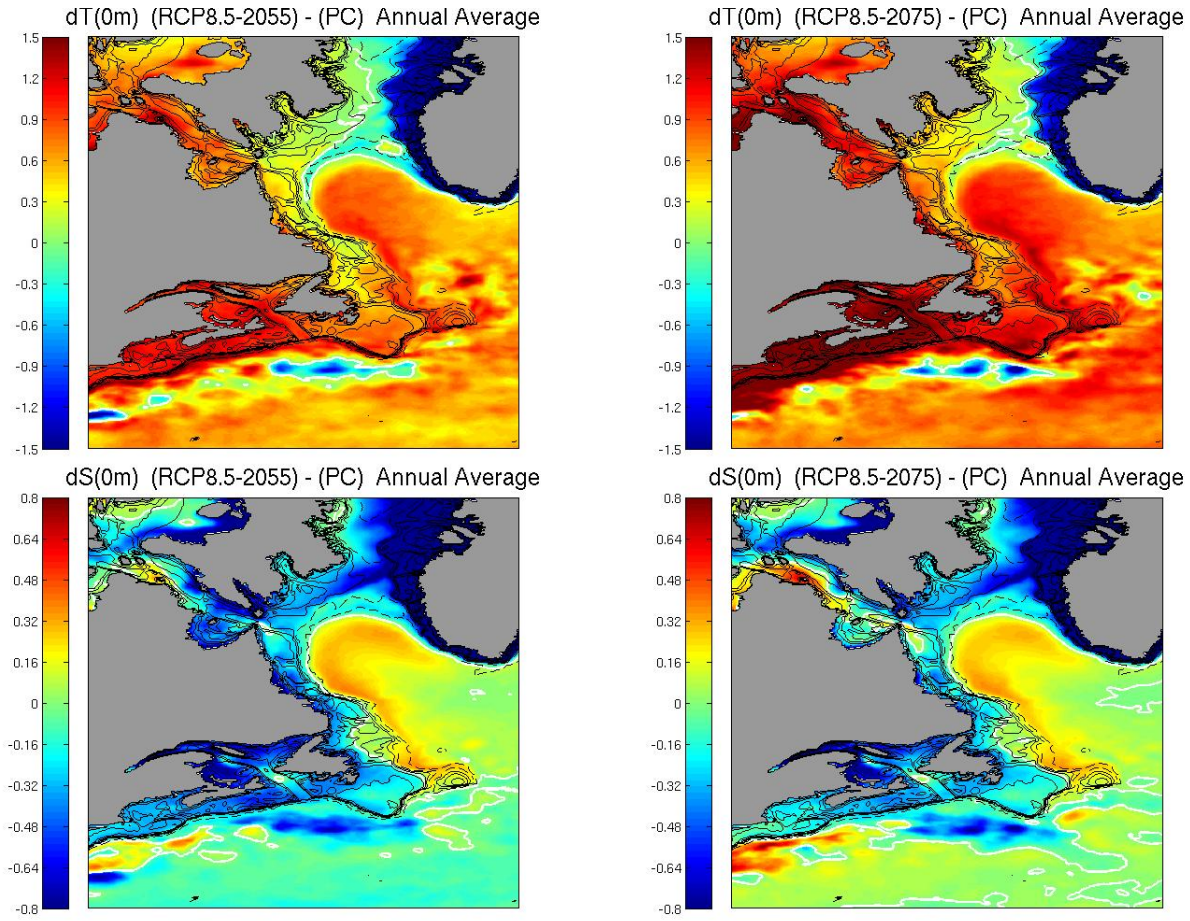

(a) (b)

Figure 14: Predicted annual change in T and S at 0m for RCP8.5 for (a) 2055 climatology and (b) 2075 climatology.

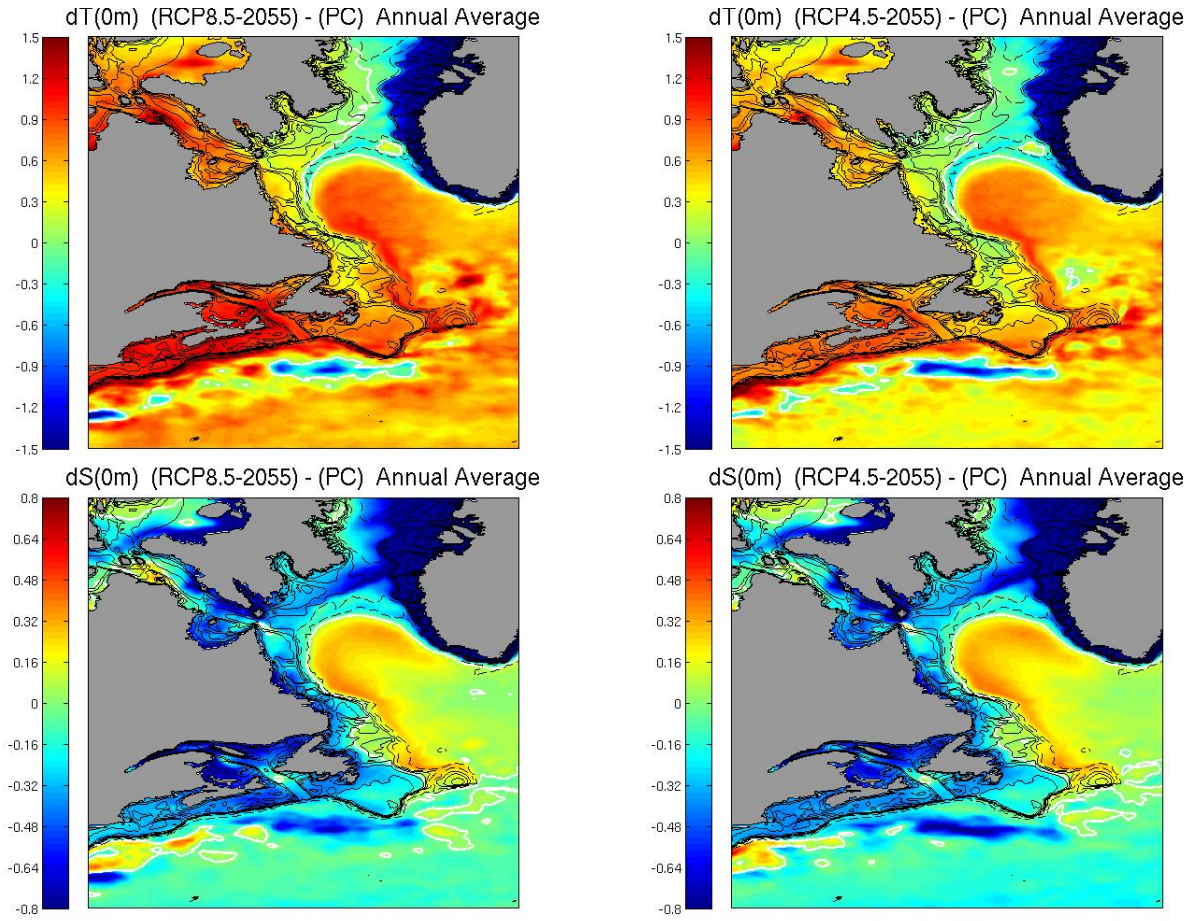

(a) (b)

Figure 15: Predicted annual change in T and S at 0m, 2055 climatology, for (a) RCP8.5 and (b) RCP4.5.

It was also found that spatial plots of seasonal changes were not revealing so we present this information as regional plots with the season of extreme values annotated (e.g. figure 16; where winter is season 1, etc.), with detailed information placed in a corresponding table (e.g. table 5). The season of extreme value was chosen to account for possible positive and negative changes in properties: if the mean change is negative (for example, surface T in the west Greenland coastal zone) then the season of extreme value is the season in which the predicted change is most negative – and vice versa.

For each set of variables, we will present the results for one scenario in the main text, and place the majority of figures and tables in Appendix B.

4.3 Changes in surface T and S

Predicted annual changes for surface T and S for the RCP8.5-2055 climatology are shown in figure 17, and summarized in table 5. As mentioned above, the model's prediction is cooler/fresher water on the west Greenland shelf region, warmer/fresher water on (most of) the remaining shelf area, and warmer/saltier water in the northern Labrador Sea. The seasonal changes indicate maximum changes in surface T in the summer-fall for the northern regions, changing to winter-spring in the maritime Canada region (i.e GSL, Scotian Shelf, Gulf of Maine). No clear seasonal pattern emerges for regional changes in surface S. Average changes in temperature, on an annual basis, increase from about 0.5° on the Labrador shelf to about 1.0° in the GSL, Scotian Shelf and Gulf of Maine regions. The latter values are about $1 - 2°$ smaller than those derived from coarse resolution ocean climate models (Loder and van der Baaren, 2013, figure 5-9c). Average changes in salinity (outside of the Greenland shelf area), on an annual basis, range from about -0.3 to -0.6PSU with lowest values in the GSL. These decreases are about 0.1-0.2PSU lower than average AOGCM results (Loder and van der Baaren, 2013, figure 6-9c) but within the range of values. The increase in salinity in the Labrador Sea is not reported in the AOGCM results.

Figures and tables for the other scenarios can be found in Appendix B (figures A4, A9, A14; tables A4, A9, A14).

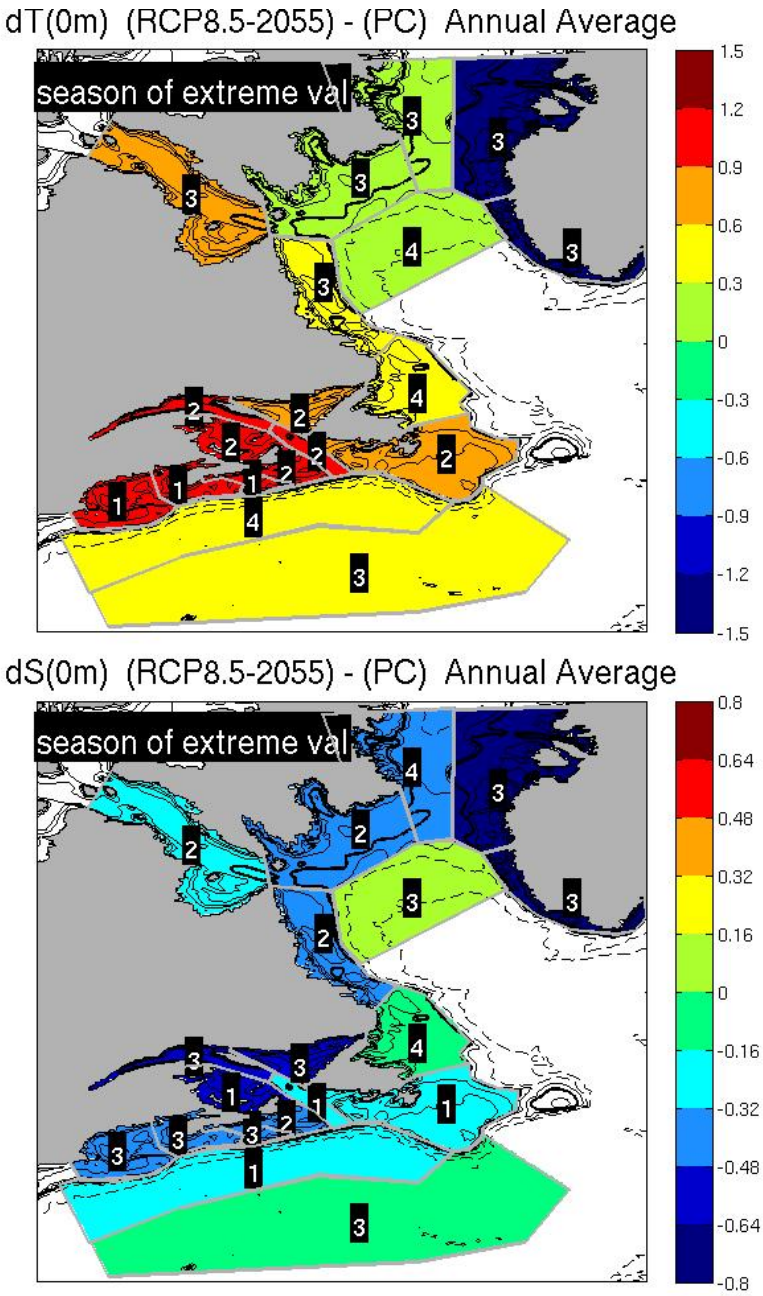

Figure 16: Predicted annual change in T and S at 0m, by region, for RCP8.5-2055. The season of extrema in T and S change is annotated. In this and subsequent plots winter is season 1, etc.

4.4 Changes in bottom T and S

Predicted annual changes for bottom T and S for the RCP8.5-2055 climatology are shown in figure 18, and summarized in table 6. Bottom temperatures are predicted to increase over the entire shelf region except for the area affected by the Greenland glacier melt. Average values, on an annual

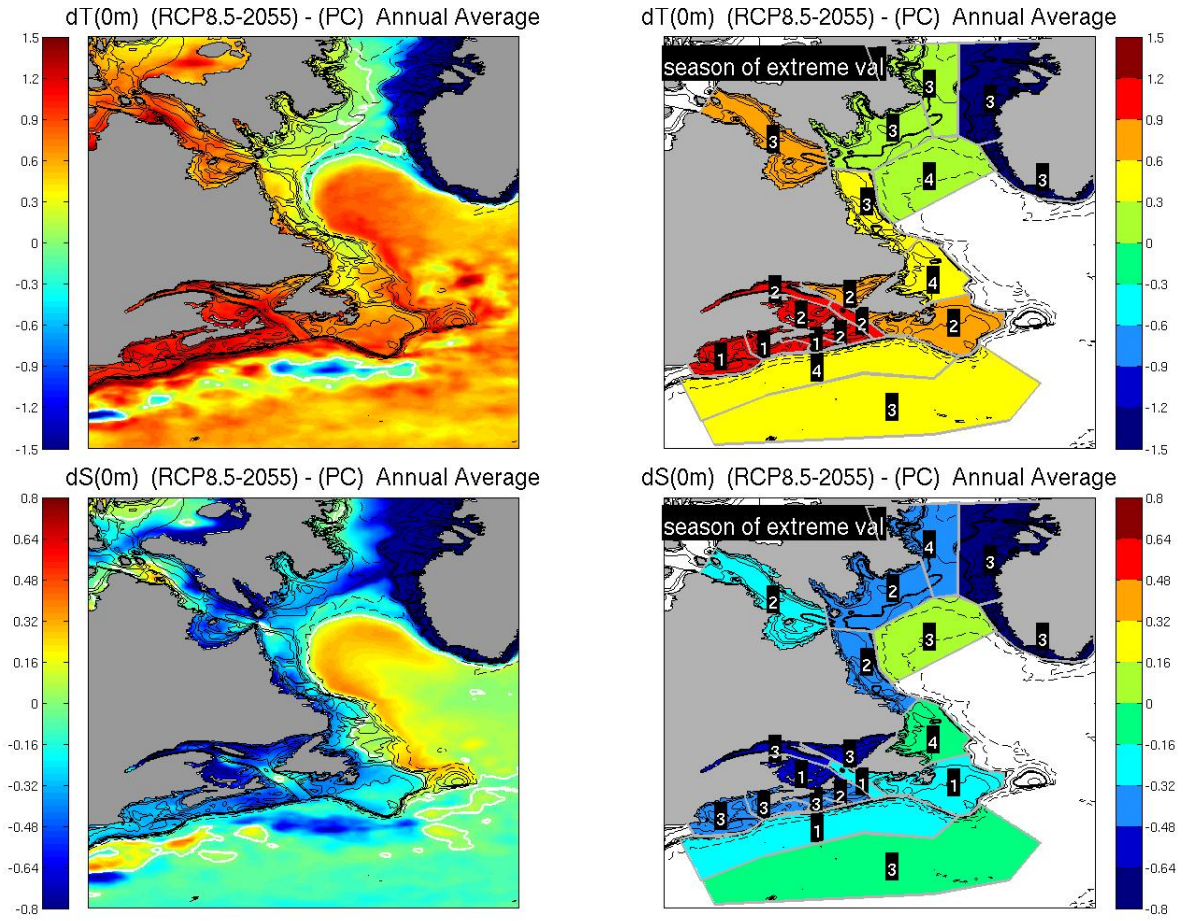

(a) (b)

Figure 17: Predicted annual change in T and S at 0m for RCP8.5-2055. (a) Spatial plot. (b) Region plot. The season of extrema in T and S change is annotated.

basis, are typically $< 0.5°$ with the highest values on the Scotian Shelf and Gulf of Maine. The latter values ($\sim 1.6°$) are about 1° smaller than those derived from coarse resolution ocean climate models (based on an analysis of simulations from the 6 AOGCMs listed in table 1; see figure A45). Seasonally, there is a tendency toward maximum changes in bottom T in the summer-fall for the northern regions, changing to winter-spring in the maritime Canada region. Bottom salinity onshelf exhibits a more complicated pattern with most of the region decreasing, but with some areas of increase, likely due to the effects of enhanced surface evaporation (i.e. Hudson Strait) or incursions of saltier offshelf waters (e.g. central Gulf of Maine). Seasonally, most of the shelf region exhibits maximum changes in bottom S in winter-spring, the exceptions being the west Greenland and Davis Strait regions.

Figures and tables for the other scenarios can be found in Appendix B (figures A5, A10, A15; tables A5, A10, A15).

4.5 Changes in sub-surface T and S

Predicted annual and seasonal changes for T and S were also computed at other sub-surface depths for which we report depths 50, 100, and 150m in this document. For the regional analyses, a particular depth may be below the bottom for part of a region. In these cases, the average value was computed using only the cells above bottom. Note that for plotting purposes a given region is completely filled with the computed colour (i.e. value), as opposed to just filling the area that was above the bottom.

In general, the results are qualitatively similar to the surface T and S, so we relegate all figures and tables to Appendix B (figures A1, A2, A3, A6, A7, A8, A11, A12, A13, A16, A17, A18; tables A1, A2, A3, A6, A7, A8, A11, A12, A13, A16, A17, A18).

4.6 Changes in density and stratification

Predicted annual changes in stratification for the RCP8.5-2055 climatology are shown in figure 19, and summarized in table 7. As discussed above, stratification is predicted to increase over the shelf regions (except for parts of Hudson Strait) and decrease in the northern Labrador Sea.

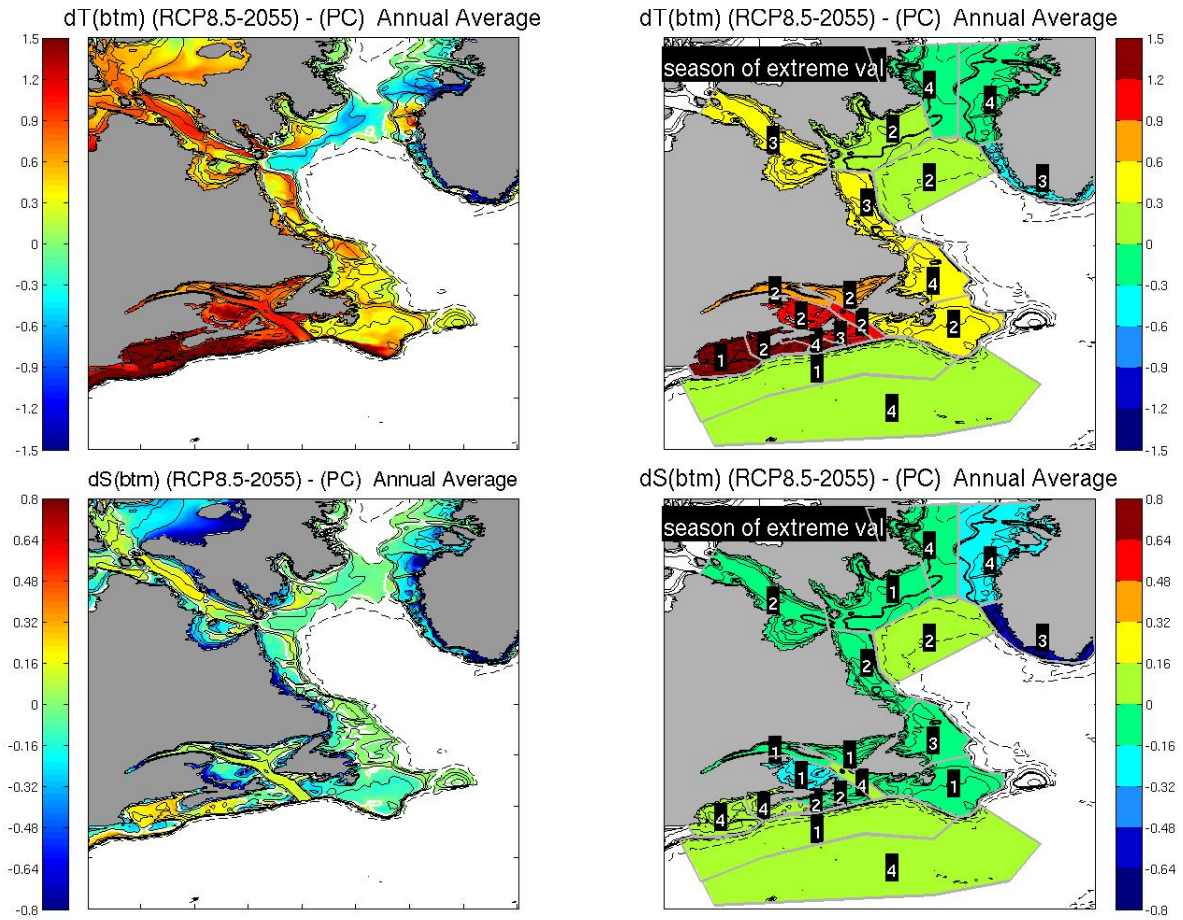

(a) (b)

Figure 18: Predicted annual change in bottom T and S for RCP8.5-2055. (a) Spatial plot. Deep water region is masked out for clarity. (b) Region plot. The season of extrema in T and S change is annotated.

The increase in stratification can be attributed to a greater decrease in the surface versus the 50m densities. In the Labrador Sea, circulation adjustments lead to a surface intensified *increase* in upper layer density, resulting in a *decrease* in stratification.

Figures and tables for the other scenarios can be found in Appendix B (figures A19, A20, A21; tables A19, A20, A21).

4.7 Changes in sea ice

The spatial patterns for ice metrics are similar between RCPs and bi-decadal periods, so we illustrate results here using the RCP8.5-2055 scenario and relegate most details for the other scenarios to Appendix B.

In general, the development, growth and retreat of sea ice is predicted to be similar to present climate in space and time (figures 20 and 21). However, warmer air temperatures lead to less ice production in all regions with the exception of Baffin Bay and Davis Strait (figure 22). Here the increased stratification and surface freshening (freezing point elevation) cause an increase in ice production. The effect is most pronounced off the west coast of Greenland. The increase in ice production in these regions increases the southwards ice advection along the shelf break leading to more ice in the northern Labrador Sea January to April. Both Hudson Bay and Hudson Strait continue to be completely ice covered January to March (figure 20).

Figures 23 and 24 show the percentage change from present climate of monthly ice box area and volume for all combinations of RCP and bi-decade. In these plots, a percentage change of 100% indicates that the month is ice free relative to present climate. Ice decreases for all boxes except Davis Strait. There is also a small increase in ice area for the northern Labrador Sea, February to April, but ice volume only increases for RCP4.5-2055 i.e. there is less ice spread over a larger area for the other three scenarios. The amount of ice in the Gulf of St.Lawrence dramatically decreases for all scenarios, particularly late season ice. For RCP8.5-2075, significantly less ice is predicted. For example, the GSL is almost ice-free while the decrease in Hudson Bay ice volume is 2-4 times greater than for the other three scenarios. For the RCP8.5-2075 scenario all regions are almost ice free a month earlier than present climate.

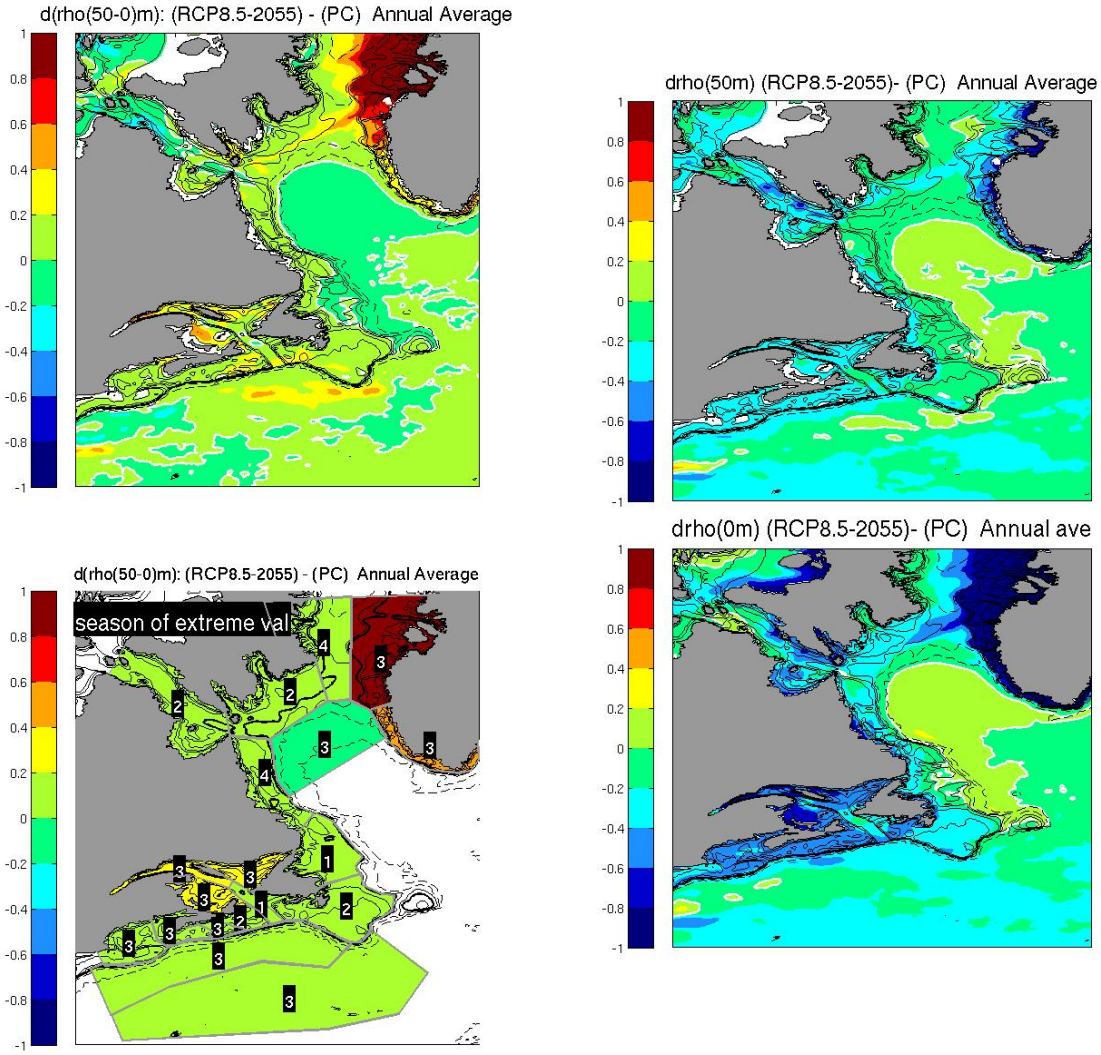

(b)

(a)

Figure 19: (a) Predicted annual change in 50m-0m stratification for RCP8.5-2055 – spatial and regional plots. The season of extrema in stratification change is annotated. (b) Predicted annual change in 50m and 0m density for RCP8.5-2055.

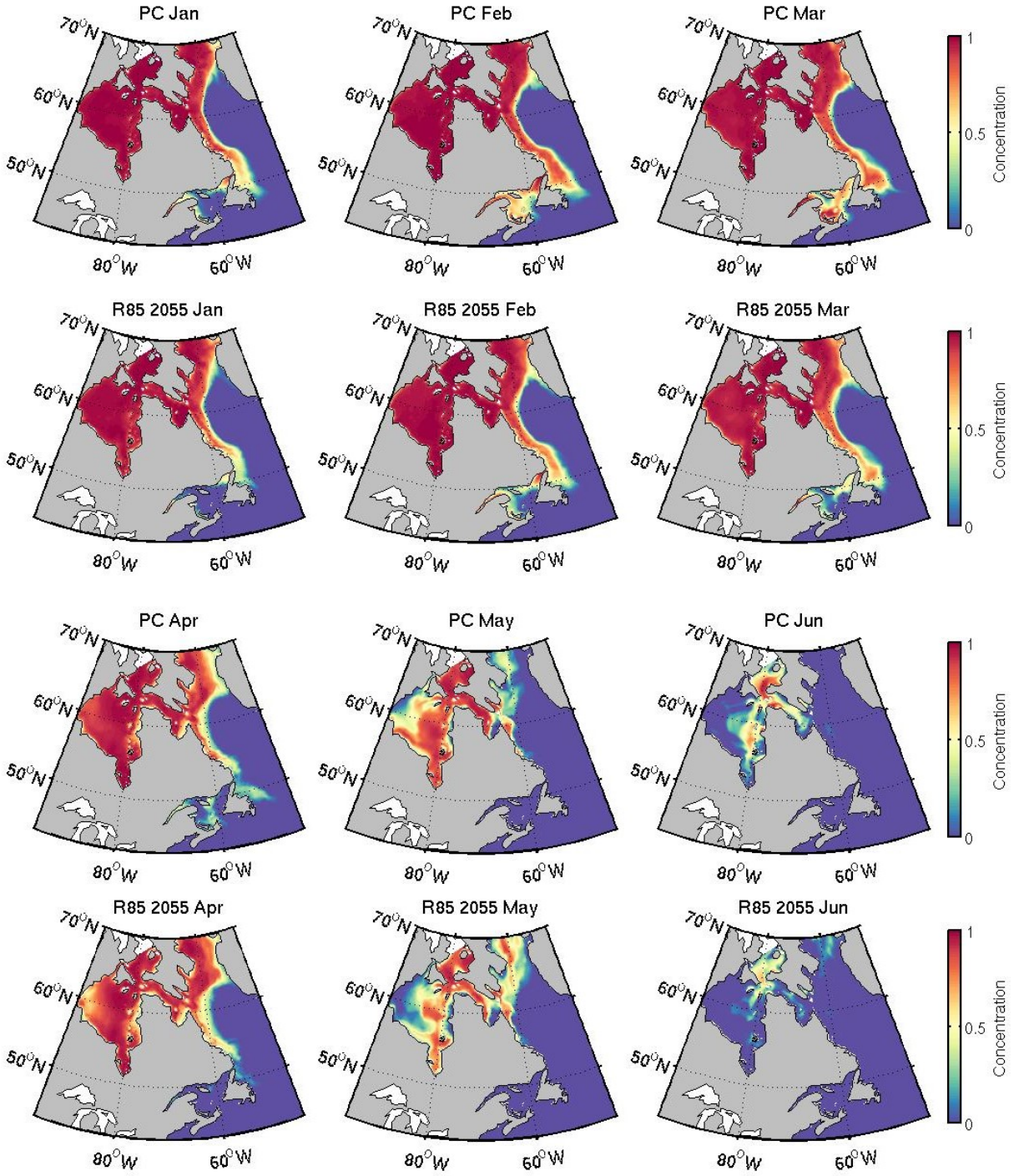

Figure 20: Model present climate vs RCP8.5-2055 ice concentration, January to June.

Figures for the other scenarios can be found in Appendix B. (figures A31 – A44). Appendix B table A22 lists the percentage change from present climate of the **annual mean** ice area, volume

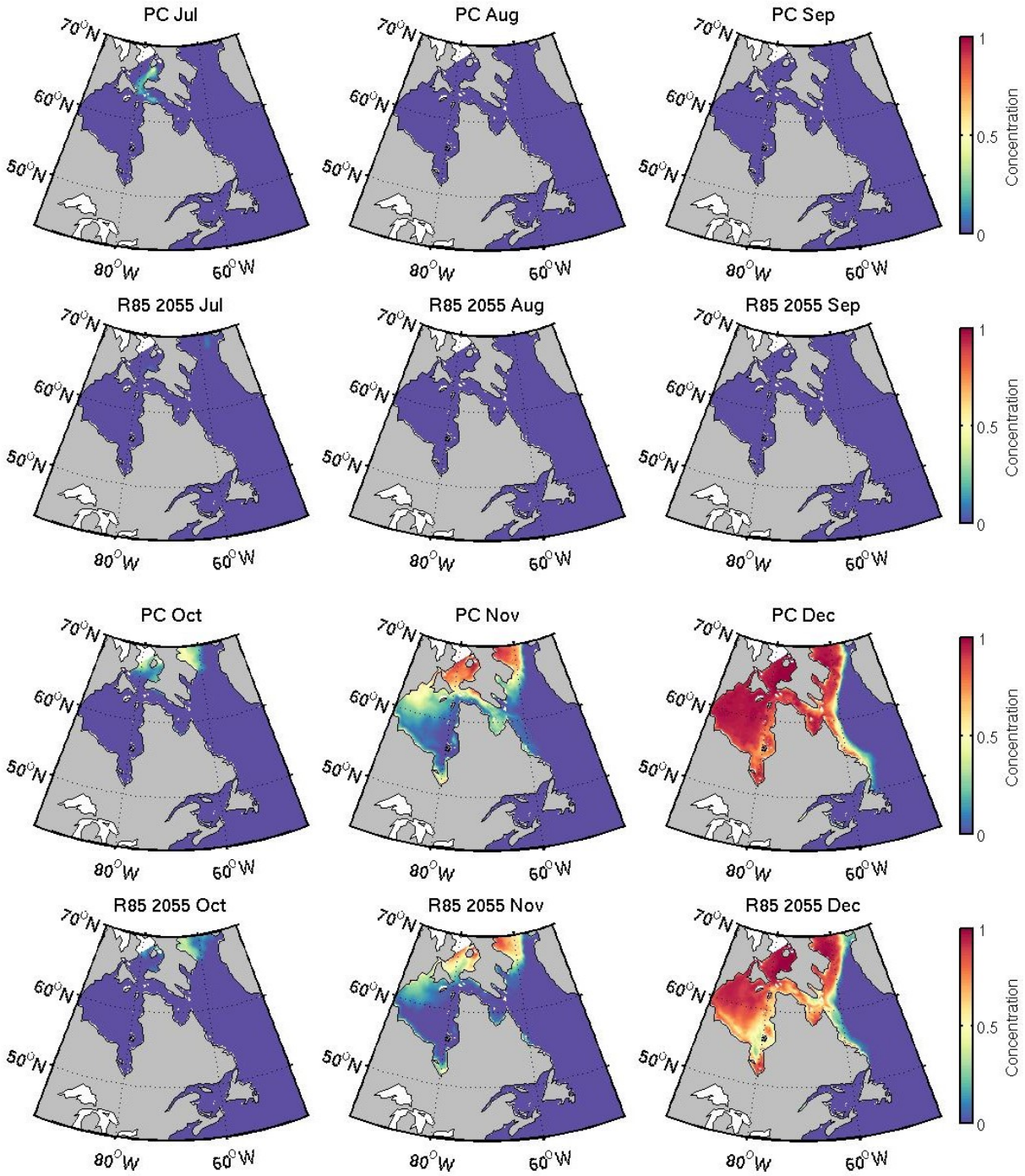

Figure 21: Model present climate vs RCP8.5-2055 ice concentration, July to December.

and extent, for each ice box, and the sum over all ice boxes. Similarly, table A23 lists the annual mean percentage change from present climate of the **maximum** ice area, volume and extent, for each ice box, and the sum over all ice boxes. (NB: ice extent defines a region as ice-covered or not

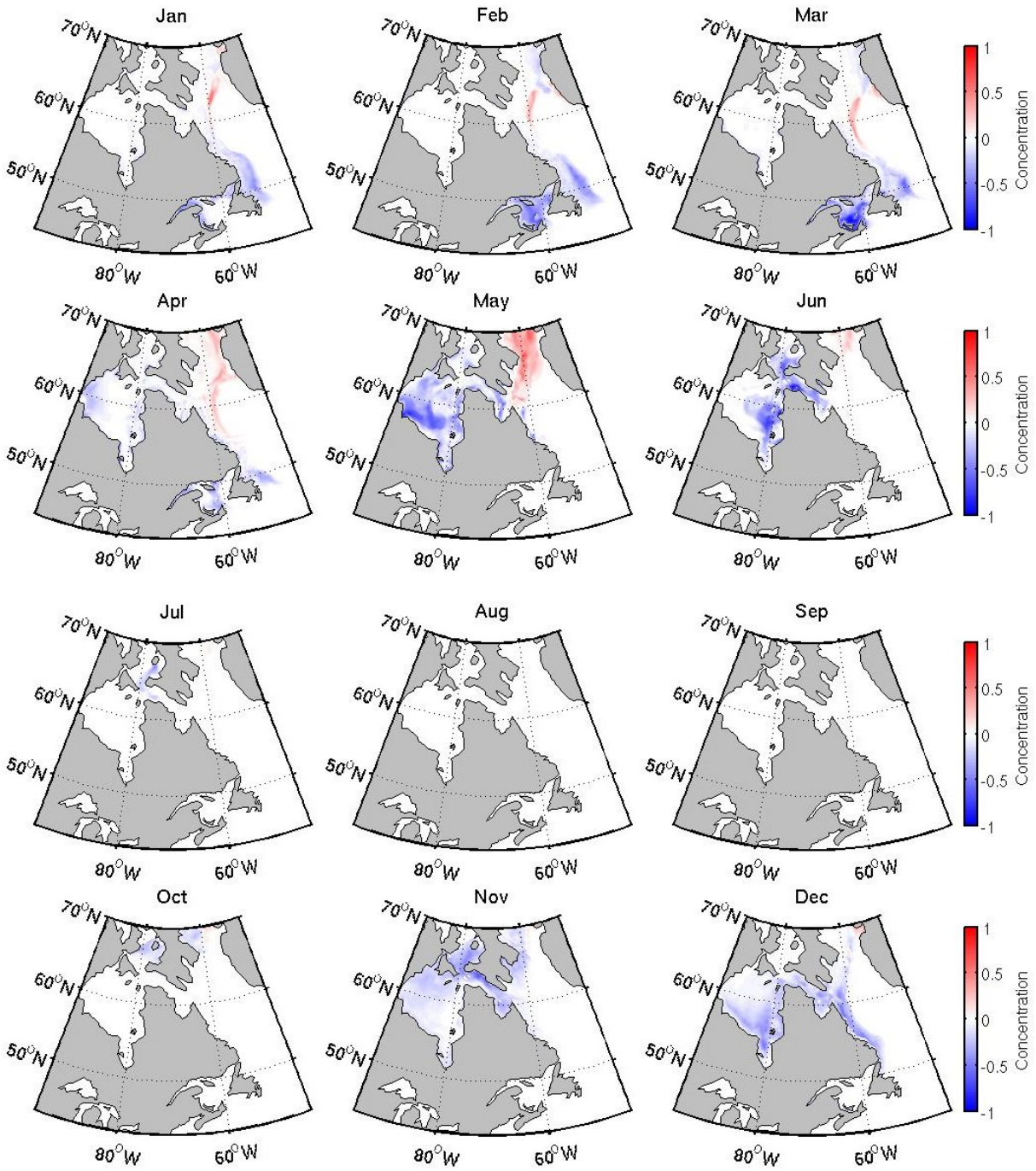

Figure 22: Change in ice concentration: (RCP8.5-2055) - (PC).

ice-covered based on a threshold concentration. The threshold used here was 15 percent.)

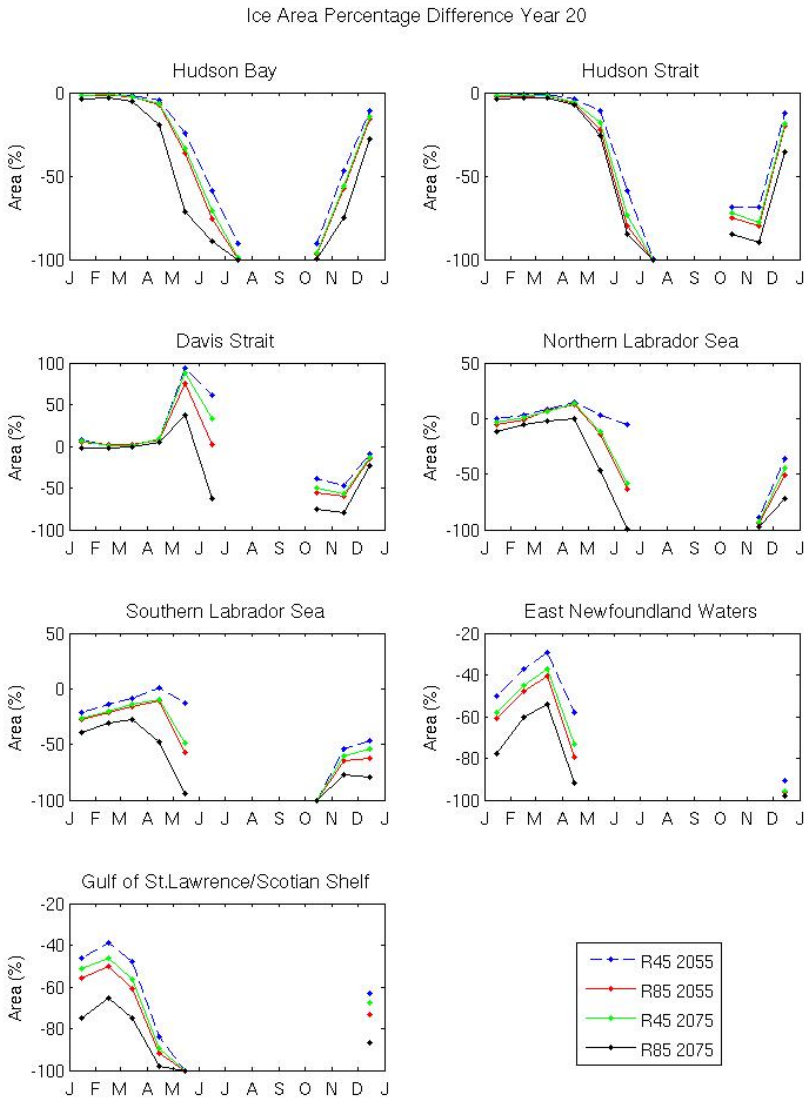

Figure 23: Percentage change from PC, ice box monthly ice area, for all combinations of RCP and bi-decade.

4.8 Changes in circulation: transports

Velocity data were extracted from the model simulation at section locations shown in figure 25. From these, depth-integrated transports through various subsections were created where the subsections were chosen based on the principal current streams found in the region. The transports computed

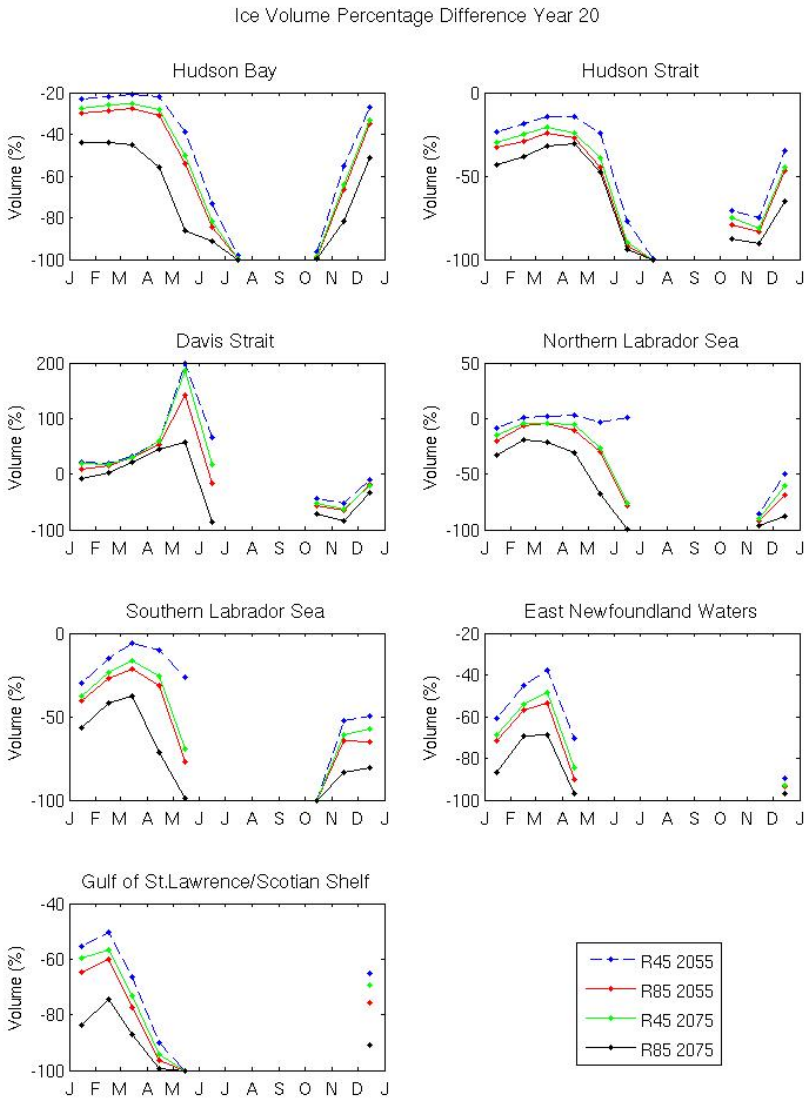

Figure 24: Percentage change from PC, ice box monthly ice volume, for all combinations of RCP and bi-decade.

were: the Greenland coastal and Greenland coastal plus shelfbreak regions of the (eastern) AR7W section; the coastal and shelfbreak regions of the Seal Island section (i.e. the inshore and offshore Labrador currents); the net transport through the Strait of Belle Isle; the inner and shelfbreak regions of the Bonavista, Flemish Cap, and southeast Grand Banks sections; Cabot Strait transports; inner and shelfbreak regions of the Louisbourg and Halifax sections; inner shelf region of the Cape

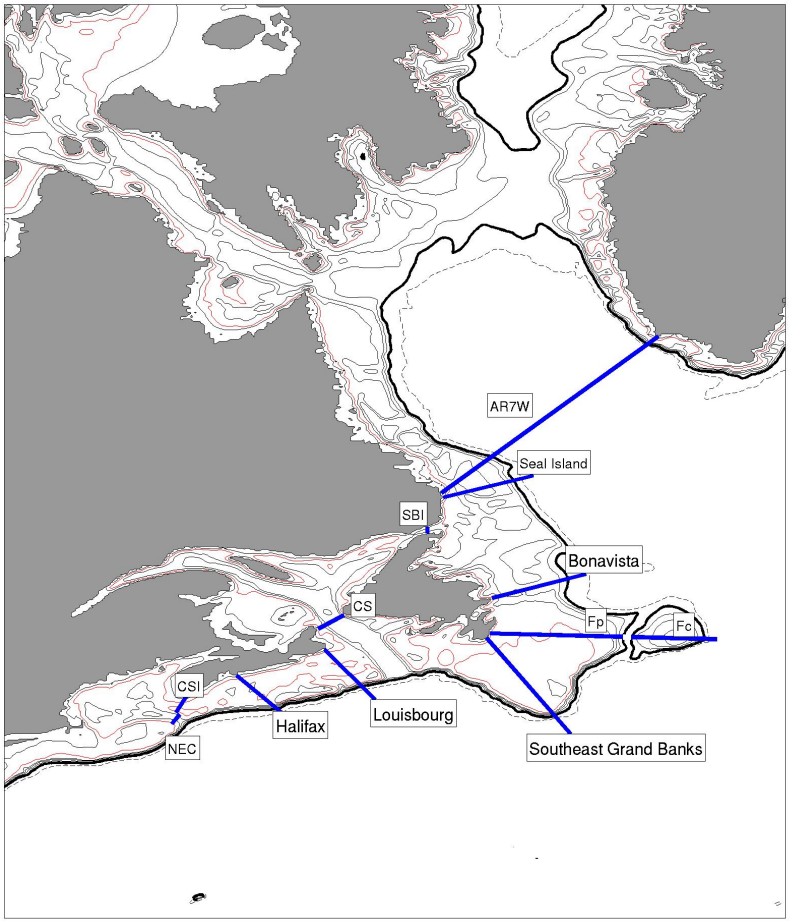

Figure 25: Sections for which transports were computed for various subsections. The Flemish Cap section was broken into Flemish Pass (Fp) and Flemish Cap (Fc) subsections. See table 3 for abbreviations. Contours are at 50, 100 (red), 200, 300, 500, 1000 (bold), and 2000 (dashed) meters.

Sable Island section; and the transport into and out of the Gulf of Maine through a section across the Northeast Channel. (Note that for analysis purposes the Flemish Cap section is divided into Flemish Pass and Flemish Cap subsections (see figure 25).) Section names and their abbreviations used in the text are contained in table 3. The division of sections into fixed inner (where "inner" denotes the subsection that abuts the coastline) and shelfbreak regions was based on identifying the location of these current streams in monthly mean model velocity sections. Computation of inflow

and outflow through sections was based on the sign of the velocity (at a given time), as opposed to dividing the section into fixed inflow and outflow subsections.

Name	**Abbreviation**
AR7W	AR7W
Seal Island	SI
Strait of Belle Isle	SBI
Bonavista	BV
Flemish Pass	Fp
Flemish Cap	Fc
southeast Grand Banks	se-GB
Cabot Strait	CS
Louisbourg	Lb
Halifax	Hfx
Cape Sable Island	CSI
Northeast Channel	NEC

Table 3: Key section names and their abbreviations. In the text and tables, nearshore and shelfbreak subsections are denoted by "inner" and "sb" appendices respectively.

Fractional changes in transports were computed as (Γ(F)-Γ(PC))/Γ(PC), where Γ is the transport through a given region, and F and PC are future and present climate respectively. A qualitative depiction of the result for the RCP8.5-2055 simulation (Atlantic Canada region) is shown in figure 26. Results for all scenarios are reported in table 8. In general, differences in transports are predicted to be small (less than 5%), except for the west Greenland shelf ($\sim$30%) which is strongly influenced by glacier melt. Differences tend to be highest in shelfbreak flows, particularly at the tail of the Grand Banks and along the Scotian Shelf, likely expressing the influence of the Gulf Stream. In terms of spatial pattern, there is a general tendency in all scenarios of increased transports along the NL shelf (inshore and shelfbreak) with decreased transport into the Gulf of Maine via CSI and NEC.

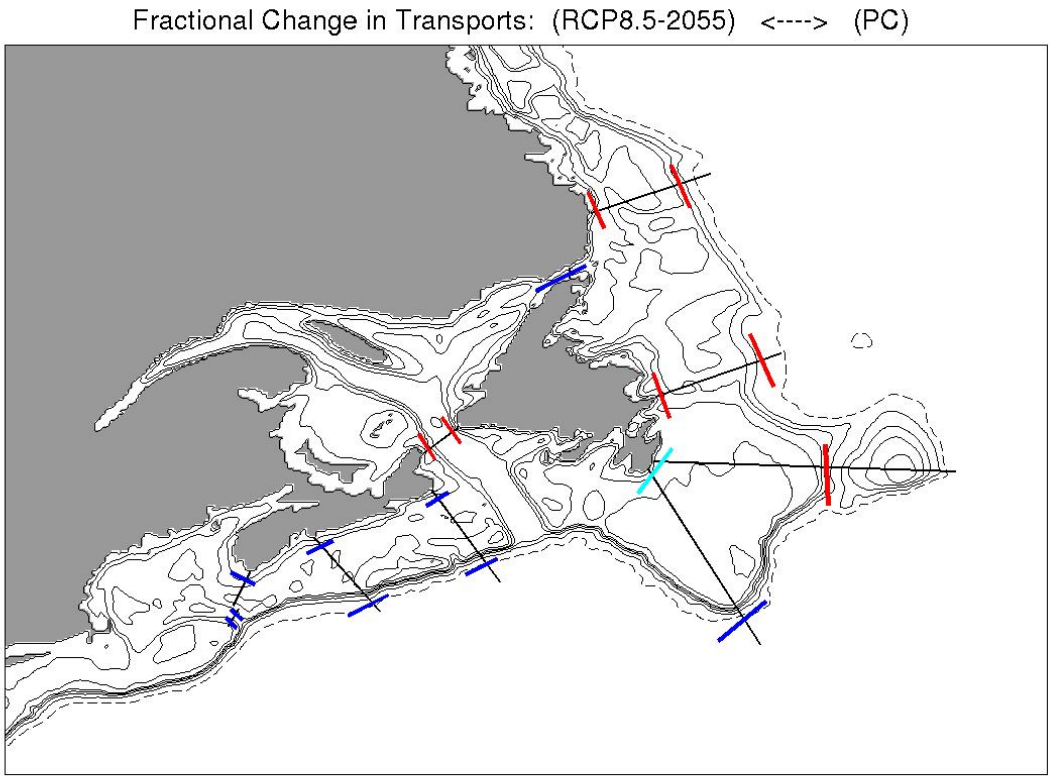

Figure 26: Fractional change in transports through various AZMP subsections in Atlantic Canada, for RCP8.5-2055. The red lines denote increased transport, the blue lines decreased transport, the cyan line no change in transport. See table 8 for values.

4.9 Results for Hudson Bay

Results for Hudson Bay, for the 4 scenarios, are shown in (Appendix B) figures A22-A30 (and note that the 150m level is omitted as most of Husdon Bay is shallower than this depth). Consistent with the NW Atlantic region reported above, there are qualitative similarities between RCPs and periods.

In general, the predicted response is complicated, reflecting the competing effects of circulation and changes in surface forcing. The effect of higher surface air temperature results in an increase in ocean temperature throughout the water column over all of the Bay. Salinity is predicted to decrease over the majority of the region but with areas of increased salinity located typically toward the central

Bay. This response can be attributed to the effects of enhanced surface evaporation versus increased precipitation and runoff. The latter would be expected to reduce salinity predominately in the coastal zone, which is evident in the plots (figures A22- A29). Stratification is predicted to decrease in the south part of the Bay and increase in the north, with a region of decreased stratification in the northeast (figure A30). This latter region merges with the decreased stratification region of Hudson Strait, likely a signature of the outflow from Hudson Bay into the Strait (figures 19 and A19–A21).

5 Summary

In this report we presented results from future climate simulations using a high resolution ocean model of the entire north Atlantic ocean, with a focus on Atlantic Canadian waters. The present climate simulation of the ocean model was forced using the CORE normal year forcing of Large and Yeager (2004). Future climate forcing was created by adding anomalies of surface air temperature and precipitation to the CORE normal year forcing where these anomalies were derived from an ensemble of 6 ESM future climate simulations (table 1). A representation of the predicted melting of the Greenland glacier was included in the future climate forcing. Due to computational constraints, simulations were limited to 2 time periods (2046-2065, 2066-2085) and 2 RCPs (RCP4.5, RCP8.5) – producing RCP4.5-2055, RCP4.5-2075, RCP8.5-2055, and RCP8.5-2075 climatologies.

The model was found to have a characteristic response to the future climate forcing consisting of: cooler/fresher water on the west Greenland shelf region, warmer/fresher water on (most of) the remaining shelf area, warmer/saltier water in the northern Labrador Sea, and a chaotic pattern of variability in the Gulf Stream and slope recirculation area (figure 12).

Key predictions of the simulations are:

• Changes in surface T and S (tables 5, A4, A9, A14):

– Average changes in **SST** (figure 27), on an annual basis, for all scenarios except RCP8.5-2075,

increase from about 0.5° on the Labrador shelf to about 1.0° in the GSL, Scotian Shelf and Gulf of Maine regions. The latter values are about $1-2°$ smaller than those derived from coarse resolution ocean climate models for the same period (Loder and van der Baaren, 2013). The RCP8.5-2075 scenario is about 0.5° warmer than the others for these regions.

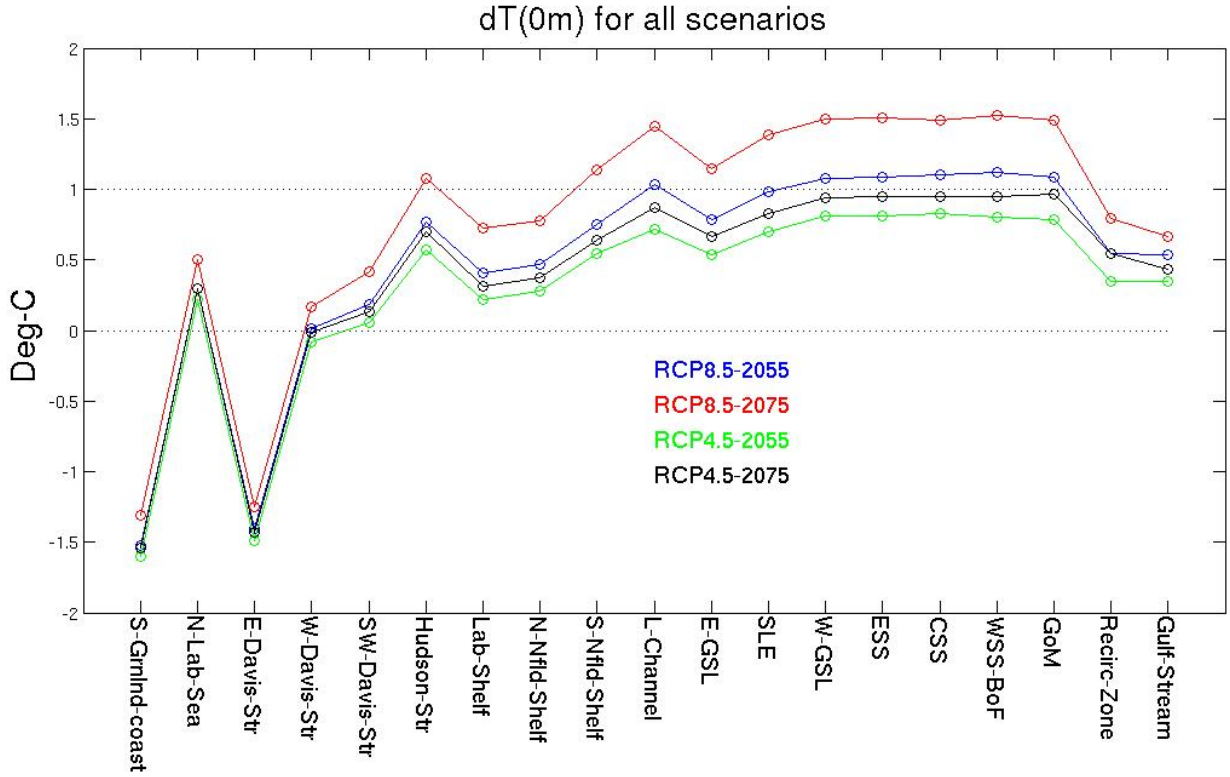

Figure 27: Predicted surface temperature changes for all regions and all scenarios. For abbreviations see table 4

.

− Average changes in **SSS** (figure 28), (outside of the Greenland shelf area), on an annual basis, for all scenarios, range from about -0.3 to -0.6PSU with lowest values in the GSL. These decreases are about 0.1-0.2PSU lower than average AOGCM results for the same period (Loder and van der Baaren, 2013) but within the range of values reported. Salinity is found to increase in the Labrador Sea, a result not reported in the AOGCM results.

• Changes in bottom T and S (tables 6, A5, A10, A15):

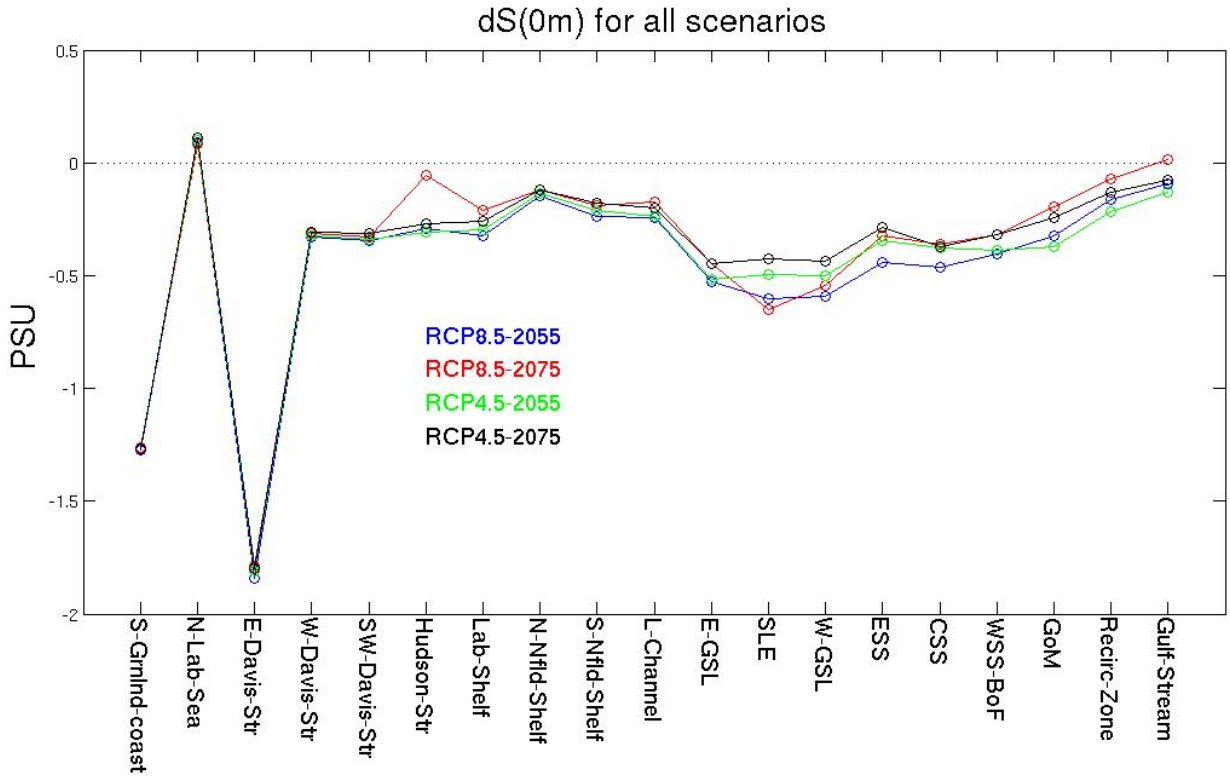

Figure 28: Predicted surface salinity changes for all regions and all scenarios.

– Bottom temperatures (figure 29), are predicted to increase over the entire shelf region except for the area affected by the Greenland glacier melt. Average increases, on an annual basis, for all scenarios except RCP8.5-2075, are about $0.5 - 1.0°$ rising to $1.0 - 1.5°$ on the Scotian Shelf and Gulf of Maine. The latter values ($\sim 1.5°$) are about $1°$ smaller than those derived from coarse resolution ocean climate models (figure A45). The RCP8.5-2075 scenario is warmer than the others by $0.1 - 0.5°$.

– Bottom salinity onshelf (figure 30), exhibits a more complicated pattern with most of the northern regions decreasing by < 0.25PSU, likely reflecting the direct effect of glacial melt being advected downstream. Salinity decreases throughout the GSL, with greatest decrease in the W-GSL, likely due to increased river runoff. Some areas increase in salinity, notably the Laurentian Channel and regions downstream toward the Gulf of Maine. This pattern supports a mechanism whereby the general tendency toward decreasing salinity due to NE-SW advection of fresh water is offset by incursions of saltier offshelf waters via deep channels – an effect that increases in the downstream

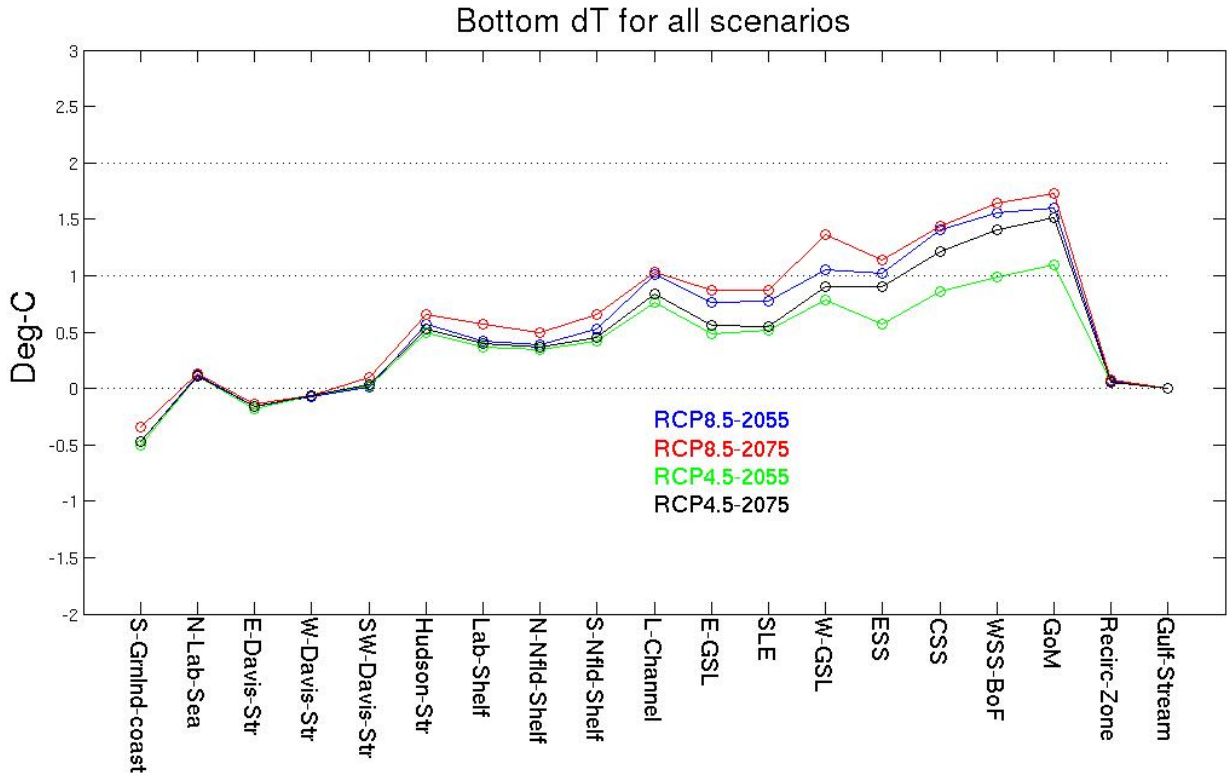

Figure 29: Predicted bottom temperature changes for all regions and all scenarios.

(i.e. southwestern) direction from the SS to the GoM. The above is another example of a result unique to a high resolution simulation – i.e. one not reported in the AOGCM results.

From the above we note that changes in temperature increase in scenario order from RCP4.5-2055, RCP4.5-2075, RCP8.5-2055, to RCP8.5-2075, but no sequential "intensity" pattern exists for salinity.

• Changes in density and stratification (tables 7, A19, A20, A21):

– Stratification (figure 31), is predicted to increase over most of the shelf regions and decrease in the northern Labrador Sea. The increase in stratification can be attributed to a greater decrease in the surface versus the 50m densities. In the Labrador Sea, circulation adjustments lead to a surface intensified *increase* in upper layer density, resulting in a *decrease* in stratification. There is little difference between the 4 scenarios except in the GSL where the RCP8.5 scenarios are predicted to be about 0.1-0.2 kg/m^3 more stratified than the RCP4.5 scenarios. Taking the present climate

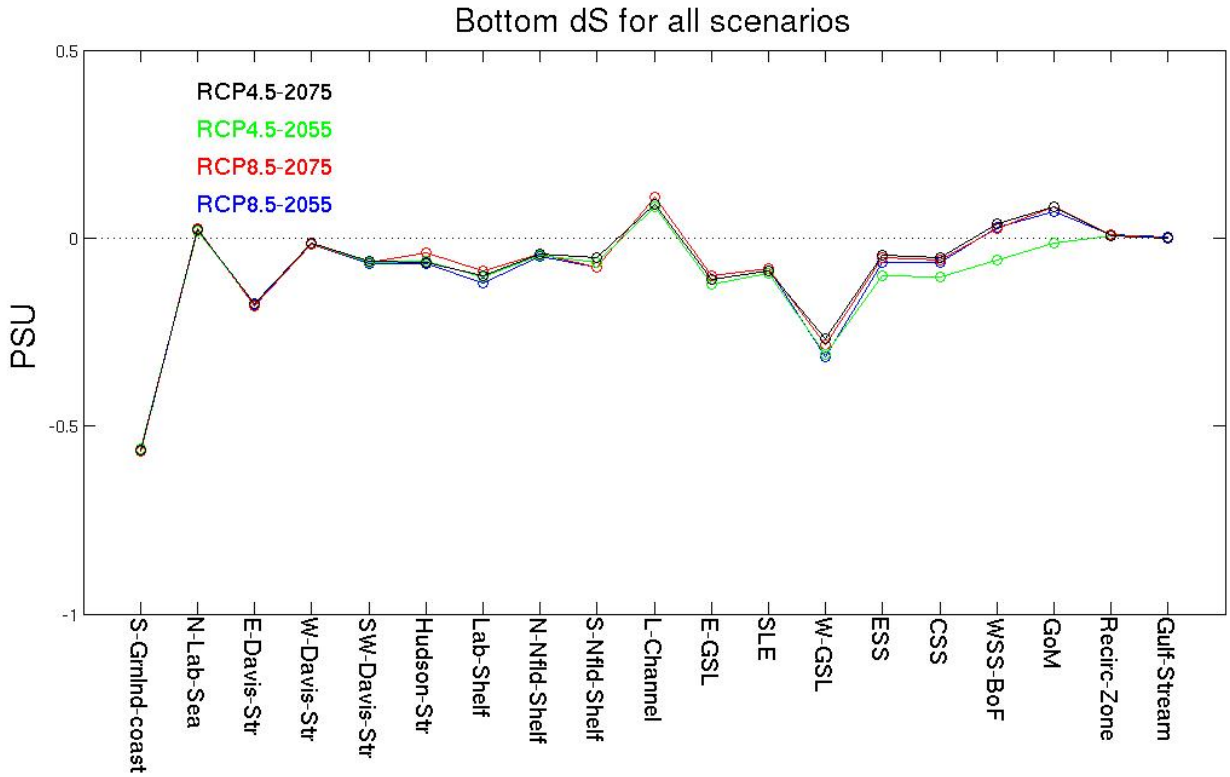

Figure 30: Predicted bottom salinity changes for all regions and all scenarios.

to be centred at 1995 the rates of increase in stratification for the Scotian Shelf/Gulf of Maine region are about 0.008 and 0.006 kg/m^4/century for 2055 and 2075 respectively with corresponding values of 0.01 and 0.009 kg/m^4/century for the GSL. This can be compared to the present climate estimates of Hebert (in Loder et al., 2013) of about 0.01-0.02 kg/m^4/century depending on series length (1951-2011 or 1979-2011). Thus the model predicts stratification trends similar to those based on the historical record.

• Changes in sea ice (figures A31 – A44; tables A22 and A23)

– Less ice production is predicted in all regions with the exception of Baffin Bay and Davis Strait, the latter due to processes associated with Greenland glacier melt and subsequent downstream advection of sea ice.

– The amount of ice in the Gulf of St.Lawrence dramatically decreases for all scenarios, particularly late season ice. However, no scenario predicts an ice-free GSL.

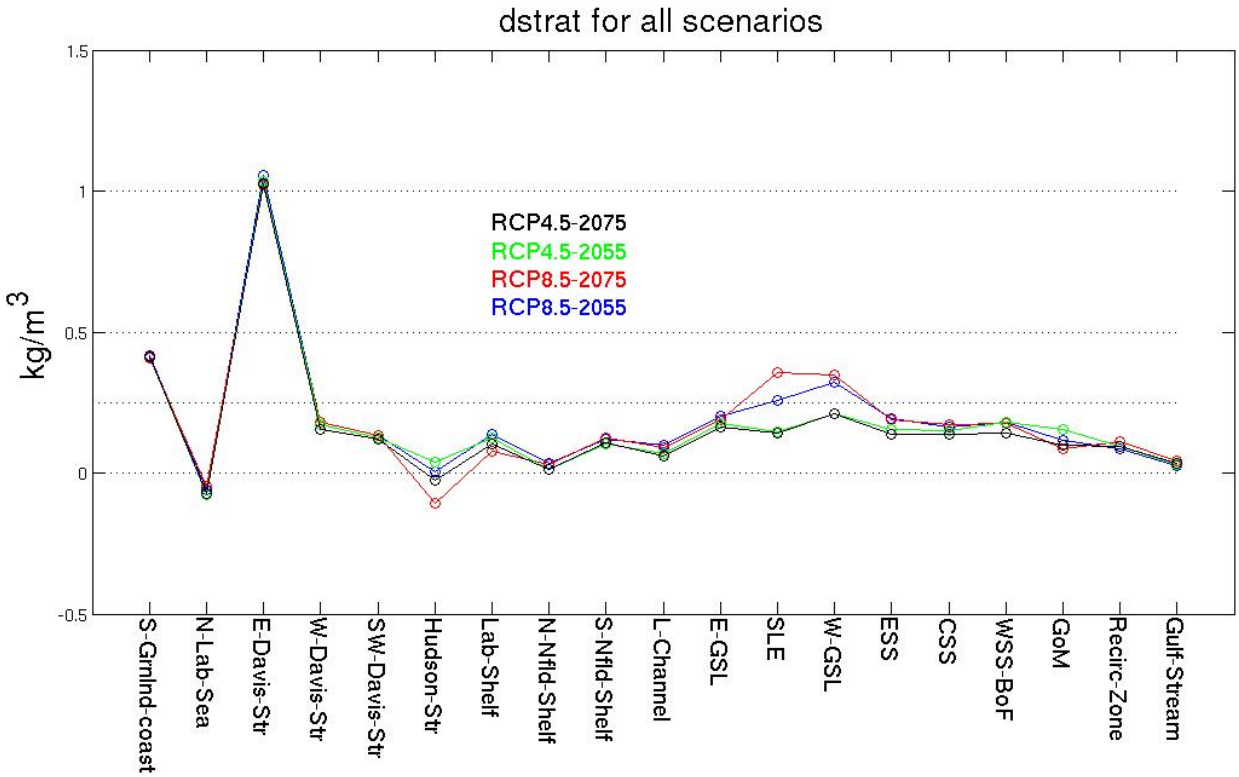

Figure 31: Predicted stratification changes for all regions and all scenarios.

– For the RCP8.5-2075 scenario all regions are almost ice free a month earlier than present climate.

• Changes in circulation: transports (table 8)

– In general, changes in transports are predicted to be small (less than 5%), except for the west Greenland shelf (∼30%) which is strongly influenced by glacier melt. Differences tend to be highest in shelfbreak flows, particularly at the tail of the Grand Banks and along the Scotian Shelf. In terms of spatial pattern, there is a general tendency in all scenarios of increased transports along the NL shelf (inshore and shelfbreak) with decreased transport into the Gulf of Maine via CSI and NEC.

Acknowledgements

The authors thank Dr. Y. Wu and Dr. B. Greenan (Fisheries and Oceans Canada, BIO) for their reviews of this report. This work received funding from the government of Canada's Aquatic Climate Change Adaptation Services Program.

Tables

Table 4: Numbers and names of regions used for bulk calculations.

Region #	Region Abbreviation	Region Name
1	S-Grnlnd-coast	south Greenland coast
2	N-Lab-Sea	north Labrador Sea
3	E-Davis-Str	east Davis Strait
4	W-Davis-Str	west Davis Strait
5	SW-Davis-Str	southwest Davis Strait
6	Hudson-Str	Hudson Strait
7	Lab-Shelf	Labrador shelf
8	N-Nfld-Shelf	north Newfoundland shelf
9	S-Nfld-Shelf	south Newfoundland shelf
10	L-Channel	Laurentian Channel
11	E-GSL	east Gulf of St. Lawrence
12	SLE	St. Lawrence Estuary
13	W-GSL	west Gulf of St. Lawrence
14	ESS	eastern Scotian shelf
15	CSS	central Scotian shelf
16	WSS-BoF	western Scotian shelf - Bay of Fundy
17	GoM	Gulf of Maine
18	Recirc-Zone	recirculation zone
19	Gulf-Stream	Gulf Stream
20	H-Bay	Hudson Bay

Table 5: Predicted changes in 0m T and S, (RCP8.5-2055)-(PC), by region, season, and on an annual basis.

	dT(°C)					**dS(PSU)**				
Region	**winter**	**spring**	**summer**	**fall**	**annual**	**winter**	**spring**	**summer**	**fall**	**annual**
S-Grnlnd-coast	-0.931	-1.479	-2.365	-1.314	-1.523	-0.598	-0.947	-2.460	-1.084	-1.272
N-Lab-Sea	0.132	0.136	0.404	0.526	0.300	-0.049	0.063	0.252	0.091	0.089
E-Davis-Str	-0.017	-1.690	-3.034	-0.873	-1.403	-0.780	-1.511	-3.467	-1.599	-1.839
W-Davis-Str	-0.017	-0.234	0.258	0.060	0.017	-0.389	-0.290	-0.100	-0.532	-0.328
SW-Davis-Str	-0.050	-0.044	0.467	0.378	0.188	-0.366	-0.548	-0.283	-0.179	-0.344
Hudson-Str	0.032	0.699	1.558	0.785	0.769	-0.281	-0.489	-0.152	-0.249	-0.293
Lab-Shelf	0.006	0.398	0.687	0.525	0.404	-0.257	-0.383	-0.319	-0.339	-0.324
N-Nfld-Shelf	0.375	0.541	0.368	0.595	0.470	-0.219	-0.147	0.005	-0.226	-0.147
S-Nfld-Shelf	0.735	0.840	0.713	0.716	0.751	-0.313	-0.277	-0.176	-0.192	-0.240
L-Channel	1.101	1.285	0.857	0.906	1.037	-0.332	-0.187	-0.210	-0.239	-0.242
E-GSL	0.443	1.138	0.763	0.797	0.785	-0.542	-0.554	-0.600	-0.418	-0.529
SLE	0.461	1.457	1.057	0.969	0.986	-0.670	-0.444	-0.780	-0.521	-0.604
W-GSL	0.703	1.510	0.957	1.131	1.075	-0.671	-0.597	-0.529	-0.561	-0.589
ESS	1.201	1.217	0.904	1.013	1.084	-0.370	-0.530	-0.403	-0.455	-0.439
CSS	1.192	1.149	0.896	1.162	1.100	-0.432	-0.483	-0.498	-0.444	-0.464
WSS-BoF	1.219	1.219	0.957	1.071	1.117	-0.390	-0.466	-0.467	-0.297	-0.405
GoM	1.212	1.126	0.892	1.129	1.090	-0.250	-0.362	-0.409	-0.269	-0.322
Recirc-Zone	0.493	0.546	0.522	0.612	0.543	-0.210	-0.172	-0.167	-0.105	-0.164
Gulf-Stream	0.412	0.562	0.578	0.578	0.533	-0.098	-0.072	-0.110	-0.089	-0.092
H-Bay	0.031	0.945	1.397	0.838	0.803	-0.364	-0.393	0.004	-0.170	-0.231

Table 6: Predicted changes in bottom T and S, (RCP8.5-2055)-(PC), by region, season, and on an annual basis.

	dT(°C)					**dS(PSU)**				
Region	**winter**	**spring**	**summer**	**fall**	**annual**	**winter**	**spring**	**summer**	**fall**	**annual**
S-Grnlnd-coast	0.038	-0.506	-1.069	-0.335	-0.468	-0.347	-0.430	-0.948	-0.543	-0.567
N-Lab-Sea	0.087	0.156	0.131	0.099	0.118	0.018	0.029	0.022	0.017	0.022
E-Davis-Str	-0.029	-0.070	-0.249	-0.273	-0.155	-0.131	-0.116	-0.211	-0.249	-0.177
W-Davis-Str	-0.038	-0.044	-0.088	-0.115	-0.071	-0.017	-0.012	-0.012	-0.021	-0.016
SW-Davis-Str	-0.054	0.148	0.038	-0.065	0.017	-0.082	-0.064	-0.061	-0.072	-0.070
Hudson-Str	0.468	0.553	0.661	0.585	0.567	-0.051	-0.089	-0.069	-0.069	-0.069
Lab-Shelf	0.312	0.484	0.504	0.396	0.424	-0.118	-0.163	-0.089	-0.105	-0.119
N-Nfld-Shelf	0.376	0.382	0.364	0.437	0.390	-0.050	-0.050	-0.055	-0.034	-0.047
S-Nfld-Shelf	0.561	0.612	0.489	0.442	0.526	-0.102	-0.058	-0.063	-0.086	-0.077
L-Channel	0.999	1.019	1.015	0.984	1.004	0.106	0.109	0.111	0.114	0.110
E-GSL	0.720	0.822	0.728	0.774	0.761	-0.147	-0.127	-0.067	-0.063	-0.101
SLE	0.683	0.845	0.802	0.786	0.779	-0.147	-0.101	-0.043	-0.033	-0.081
W-GSL	0.959	1.309	0.962	0.976	1.051	-0.429	-0.360	-0.254	-0.221	-0.316
ESS	0.931	1.043	1.077	1.036	1.022	-0.074	-0.090	-0.048	-0.043	-0.064
CSS	1.391	1.353	1.299	1.603	1.412	-0.050	-0.090	-0.065	-0.053	-0.064
WSS-BoF	1.585	1.605	1.472	1.579	1.560	0.020	-0.002	0.010	0.083	0.028
GoM	1.668	1.572	1.493	1.662	1.599	0.076	0.034	0.050	0.115	0.069
Recirc-Zone	0.077	0.071	0.060	0.063	0.068	0.009	0.007	0.007	0.008	0.008
Gulf-Stream	0.006	0.005	0.005	0.007	0.006	0.001	0.001	0.001	0.001	0.001
H-Bay	0.515	0.663	0.769	0.705	0.663	-0.148	-0.169	-0.110	-0.136	-0.141

Table 7: Predicted changes in 50m-0m stratification, (RCP8.5-2055)-(PC), by region, season, and on an annual basis. The units are kg·m^{-3}.

Region	**winter**	**spring**	**summer**	**fall**	**annual**
S-Grnlnd-coast	0.149	0.364	0.898	0.249	0.415
N-Lab-Sea	0.025	-0.042	-0.167	-0.064	-0.062
E-Davis-Str	0.342	0.898	2.185	0.797	1.056
W-Davis-Str	0.091	0.151	0.101	0.370	0.178
SW-Davis-Str	0.032	0.239	0.193	0.063	0.132
Hudson-Str	-0.025	0.119	-0.059	-0.024	0.003
Lab-Shelf	0.090	0.131	0.144	0.181	0.137
N-Nfld-Shelf	0.106	0.049	-0.098	0.077	0.034
S-Nfld-Shelf	0.114	0.147	0.138	0.087	0.122
L-Channel	0.124	0.078	0.108	0.090	0.100
E-GSL	0.119	0.206	0.321	0.156	0.200
SLE	0.233	0.073	0.478	0.249	0.258
W-GSL	0.264	0.332	0.352	0.340	0.322
ESS	0.108	0.241	0.223	0.204	0.194
CSS	0.108	0.195	0.244	0.111	0.164
WSS-BoF	0.118	0.226	0.270	0.104	0.180
GoM	0.014	0.161	0.215	0.069	0.115
Recirc-Zone	0.089	0.079	0.124	0.055	0.087
Gulf-Stream	0.006	0.012	0.057	0.024	0.025
H-Bay	0.071	0.128	-0.100	-0.075	0.006

Table 8: Predicted fractional changes in transport (Γ(F)-Γ(PC))/Γ(PC) through various subsections, for the 2 RCPs and 2 future periods. Negative values denote a decrease in transport. AR7W:w-GL-coast denotes the west Greenland coastal region of the AR7W line. AR7W:w-GL-shelf denotes the region of the (eastern) AR7W line from the shelf slope to the west Greenland coastline. Fp:sb denotes the southward flow through Flemish Pass. See table 3 for other abbreviations.

Section	**(RCP-8.5: 2055)**	**(RCP-8.5: 2075)**	**(RCP-4.5: 2055)**	**(RCP-4.5: 2075)**
AR7W-east:w-GL-coast	0.306	0.293	0.292	0.299
AR7W-east:w-GL	0.034	0.014	0.049	0.049
Seal-I:inner	0.041	0.042	0.043	0.050
Seal-I:outer	0.048	0.036	0.052	0.052
SBI:net	-0.045	-0.047	-0.044	-0.016
BV:inner	0.023	0.008	0.049	0.035
BV:outer	0.081	0.083	0.088	0.089
F-cap:Fp:+ve	0.020	0.016	0.021	0.038
F-cap:shf:inner	0.002	0.010	0.028	0.038
se-GB:sb	-0.038	-0.199	-0.069	0.004
se-GB:inner	-0.001	0.011	0.025	0.037
CS:inflow	0.050	-0.021	-0.012	0.023
CS:outflow	0.028	-0.023	-0.014	0.016
CS:net	-0.036	-0.031	-0.019	-0.002
Lb:inner	-0.067	-0.048	0.005	-0.004
Lb:outer	-0.188	-0.192	-0.184	-0.171
Hfx:inner	-0.107	-0.094	-0.030	-0.073
Hfx:outer	-0.101	-0.125	-0.079	-0.098
CSI:inner	-0.242	-0.156	-0.073	-0.144
NEC:inflow	-0.074	-0.026	-0.056	-0.037
NEC:outflow	-0.155	-0.103	-0.082	-0.058

References

Arora, V. K., J. F. Scinocca, G. J. Boer, J. R. Christian, K. L. Denman, G. M. Flato, V. V. Kharin, W. G. Lee, and W. J. Merryfield (2011). Carbon emission limits required to satisfy future representative concentration pathways of greenhouse gases. Geophys. Res. Lett., 38(5), L05805, doi:10.1029/2010GL046270.

Bamber, J., M. den Broeke, J. Ettema, J. Lenaerts, and E. Rignot (2012). Recent large increases in freshwater fluxes from Greenland into the North Atlantic. Geophysical Research Letters, 39(19).

Barnier, B. and 9 others (2006). Impact of partial steps and momentum advection schemes in a global ocean circulation model at eddy permitting resolution. *Ocean Dynamics*, **56**: 543-567. doi:10.1007/s10236- 006-0082-1.

Booth, B. B. B., N. J. Dunstone, P. R. Halloran, T. Andrews, and N. Bellouin (2012). Aerosols implicated as a prime driver of twentieth-century North Atlantic climate variability. Nature, 484(7393): 228-232, doi:10.1038/nature10946.

Brickman D., Z. Wang, and B. DeTracey (2015). Variability in current streams in Atlantic Canadian waters: a model study. Atmosphere-Ocean, in press. doi:10.1080/07055900.2015.1094026

Brovkin, V., L. Boysen, T. Raddatz, V. Gayler, A. Loew, and M. Claussen (2012). Evaluation of vegetation cover and land-surface albedo in MPI-ESM CMIP5 simulations. J. Adv. Model. Earth Syst., 5: 48-57, doi:10.1029/2012MS000169.

Chassé J., W. Perrie, Z. Long, D. Brickman, L. Guo and N. Lambert (2014). Regional atmosphere-ocean-ice climate downscaling results for the Gulf of St. Lawrence using the DFO Regional Climate Downscaling System. Can. Tech. Rep. Hydrogr. Ocean Sci. (under revision)

Chassé, J., N. Lambert and D. Lavoie (2013). Precipitation, Evaporation and Freshwater Flux over Canada from six Global Climate Models. Can. Tech. Rep. Hydrogr. Ocean Sci. 287: viii

+ 47 p.

CLIVAR Exchanges No. 65, Vol. 19, No. 2, July 2014 Available at: http://www.clivar.org/publications/exchanges

CORDEX. Coordinated Regional Climate Downscaling Experiment http://wcrp-cordex.ipsl.jussieu.fr/

Diffenbaugh, N. S. and F. Giorgi (2012). Climate change hotspots in the CMIP5 global climate model ensemble. Climatic Change 114:813822. doi 10.1007/s10584-012-0570-x

Dunne, J. P., J. G. John, A. J. Adcroft, S. M. Griffies, R. W. Hallberg, E. Shevliakova, R. J. Stouffer, W. Cooke, K. A. Dunne, M. J. Harrison, J. P. Krasting, S. L. Malyshev, P. C. D. Milly, P. J. Phillipps, L. T. Sentman, B. L. Samuels, M. J. Spelman, M. Winton, A. T. Wittenberg, and N. Zadeh (2012). GFDLs ESM2 Global Coupled ClimateCarbon Earth System Models. Part I: Physical Formulation and Baseline Simulation Characteristics. J. Clim., 25: 66466665, doi:10.1175/JCLI-D-11-00560.

Ferry, N., L. Parent, G. Garric, B. Barnier, N. C. Jourdain and the Mercator Ocean team (2010). Mercator global eddy permitting ocean reanalysis GLORYS1V1: Description and results. Mercator Quarterly Newsletter 36, January 2010.

Fichefet, T. and M. A. Morales Maqueda (1997). Sensitivity of a global sea ice model to the treatment of ice thermodynamics and dynamics, J. Geophys. Res., 102, 12609-12646, doi:10.1029/97JC00480.

Fox-Kemper B., S. Bachman, B. Pearson, and S. Reckinger (2014). Principles and advances in subgrid modelling for eddy- rich simulations. In CLIVAR Exchanges No. 65, Vol. 19, No. 2, July 2014

Gerdes, R., W. Hurlin, and S.M. Griffies (2006). Sensitivity of a global ocean model to increased run-off from Greenland. Ocean Modelling, 12(3), 416-435.

Greene, C. H. and A. J. Pershing (2003). The flip-side of the North Atlantic Oscillation and modal shifts in slope-water circulation patterns. Limnology and oceanography 48.1:319-322.

Griffies, S., and Coauthors, 2009, Coordinated ocean-ice reference experiments (COREs). Ocean Modell., 26, 1 - 46.

IPCC (2013). Climate Change 2013: The Physical Science Basis. Contribution of Working Group I to the Fifth Assessment Report of the Intergovernmental Panel on Climate Change [Stocker, T.F., D. Qin, G.-K. Plattner, M. Tignor, S.K. Allen, J. Boschung, A. Nauels, Y. Xia, V. Bex and P.M. Midgley (eds.)]. Cambridge University Press, Cambridge, United Kingdom and New York, NY, USA, 1535 pp.

Jungclaus, J. H., H. Haak, M. Esch, E. Roeckner, and J. Marotzke (2006). Will Greenland melting halt the thermohaline circulation?. Geophysical Research Letters, 33(17).

Kara, A. B., A. J. Walcraft and H. E. Hurlburt (2007). A correction for land contamination of atmospheric variables near land-sea boundaries, J. Phys. Oceanogr., 37: 803-818, doi:10.1175/JPO2984.1.

Lambert, N., J. Chassé, W. Perrie, Z. Long, L. Guo, and J. Morrison (2013). Projection of future river runoffs in Eastern Atlantic Canada from Global and Regional climate models. Can. Tech. Rep. Hydrogr. and Ocean. Sci. 288: viii + 34 p.

Large, W. and S. Yeager (2004). Diurnal to decadal global forcing for ocean and sea-ice models: the data sets and flux climatologies. CGD Division of the National Center for Atmospheric Research, NCAR Technical Note: NCAR/TN-460+STR.

Lavoie, D., N. Lambert, S. ben Mustafa, and A. van der Baaren (2013). Projections of future physical and biogeochemical conditions in the Northwest Atlantic from CMIP5 Global Climate Models, Can. Tech. Rep. Hydrog. Ocean. Sci. 285: xiv + 156 p.

Lavoie, D. and N. Lambert (2013). Projections of future physical and biogeochemical conditions in Hudson and Baffin Bays CMIP5 Global Climate Models, Can. Tech. Rep. Hydrog. Ocean.

Sci. 289: xiii + 129 p.

Loder, J and A. van der Baaren (2013). Climate change projections for the Northwest Atlantic from six CMIP5 Earth System Models, Can. Tech. Rep. Ocean. Hydrogr. Sci. 286: xiv + 112 p.

Loder, J.W., G. Han, P.S. Galbraith, J. Chassé, and A. van der Baaren (Eds.). 2013. Aspects of climate change in the Northwest Atlantic off Canada. Can. Tech. Rep. Fish. Aquat. Sci. 3045: x + 190 p.

Madec G. (2008). NEMO ocean engine. Note du Pole de modélisation, Institut Pierre-Simon Laplace (IPSL), France, No 27 ISSN No 1288-1619.

Magnusdottir, G., C. Deser, and R. Saravanan (2004). The Effects of North Atlantic SST and Sea Ice Anomalies on the Winter Circulation in CCM3. Part I: Main Features and Storm Track Characteristics of the Response J. Climate V.17 #5 857-876

Marti, O., P. Braconnot, J.-L. Dufresne, J. Bellier, R. Benshila, S. Bony, P. Brockmann, P. Cadule, A. Caubel, F. Codron, N. de Noblet, S. Denvil, L. Fairhead, T. Fichefet, M.-A. Foujols, P. Friedlingstein, H. Goosse, J.-Y. Grandpeix, E. Guilyardi, F. Hourdin, A. Idelkadi, M. Kageyama, G. Krinner, C. Lvy, G. Madec, J. Mignot, I. Musat, D. Swingedouw, and C. Talandier (2010). Key features of the IPSL ocean atmosphere model and its sensitivity to atmospheric resolution. Clim. Dyn., 34(1): 1-26, doi:10.1007/s00382-009-0640-6.

Miller, A. J, D. R. Cayan, T. P. Barnett, N. E. Graham, and J. M. Oberhuber (1994). Interdecadal variability of the Pacific Ocean: model response to observed heat flux and wind stress anomalies Climate Dynamics 9:287-302

Ming, J., and T. M. Smith (1995). Ocean model response to temperature data assimilation and varying surface wind stress: Intercomparisons and implications for climate forecast. Monthly weather review 123.6 (1995): 1811-1821.

NARCCAP, North American Regional Climate Change Assessment Program. http://www.narccap.ucar.edu/

Petrie, B. (2007). Does the North Atlantic Oscillation Affect Hydrographic Properties on the Canadian Atlantic Continental Shelf? Atmosphere-Ocean, **V45(3)**, 141-151.

Press, W. H., B. P. Flannery, S. A. Teukolsky, and W. T. Vettering. (1986). Numerical Recipes, Cambridge Univ. Press, New York.

Rignot, E., I. Velicogna, M. R. Van den Broeke, A. Monaghan, and J. T. M. Lenaerts (2011). Acceleration of the contribution of the Greenland and Antarctic ice sheets to sea level rise. Geophysical Research Letters, 38(5).

Schubert, S. D., and 32 others (2009). A U.S. CLIVAR Project to Assess and Compare the Responses of Global Climate Models to Drought-Related SST Forcing Patterns: Overview and Results. Journal of Climate, 22(19), 5251-5272. doi: 10.1175/2009JCLI3060.1

Somot, S., E. F. Sevault, and E. M. Deque (2006). Transient climate change scenario simulation of the Mediterranean Sea for the twenty-first century using a high-resolution ocean circulation model. Clim Dyn (2006) 27:851879 DOI 10.1007/s00382-006-0167-z

Stouffer, R. J., J. Yin, J. M. Gregory, K. W. Dixon, M. J. Spelman, W. Hurlin, A. J. Weaver, M. Eby, G. M. Flato, H. Hasumi, A. Hu, J. H. Jungclaus, I. V. Kamenkovich, A. Levermann, M. Montoya, S. Murakami, S. Nawrath, A. Oka, W. R. Peltier, D. Y. Robitaille, A. Sokolov, G. Vettoretti, and S. L. Weber (2006). Investigating the Causes of the Response of the Thermohaline Circulation to Past and Future Climate Changes. J. Climate, 19, 13651387.

Taylor, K. E., R. J. Stouffer, and G. A. Meehl (2012). An overview of CMIP5 and the experiment design, Bull. Amer. Meteor. Soc., 93: 485-498, doi:10.1175/BAMS-D-11-00094.1.

Visbeck, M., H. Cullen, G. Krahmann, and N. Naik (1998). An ocean model's response to North Atlantic Oscillations-like wind forcing Geophysical Research Letters, Vol. 25, No.24, 4521-4524.

Watanabe, S., T. Hajima, K. Sudo, T. Nagashima, T. Takemura, H. Okajima, T. Nozawa,H. Kawase, M. Abe, T. Yokohata, T. Ise, H. Sato, E. Kato, K. Takata, S. Emori, and M. Kawamiya (2011). MIROC-ESM 2010: model description and basic results of CMIP5-20c3m experiments, Geosci. Model Dev., 4: 845-872, doi:10.5194/gmd-4-845-2011.

Weijer, W., M. E. Maltrud, M. W. Hecht, H. A. Dijkstra, and M.A. Kliphuis (2012). Response of the Atlantic Ocean circulation to Greenland Ice Sheet melting in a stronglyeddying ocean model. Geophysical Research Letters, 39(9).

Zebiak, S. E., and M. A. Cane (1987). A Model El Niño-Southern Oscillation. Monthly Weather Review 115.10: 2262-2278.

Appendix: A – Model Equilibration

One of the main objectives of this project was to produce present and future climatologies from which difference fields of various ocean variables could be computed. Areas of the ocean where the simulations do not achieve an equilibrium (i.e. there is still significant interannual variability) are regions where there is less confidence in the model results.

The questions of the definition of equilibrium and the model run length required to achieve this have no simple answers. This fact, combined with the large volume of model output, makes it difficult to produce a simple quantitative summary of this investigation. Thus our analyses will be more qualitative, designed to highlight aspects of the model's approach to equilibrium that are likely relevant to any model being run in climatology mode, and to identify where the model's continued interannual variability affects the reliability of its predictions. It is noted that this presentation is not meant to be exhaustive, but rather to give readers a sense of the type of analyses that were undertaken.

To simplify comparisons and eliminate seasonal effects, all data used in this section were layer and annually averaged. The future climate scenario chosen for comparison was RCP8.5-2055. To illustrate the model's approach to equilibrium, profiles of TS data, for the present and future climates, were extracted at a number of onshelf locations. Due to the large data volume, only 13 of the 20 years of data (the last 8 and 5 other years) were analyzed. An example, exhibiting typical onshelf behaviour, is taken from the ∼150m isobath along the AR7W line on the southern Labrador Shelf (figure 32, and see figure 25 for the location). It can be seen that the model approaches a reasonable equilibrium in 20 years, and that there is a clear distinction between the present and future climates at all levels. In this example it is reasonable to be confident that these differences are significant. A worse case example (figure 33) comes from the Northeast Channel (see figure 25) – a location where offshelf waters enter the Gulf of Maine. In this case there is more interannual variability evident in the last 8 years of the series. For temperature it is still reasonable to conclude that the future climate will be warmer than the present climate although there would be less confidence in the magnitude of the differences. For salinity the top 50m are clearly predicted to be fresher in 2055, but this signal changes sign with depth, with no change in the 50-100m layer and the 100-300m layer being saltier with high variability. The NEC profile

highlights that water column properties are a combination of direct surface forcing and horizontal advective effects. The former decrease with depth in the water column, allowing the latter to increase in importance. Advective effects are most noticible in regions where offshelf waters (with different properties) penetrate onshelf regions. When considering model equilibration these deep offshelf waters can maintain high variability for long timescales so places where they penetrate onshelf can be regions where the model predictions are less reliable.

The above examples provide an overall picture of the types of results observed but represent a small sample size upon which to base conclusions. To increase the sample size we performed 2 analyses, both using the annual and layer-averaged TS data described above.

The TS timeseries plots suggest a simple probabilistic analysis which could be used to assess the reliability of the model's predictions. The idea is to use the last 5 years of the timeseries to assess the chance of being (e.g.) saltier in the future. So, for the NEC (figure 33), one would say that the top 50m have a 10-out-of-10 chance of being fresher, while the 50-100m layer has a 3-out-of-5 chance of being fresher, etc. The former case could be considered a highly certain result, while the latter would indicate essentially no change predicted by the model. For a single grid cell this "N=5" sample size is small, but computing this for all grid cells increases the confidence over larger spatial regions. Figures 34 and 35 show the results for various TS layers. In these figures, a positive probability indicates a warmer/saltier future climate while a negative probability indicates a colder/fresher prediction.

The 0-25m layer (figure 34, top) is indicative of the top 50m of the water column. It can be seen that the probability pattern is similar to the general TS change pattern shown in figure 12, thus supporting high confidence in the model results. Similarly the bottom TS change shown in figure 18 is highly probable almost everywhere onshelf including the deep basins (figure 34, bottom). The situation is different at intermediate depths. For example, the predicted T change in the 100-150m layer (figure 35) is highly likely but the S change indicates low confidence in the results up the Laurentian Channel into the GSL, and along the shelfbreak of the northern Newfoundland Shelf. The above plots in general highlight that temperature changes are more certain than salinity, likely reflecting a stronger surface forcing for temperature changes than salinity.

In the other analysis we grouped the model data based on the 19 regions described in section 4 (see figure 11). For each grid cell in a region, and for each of the last 5 years of the model run, we computed the pair-wise future minus present climate T (and S) differences, and investigated the null hypothesis that if the two climate states were the same then the histogram of the differences would be a zero mean normal distribution. The Kolmogorov-Smirnov test was used in an iterative procedure to determine whether the null hypothesis held (see Numerical Recipes, Press et al., 1986). To illustrate the results we choose the Laurentian Channel box identified above as a region in which the model's results are problematic. Figure 36 shows the results for 2 TS layers. The histograms for the 0-25m layer are clearly not $N(0, \sigma)$, and confirm the predicted warm, fresh change seen in figure 34 for the 0-25m layer. Similarly, the histograms for the 150-300m layer are consistent with the predicted warm, salty change seen in figure 34 for the bottom layer. The histograms for the 100-150m layer (figure 37) have a more complicated structure. The temperature change histogram supports an increase in temperature for the region, but the salinity change histogram has a bimodal structure with a peak near zero. This suggests the existence of a subset of grid cells where the future climate may be indistinguishable from the present. We consider that this analysis generally supports the conclusions based on figures 34 and 35.

From the two analyses above we conclude that caution should be exercised when considering model predictions for intermediate layers (50-150m) in regions where offshelf waters penetrate onshelf through deep channels. Key examples are the Laurentian Channel, which feeds the deep GSL, and the Northeast Channel which feeds the deep GoM.

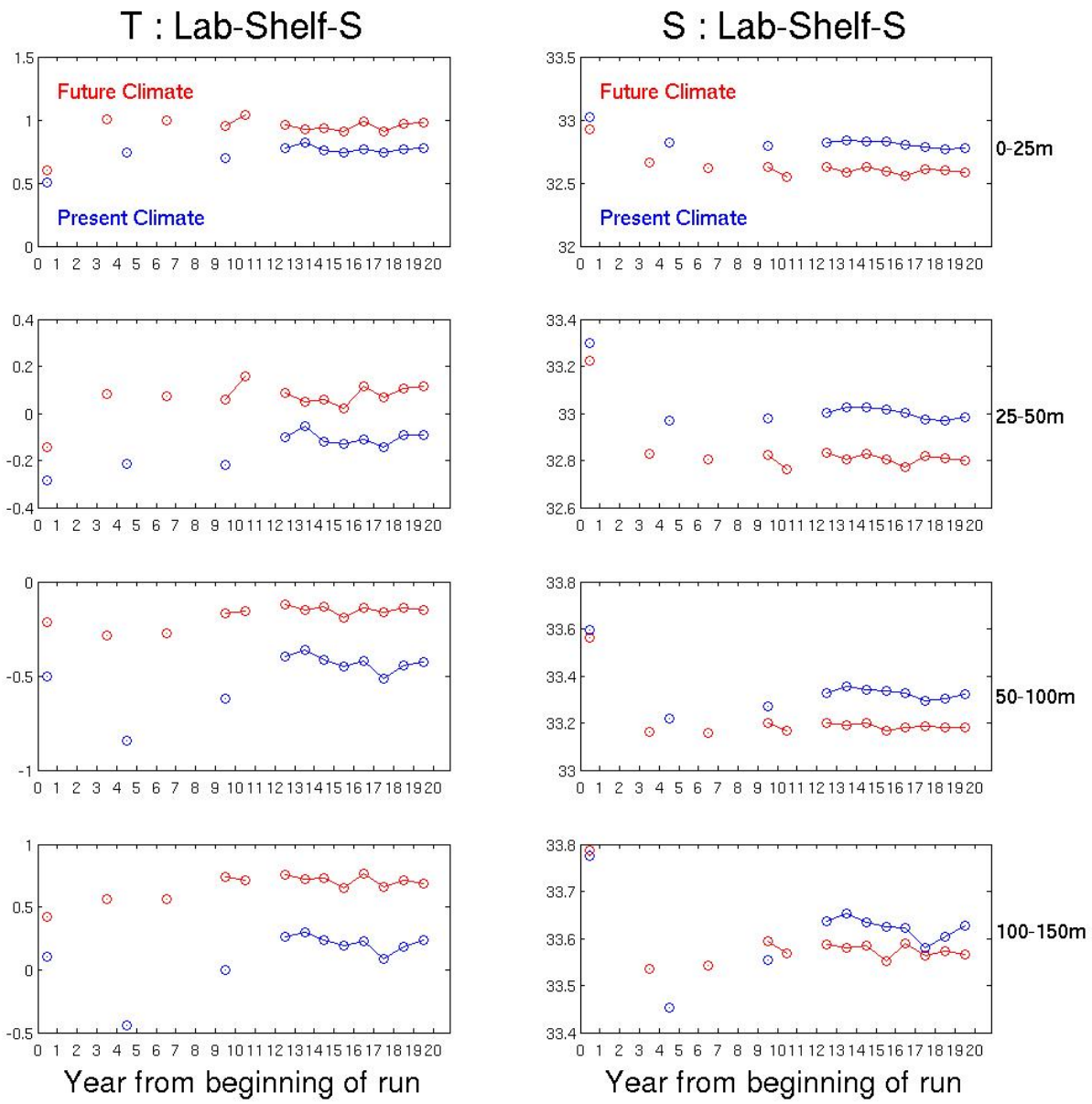

Figure 32: Future (red) and present (blue) climate timeseries of T and S in various layers, for a location along the AR7W line on the southern Labrador Shelf.

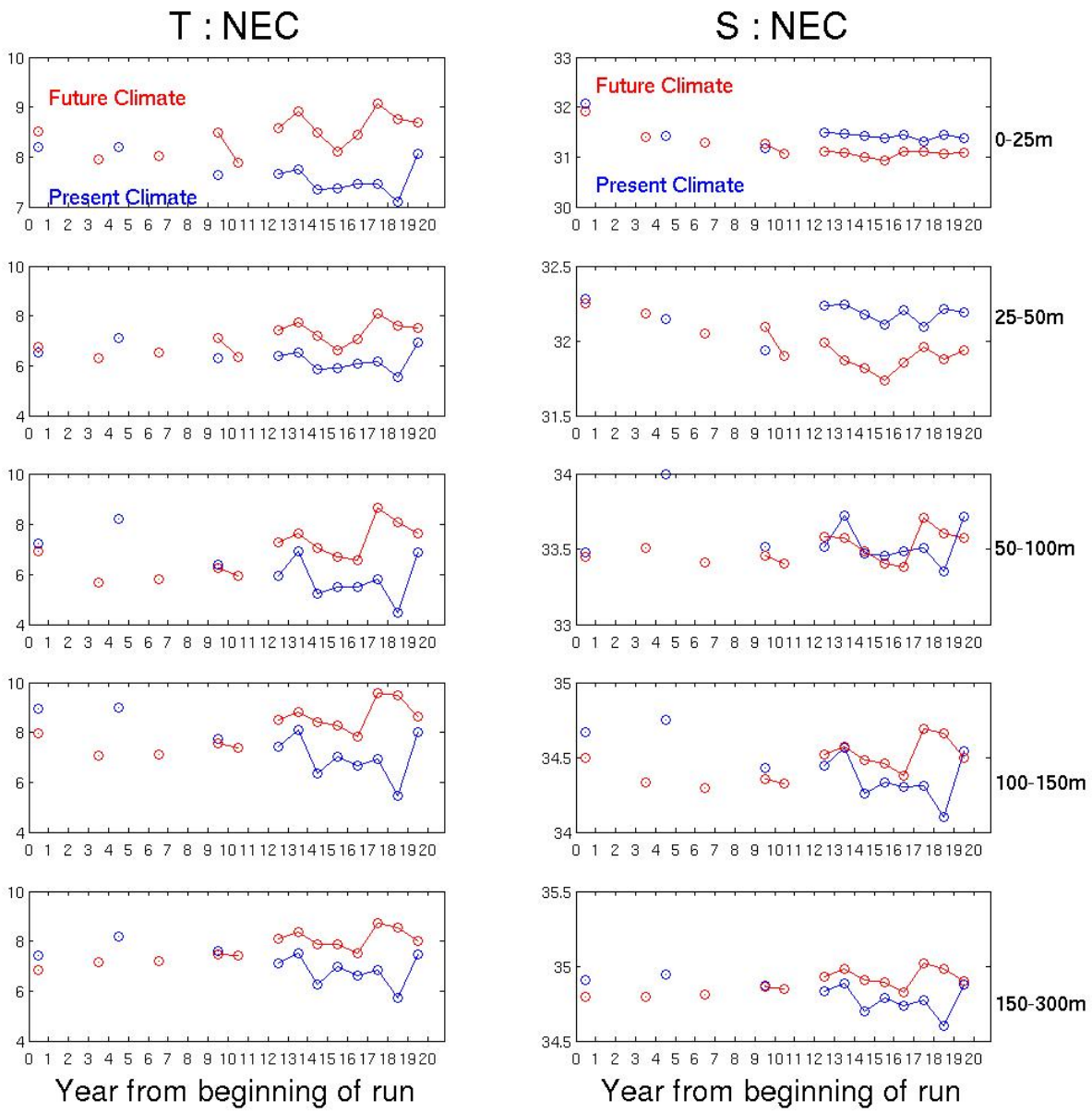

Figure 33: Future (red) and present (blue) climate timeseries of T and S in various layers, for a location in NEC.

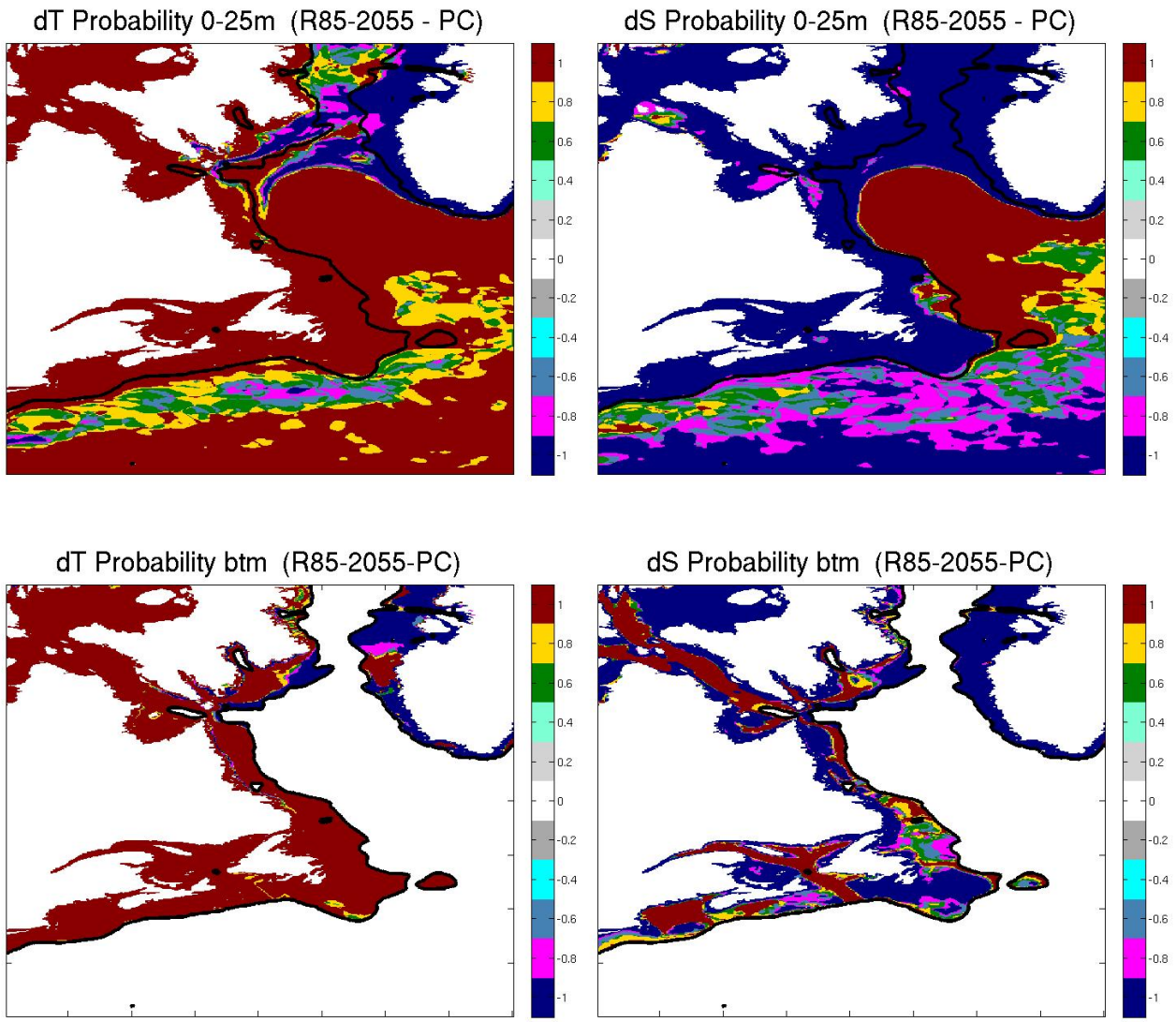

Figure 34: Probability of T and S changes for the 0-25m layer (top panel), and for the bottom layer (bottom panel). P>0 implies future warmer/saltier than present climate, and vice versa. Due to the nature of the calculation, the only possible values are ±(0.6,0.8,1.0). The thick black line is the 500m isobath.

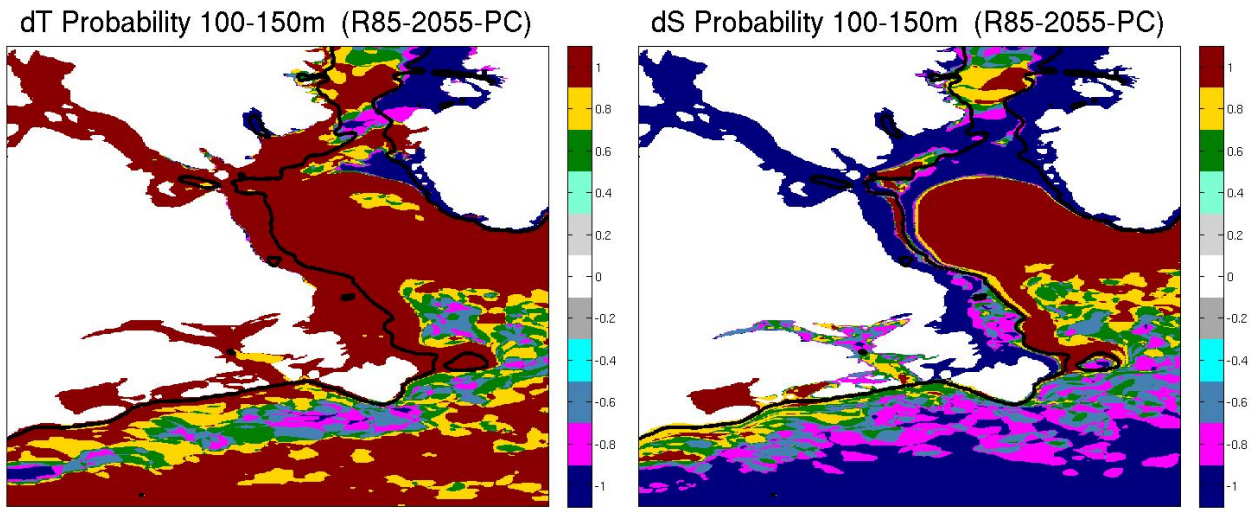

Figure 35: Probability of T and S changes for the 100-150m layer. P>0 implies future warmer/saltier than present climate, and vice versa. Due to the nature of the calculation, the only possible values are ±(0.6,0.8,1.0). The thick black line is the 500m isobath.

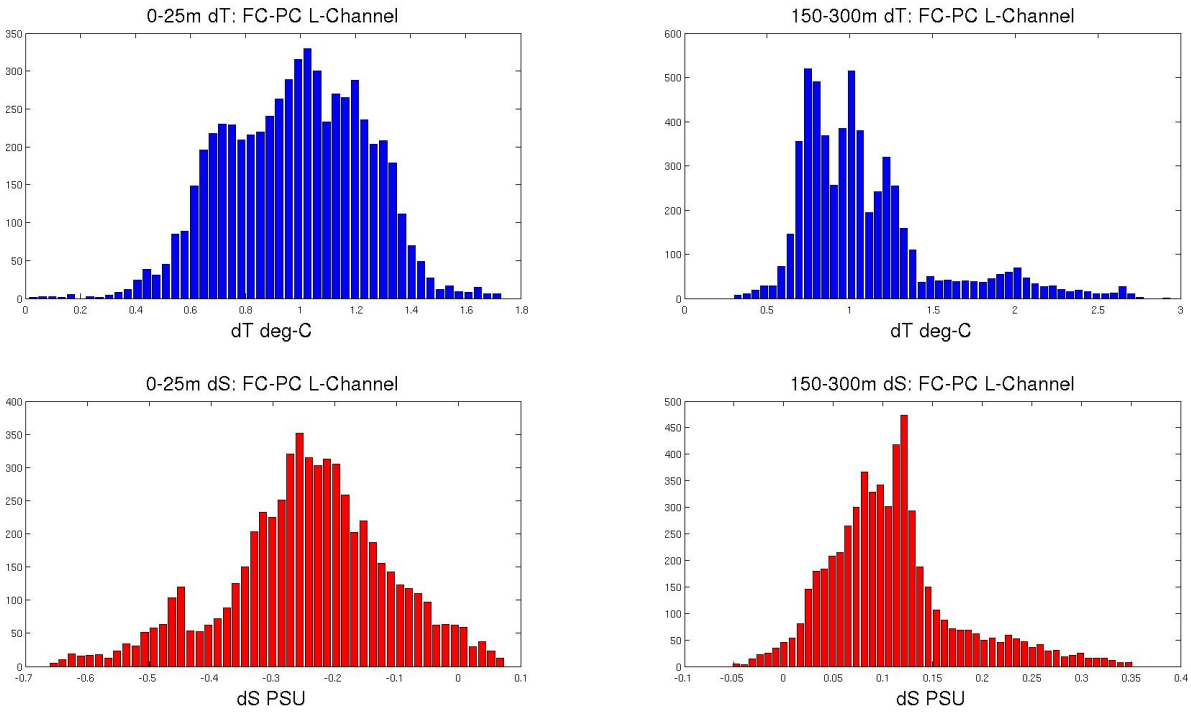

(a) (b)

Figure 36: (RCP8.5-2055) - present climate dT, dS histograms for the (a) 0-25m and (b) 150-300m layers from the Laurentian Channel box.

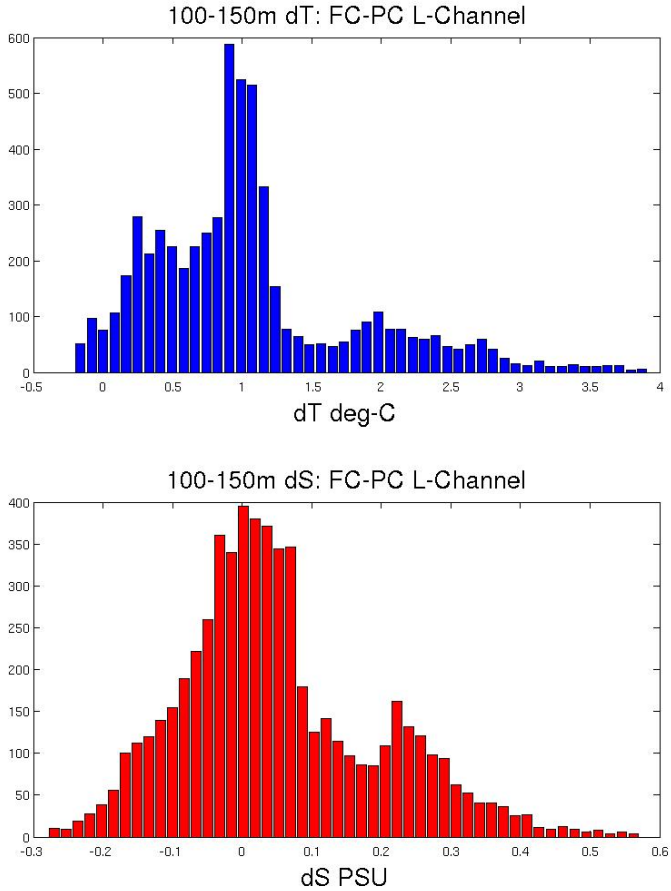

Figure 37: (RCP8.5-2055) - present climate dT, dS histograms for the 100-150m layer from the Laurentian Channel box.

Appendix: B

Supplementary figures and tables

Results for RCP 8.5 – 2055 Climatology

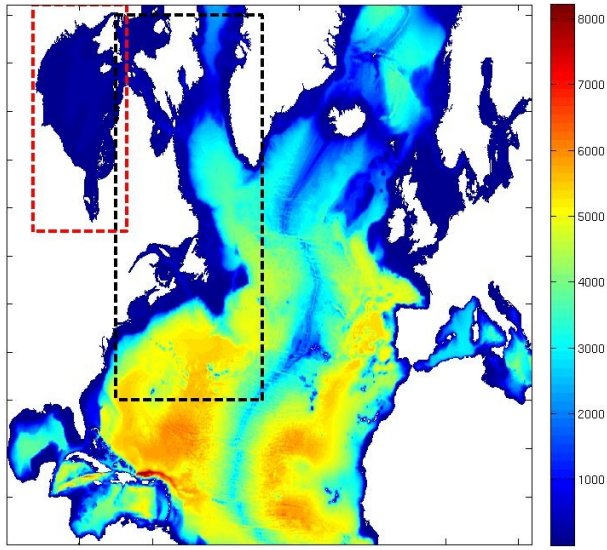

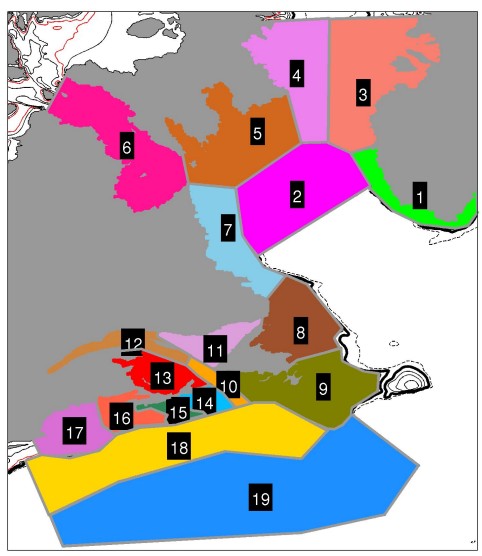

Reminder of model domains and regions used for various analyses.

For region names see table 4

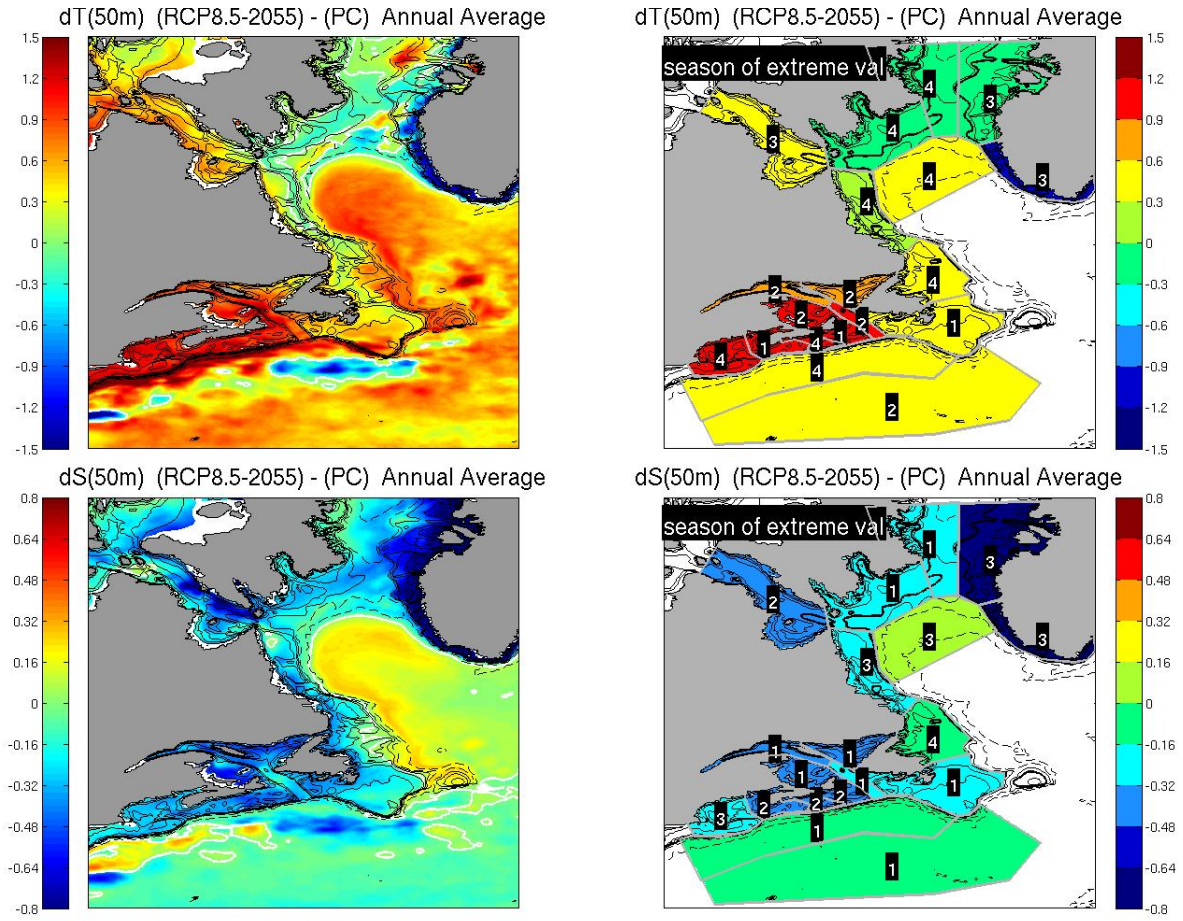

(a) (b)

Figure A1: Predicted annual change in T and S at 50m for RCP8.5-2055. (a) Spatial plot. (b) Region plot. The season of extrema in T and S change is annotated.

Table A1: Predicted changes in 50m T and S, (RCP8.5-2055)-(PC), by region, season, and on an annual basis.

	dT(°C)					**dS(PSU)**				
Region	**winter**	**spring**	**summer**	**fall**	**annual**	**winter**	**spring**	**summer**	**fall**	**annual**
S-Grnlnd-coast	-0.539	-1.039	-1.789	-0.986	-1.088	-0.478	-0.535	-1.656	-0.893	-0.890
N-Lab-Sea	0.257	0.224	0.321	0.476	0.319	-0.014	0.043	0.111	0.091	0.058
E-Davis-Str	0.832	-0.045	-1.050	0.122	-0.035	-0.571	-0.447	-0.974	-0.920	-0.728
W-Davis-Str	0.027	-0.157	-0.115	0.186	-0.015	-0.376	-0.125	-0.034	-0.343	-0.219
SW-Davis-Str	-0.056	-0.170	-0.216	0.366	-0.019	-0.363	-0.331	-0.187	-0.152	-0.258
Hudson-Str	0.105	0.220	0.890	0.770	0.496	-0.289	-0.389	-0.376	-0.250	-0.326
Lab-Shelf	0.015	-0.020	0.105	0.457	0.139	-0.175	-0.258	-0.297	-0.202	-0.233
N-Nfld-Shelf	0.445	0.315	0.287	0.552	0.400	-0.159	-0.146	-0.131	-0.190	-0.157
S-Nfld-Shelf	0.733	0.559	0.277	0.557	0.531	-0.289	-0.235	-0.171	-0.164	-0.215
L-Channel	1.086	1.254	0.814	0.824	0.995	-0.321	-0.270	-0.265	-0.199	-0.264
E-GSL	0.554	0.735	0.448	0.686	0.606	-0.491	-0.470	-0.401	-0.380	-0.436
SLE	0.690	1.018	0.970	0.909	0.897	-0.502	-0.469	-0.327	-0.321	-0.405
W-GSL	0.782	1.170	0.881	1.125	0.989	-0.545	-0.470	-0.367	-0.409	-0.448
ESS	1.195	1.059	0.909	1.047	1.053	-0.341	-0.463	-0.328	-0.373	-0.376
CSS	1.250	1.021	0.888	1.261	1.105	-0.383	-0.464	-0.424	-0.399	-0.417
WSS-BoF	1.287	1.100	0.939	1.083	1.102	-0.334	-0.365	-0.362	-0.246	-0.327
GoM	1.235	1.146	1.051	1.261	1.173	-0.238	-0.318	-0.341	-0.272	-0.293
Recirc-Zone	0.631	0.626	0.388	0.649	0.573	-0.143	-0.101	-0.089	-0.058	-0.098
Gulf-Stream	0.416	0.569	0.519	0.566	0.517	-0.094	-0.065	-0.080	-0.085	-0.081
H-Bay	0.333	0.518	1.001	0.871	0.681	-0.254	-0.319	-0.278	-0.178	-0.257

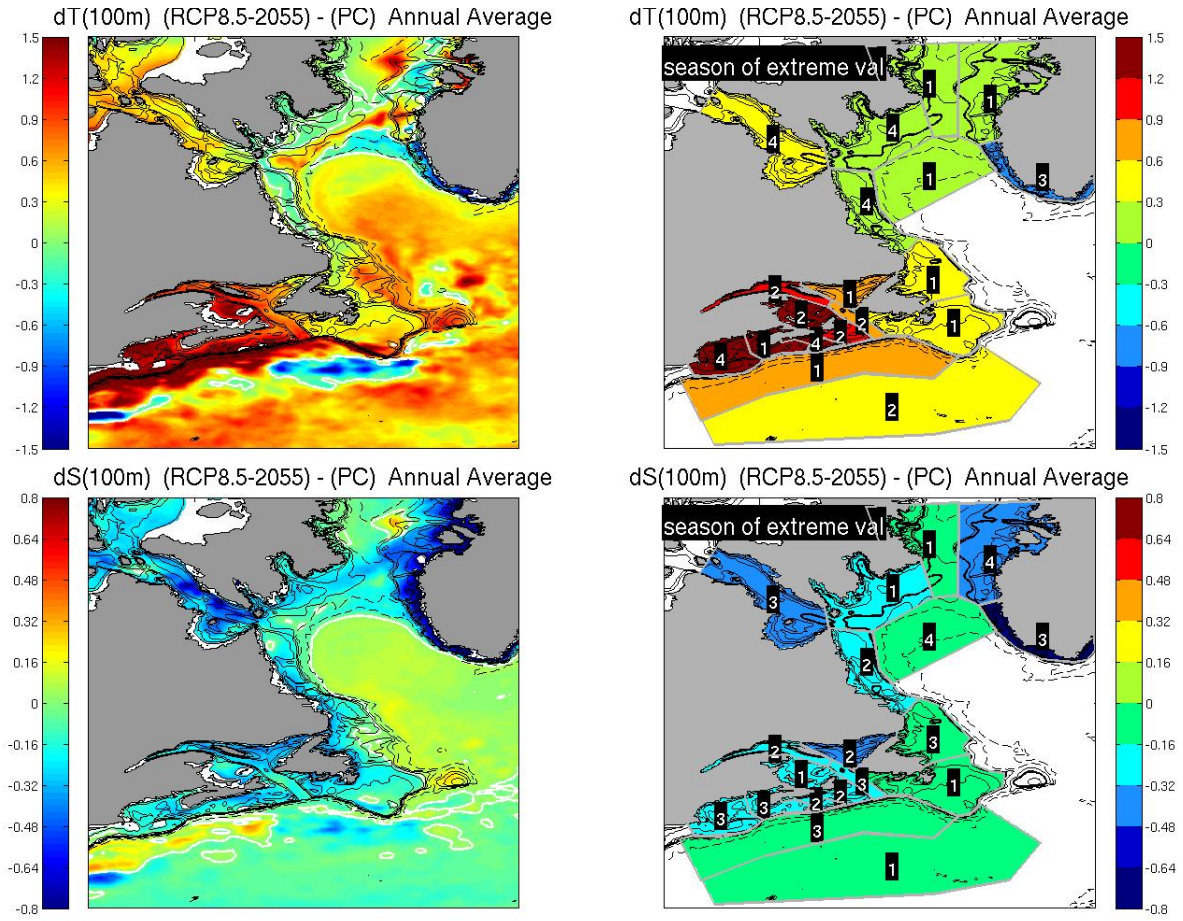

(a) (b)

Figure A2: Predicted annual change in T and S at 100m for RCP8.5-2055. (a) Spatial plot. (b) Region plot. The season of extrema in T and S change is annotated.

Table A2: Predicted changes in 100m T and S, (RCP8.5-2055)-(PC), by region, season, and on an annual basis.

	dT(°C)					**dS(PSU)**				
Region	**winter**	**spring**	**summer**	**fall**	**annual**	**winter**	**spring**	**summer**	**fall**	**annual**
S-Grnlnd-coast	-0.041	-0.863	-1.266	-0.599	-0.692	-0.357	-0.425	-1.159	-0.706	-0.662
N-Lab-Sea	0.180	0.141	0.172	0.143	0.159	-0.013	0.000	-0.009	-0.031	-0.013
E-Davis-Str	0.845	0.362	-0.371	0.124	0.240	-0.292	-0.263	-0.467	-0.543	-0.391
W-Davis-Str	0.326	0.070	0.004	0.128	0.132	-0.258	-0.084	-0.001	-0.075	-0.105
SW-Davis-Str	0.186	0.123	-0.149	0.233	0.098	-0.314	-0.243	-0.109	-0.113	-0.195
Hudson-Str	0.266	0.237	0.436	0.527	0.367	-0.302	-0.364	-0.396	-0.285	-0.337
Lab-Shelf	0.130	-0.009	-0.037	0.180	0.066	-0.139	-0.251	-0.236	-0.139	-0.191
N-Nfld-Shelf	0.654	0.296	0.316	0.423	0.422	-0.069	-0.116	-0.162	-0.152	-0.125
S-Nfld-Shelf	0.720	0.510	0.336	0.391	0.489	-0.165	-0.150	-0.143	-0.163	-0.155
L-Channel	0.948	1.009	0.743	0.577	0.819	-0.162	-0.154	-0.214	-0.207	-0.184
E-GSL	0.796	0.691	0.457	0.496	0.610	-0.361	-0.372	-0.313	-0.274	-0.330
SLE	0.959	0.997	0.993	0.800	0.937	-0.318	-0.328	-0.258	-0.194	-0.275
W-GSL	1.319	1.341	1.172	0.981	1.203	-0.279	-0.258	-0.197	-0.173	-0.227
ESS	0.991	1.058	0.970	0.922	0.985	-0.220	-0.279	-0.234	-0.245	-0.245
CSS	1.236	1.087	1.048	1.611	1.245	-0.242	-0.278	-0.276	-0.252	-0.262
WSS-BoF	1.486	1.160	1.006	1.227	1.220	-0.140	-0.239	-0.251	-0.166	-0.199
GoM	1.473	1.380	1.265	1.588	1.427	-0.149	-0.172	-0.207	-0.151	-0.170
Recirc-Zone	0.917	0.866	0.532	0.701	0.754	0.017	0.003	-0.052	-0.015	-0.012
Gulf-Stream	0.437	0.572	0.538	0.543	0.523	-0.082	-0.058	-0.061	-0.068	-0.067
H-Bay	0.633	0.648	0.760	0.783	0.706	-0.206	-0.226	-0.230	-0.203	-0.216

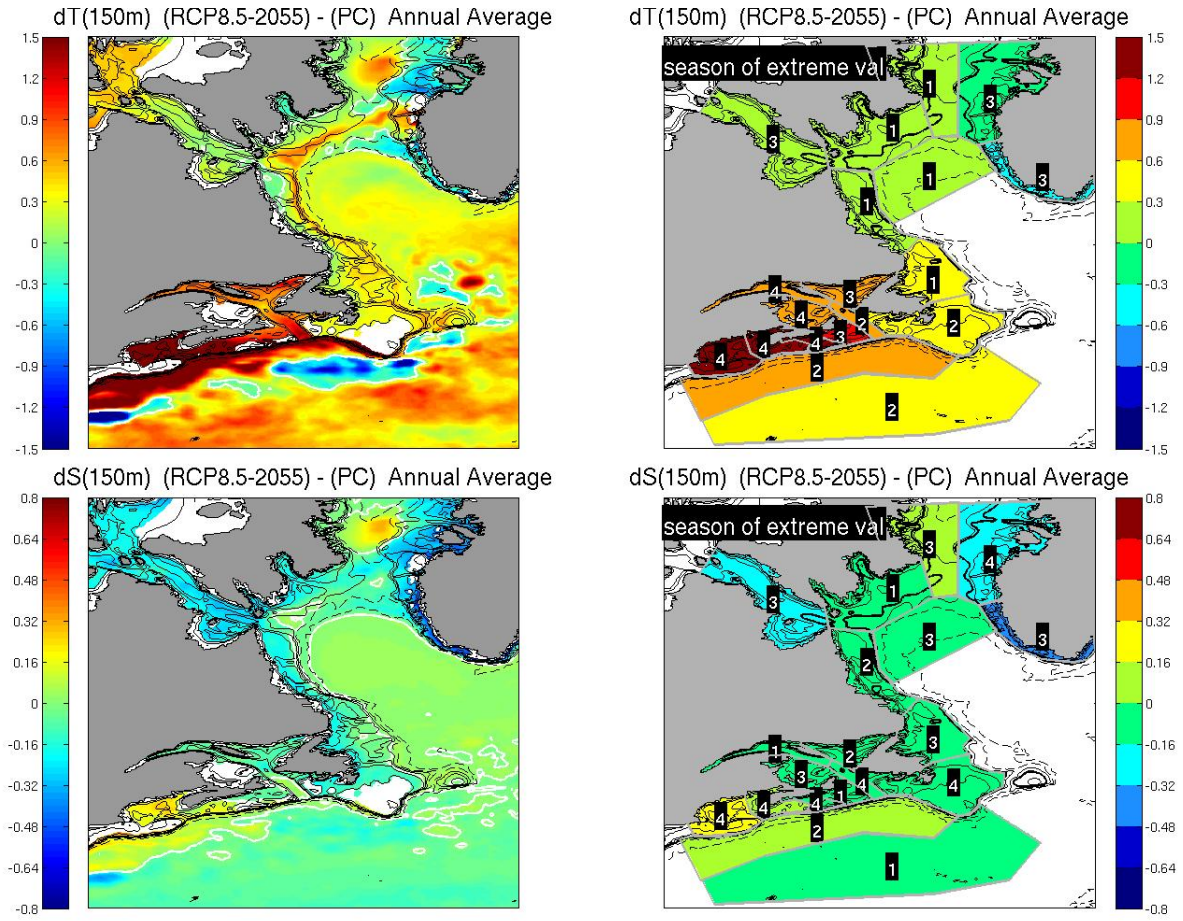

(a) (b)

Figure A3: Predicted annual change in T and S at 150m for RCP8.5-2055. (a) Spatial plot. (b) Region plot. The season of extrema in T and S change is annotated.

Table A3: Predicted changes in 150m T and S, (RCP8.5-2055)-(PC), by region, season, and on an annual basis.

	dT(°C)					**dS(PSU)**				
Region	**winter**	**spring**	**summer**	**fall**	**annual**	**winter**	**spring**	**summer**	**fall**	**annual**
S-Grnlnd-coast	-0.041	-0.542	-0.654	-0.185	-0.356	-0.283	-0.291	-0.475	-0.420	-0.367
N-Lab-Sea	0.179	0.107	0.093	0.153	0.133	-0.008	-0.011	-0.017	-0.008	-0.011
E-Davis-Str	0.071	-0.037	-0.201	-0.069	-0.059	-0.164	-0.155	-0.230	-0.272	-0.205
W-Davis-Str	0.290	0.240	0.164	0.031	0.181	-0.010	-0.000	0.031	-0.012	0.002
SW-Davis-Str	0.379	0.308	0.115	0.005	0.202	-0.158	-0.152	-0.075	-0.064	-0.112
Hudson-Str	0.131	0.140	0.146	0.122	0.135	-0.211	-0.237	-0.246	-0.220	-0.228
Lab-Shelf	0.363	0.194	0.169	0.170	0.224	-0.071	-0.212	-0.149	-0.059	-0.123
N-Nfld-Shelf	0.382	0.335	0.289	0.323	0.332	-0.039	-0.067	-0.113	-0.093	-0.078
S-Nfld-Shelf	0.544	0.578	0.397	0.341	0.465	-0.081	-0.058	-0.086	-0.120	-0.086
L-Channel	0.770	1.091	0.956	0.629	0.861	-0.043	0.030	-0.021	-0.086	-0.030
E-GSL	0.692	0.812	0.904	0.774	0.796	-0.102	-0.113	-0.064	-0.049	-0.082
SLE	0.735	0.728	0.750	0.802	0.754	-0.083	-0.080	-0.049	-0.034	-0.062
W-GSL	0.724	0.610	0.638	0.734	0.677	-0.052	-0.069	-0.075	-0.037	-0.058
ESS	0.832	0.968	1.059	0.983	0.961	-0.065	-0.052	-0.027	-0.039	-0.046
CSS	1.208	1.234	1.280	1.436	1.289	-0.005	-0.016	-0.008	0.018	-0.003
WSS-BoF	1.744	1.698	1.611	1.881	1.733	0.119	0.091	0.102	0.175	0.122
GoM	2.003	1.882	1.817	2.097	1.950	0.213	0.175	0.182	0.248	0.204
Recirc-Zone	0.711	0.872	0.754	0.837	0.793	0.002	0.025	0.000	0.001	0.007
Gulf-Stream	0.438	0.491	0.419	0.479	0.457	-0.064	-0.054	-0.058	-0.054	-0.058
H-Bay	0.599	0.597	0.612	0.624	0.608	-0.097	-0.092	-0.093	-0.099	-0.095

Results for RCP 8.5 – 2075 Climatology

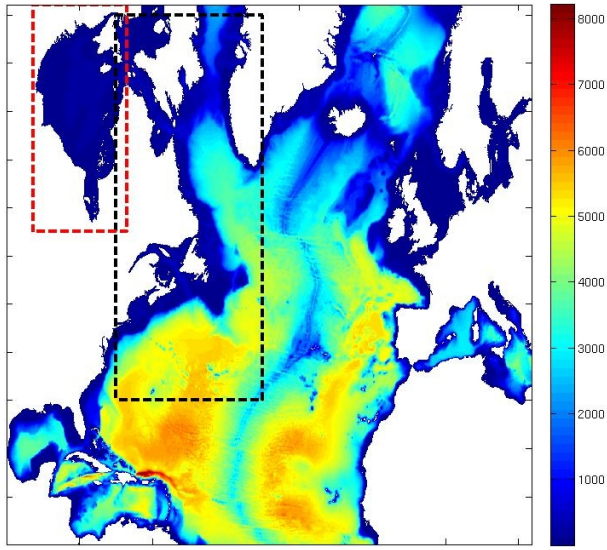

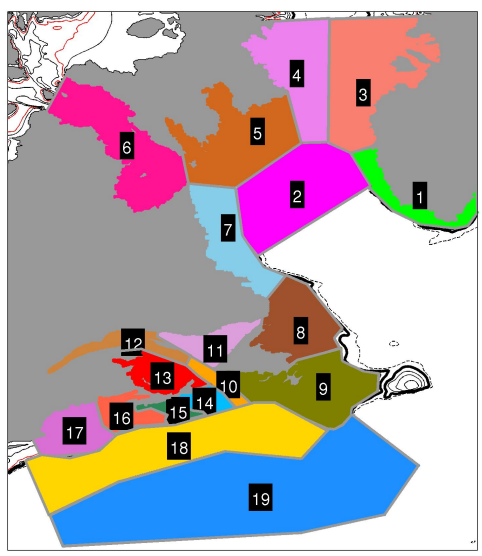

Reminder of model domains and regions used for various analyses.

For region names see table 4

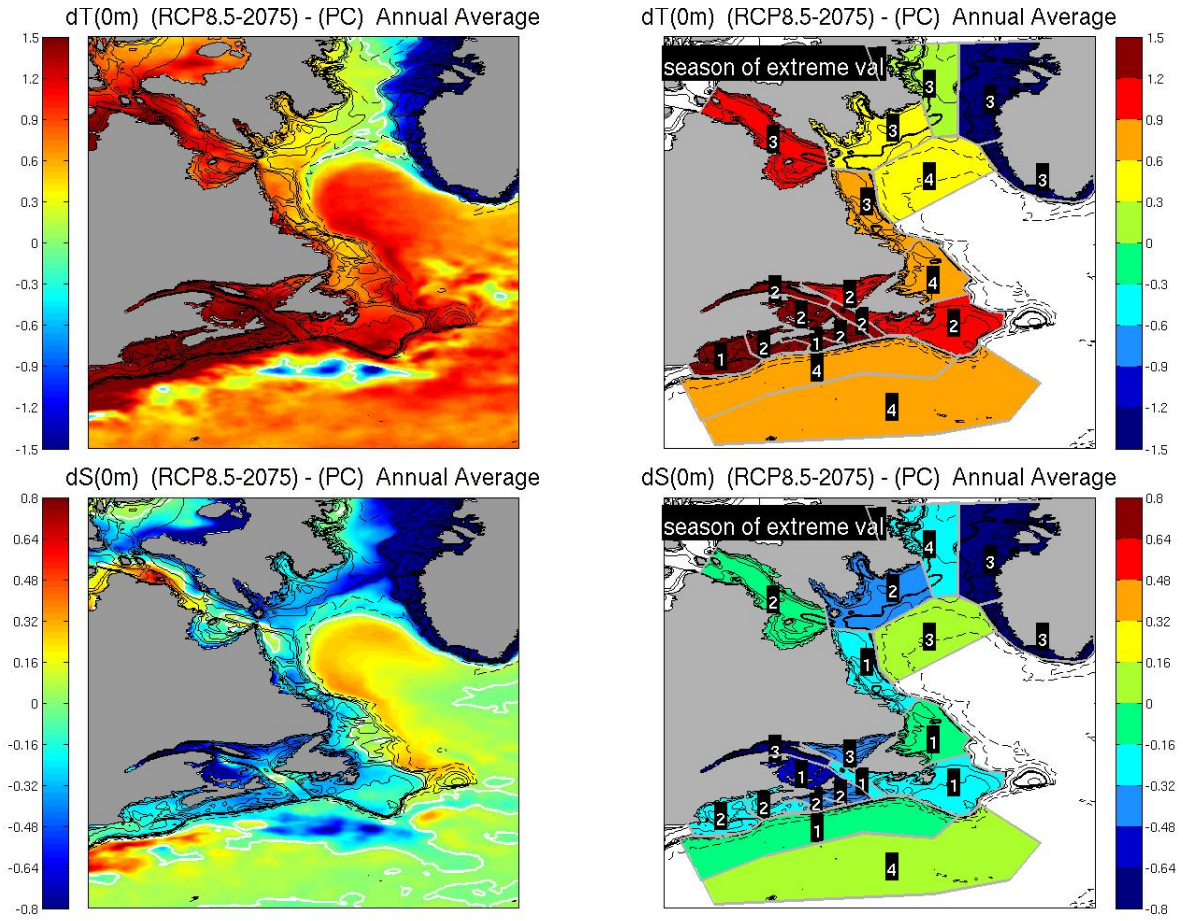

(a) (b)

Figure A4: Predicted annual change in T and S at 0m for RCP8.5-2075. (a) Spatial plot. (b) Region plot. The season of extrema in T and S change is annotated.

Table A4: Predicted changes in 0m T and S, (RCP8.5-2075)-(PC), by region, season, and on an annual basis.

	dT(°C)					**dS(PSU)**				
Region	**winter**	**spring**	**summer**	**fall**	**annual**	**winter**	**spring**	**summer**	**fall**	**annual**
S-Grnlnd-coast	-0.747	-1.301	-2.126	-1.051	-1.307	-0.591	-0.957	-2.427	-1.073	-1.262
N-Lab-Sea	0.280	0.351	0.694	0.701	0.506	-0.042	0.057	0.252	0.066	0.083
E-Davis-Str	0.003	-1.588	-2.711	-0.683	-1.245	-0.768	-1.547	-3.330	-1.514	-1.790
W-Davis-Str	-0.009	-0.081	0.583	0.177	0.168	-0.391	-0.292	-0.065	-0.513	-0.315
SW-Davis-Str	-0.028	0.239	0.868	0.597	0.419	-0.372	-0.535	-0.227	-0.172	-0.327
Hudson-Str	0.038	0.977	2.091	1.195	1.075	-0.068	-0.309	0.149	0.003	-0.056
Lab-Shelf	0.031	0.865	1.117	0.885	0.724	-0.253	-0.227	-0.149	-0.214	-0.211
N-Nfld-Shelf	0.523	0.873	0.765	0.957	0.779	-0.233	-0.120	0.054	-0.174	-0.118
S-Nfld-Shelf	1.168	1.183	1.054	1.135	1.135	-0.266	-0.253	-0.114	-0.124	-0.189
L-Channel	1.605	1.713	1.189	1.283	1.447	-0.255	-0.142	-0.162	-0.138	-0.174
E-GSL	0.735	1.497	1.153	1.200	1.146	-0.466	-0.471	-0.486	-0.361	-0.446
SLE	0.793	2.017	1.413	1.336	1.390	-0.661	-0.455	-0.859	-0.624	-0.650
W-GSL	1.130	1.973	1.323	1.578	1.501	-0.660	-0.554	-0.471	-0.489	-0.543
ESS	1.688	1.690	1.257	1.383	1.504	-0.293	-0.430	-0.282	-0.286	-0.323
CSS	1.655	1.616	1.243	1.440	1.489	-0.353	-0.405	-0.384	-0.297	-0.360
WSS-BoF	1.670	1.672	1.316	1.442	1.525	-0.345	-0.408	-0.342	-0.182	-0.319
GoM	1.675	1.558	1.235	1.474	1.486	-0.141	-0.278	-0.227	-0.142	-0.197
Recirc-Zone	0.813	0.758	0.700	0.896	0.792	-0.098	-0.088	-0.093	-0.001	-0.070
Gulf-Stream	0.572	0.638	0.722	0.741	0.668	0.019	0.015	-0.015	0.042	0.015
H-Bay	0.036	1.686	2.189	1.301	1.303	-0.316	-0.219	0.228	-0.057	-0.091

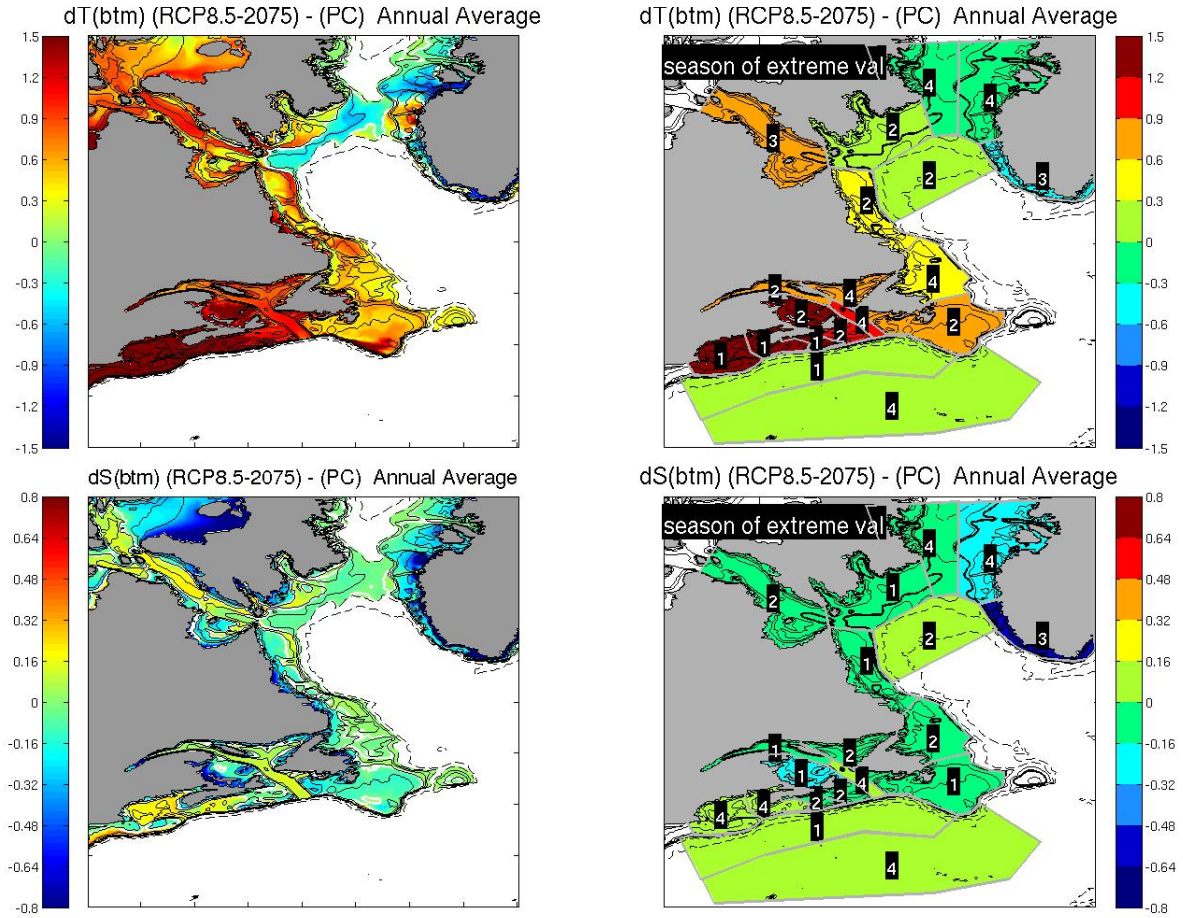

(a) (b)

Figure A5: Predicted annual change in bottom T and S for RCP8.5-2075. (a) Spatial plot. (b) Region plot. The season of extrema in T and S change is annotated. Deep water region is masked out for clarity.

Table A5: Predicted changes in bottom T and S, (RCP8.5-2075)-(PC), by region, season, and on an annual basis.

	dT(°C)					**dS(PSU)**				
Region	**winter**	**spring**	**summer**	**fall**	**annual**	**winter**	**spring**	**summer**	**fall**	**annual**
S-Grnlnd-coast	0.148	-0.439	-0.956	-0.123	-0.342	-0.346	-0.448	-0.945	-0.525	-0.566
N-Lab-Sea	0.099	0.170	0.144	0.113	0.131	0.020	0.031	0.025	0.019	0.024
E-Davis-Str	-0.013	-0.072	-0.224	-0.231	-0.135	-0.132	-0.123	-0.215	-0.252	-0.181
W-Davis-Str	-0.034	-0.031	-0.075	-0.116	-0.064	-0.016	-0.011	-0.013	-0.024	-0.016
SW-Davis-Str	-0.019	0.246	0.150	0.027	0.101	-0.085	-0.062	-0.046	-0.069	-0.065
Hudson-Str	0.517	0.630	0.788	0.687	0.655	-0.025	-0.063	-0.037	-0.037	-0.040
Lab-Shelf	0.361	0.697	0.677	0.538	0.568	-0.120	-0.119	-0.050	-0.057	-0.086
N-Nfld-Shelf	0.476	0.464	0.486	0.571	0.500	-0.046	-0.055	-0.051	-0.020	-0.043
S-Nfld-Shelf	0.703	0.707	0.604	0.618	0.658	-0.105	-0.064	-0.056	-0.082	-0.077
L-Channel	1.027	1.030	1.040	1.042	1.035	0.104	0.102	0.110	0.121	0.109
E-GSL	0.833	0.905	0.815	0.911	0.866	-0.138	-0.139	-0.078	-0.041	-0.099
SLE	0.765	0.954	0.880	0.874	0.868	-0.153	-0.098	-0.049	-0.022	-0.080
W-GSL	1.304	1.658	1.232	1.252	1.362	-0.415	-0.331	-0.212	-0.172	-0.282
ESS	1.173	1.207	1.129	1.035	1.136	-0.045	-0.064	-0.057	-0.047	-0.053
CSS	1.532	1.487	1.354	1.364	1.434	-0.035	-0.081	-0.061	-0.053	-0.057
WSS-BoF	1.706	1.638	1.620	1.591	1.639	0.018	-0.018	0.028	0.074	0.026
GoM	1.757	1.693	1.717	1.751	1.729	0.088	0.044	0.082	0.124	0.085
Recirc-Zone	0.077	0.076	0.064	0.069	0.071	0.008	0.008	0.008	0.008	0.008
Gulf-Stream	0.006	0.004	0.005	0.009	0.006	0.001	0.001	0.001	0.001	0.001
H-Bay	0.681	0.955	1.097	0.980	0.928	-0.132	-0.153	-0.062	-0.105	-0.113

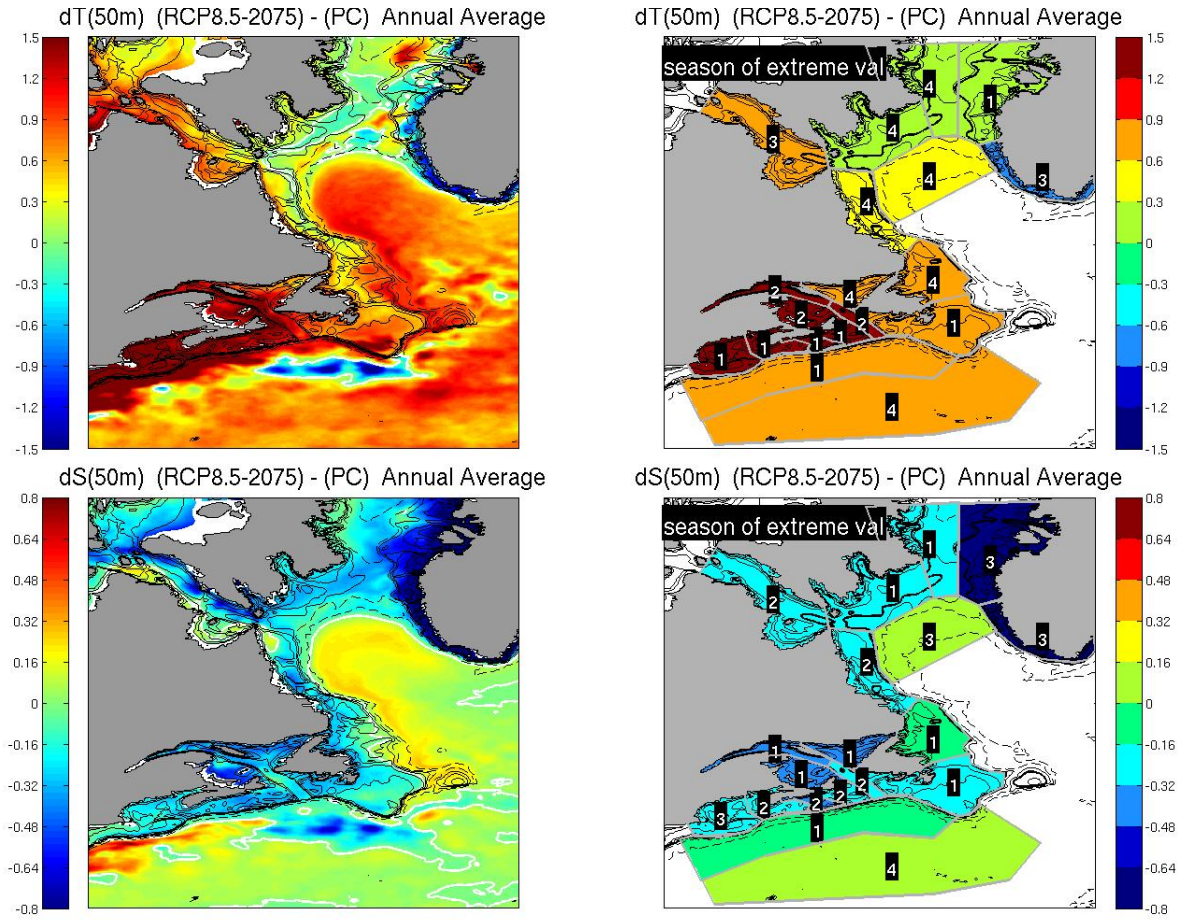

(a) (b)

Figure A6: Predicted annual change in T and S at 50m for RCP8.5-2075. (a) Spatial plot. (b) Region plot. The season of extrema in T and S change is annotated.

Table A6: Predicted changes in 50m T and S, (RCP8.5-2075)-(PC), by region, season, and on an annual basis.

	dT(°C)					**dS(PSU)**				
Region	**winter**	**spring**	**summer**	**fall**	**annual**	**winter**	**spring**	**summer**	**fall**	**annual**
S-Grnlnd-coast	-0.315	-0.900	-1.584	-0.749	-0.887	-0.461	-0.541	-1.643	-0.887	-0.883
N-Lab-Sea	0.369	0.378	0.494	0.653	0.474	-0.013	0.044	0.113	0.069	0.053
E-Davis-Str	0.886	0.023	-0.867	0.274	0.079	-0.559	-0.446	-0.937	-0.877	-0.705
W-Davis-Str	0.053	-0.109	-0.027	0.282	0.050	-0.376	-0.125	-0.024	-0.335	-0.215
SW-Davis-Str	-0.026	-0.050	0.006	0.565	0.124	-0.369	-0.336	-0.167	-0.148	-0.255
Hudson-Str	0.100	0.282	1.192	1.111	0.671	-0.115	-0.271	-0.228	-0.042	-0.164
Lab-Shelf	0.058	0.117	0.338	0.748	0.315	-0.170	-0.240	-0.236	-0.129	-0.194
N-Nfld-Shelf	0.603	0.498	0.475	0.866	0.611	-0.166	-0.145	-0.118	-0.153	-0.146
S-Nfld-Shelf	1.149	0.785	0.418	0.921	0.818	-0.243	-0.215	-0.132	-0.108	-0.174
L-Channel	1.567	1.585	1.004	1.144	1.325	-0.251	-0.260	-0.254	-0.100	-0.216
E-GSL	0.839	0.963	0.692	1.034	0.882	-0.415	-0.404	-0.323	-0.322	-0.366
SLE	1.101	1.440	1.223	1.205	1.242	-0.444	-0.414	-0.272	-0.285	-0.354
W-GSL	1.268	1.586	1.133	1.512	1.375	-0.531	-0.420	-0.272	-0.347	-0.392
ESS	1.668	1.485	1.139	1.307	1.400	-0.262	-0.380	-0.262	-0.214	-0.280
CSS	1.668	1.426	1.075	1.389	1.390	-0.325	-0.389	-0.362	-0.276	-0.338
WSS-BoF	1.713	1.491	1.207	1.342	1.438	-0.295	-0.305	-0.302	-0.153	-0.264
GoM	1.690	1.579	1.465	1.533	1.567	-0.133	-0.258	-0.262	-0.172	-0.206
Recirc-Zone	0.908	0.823	0.297	0.905	0.733	-0.047	-0.015	-0.025	0.041	-0.012
Gulf-Stream	0.574	0.608	0.586	0.732	0.625	0.022	0.030	0.024	0.044	0.030
H-Bay	0.399	0.847	1.641	1.263	1.038	-0.215	-0.297	-0.198	-0.111	-0.205

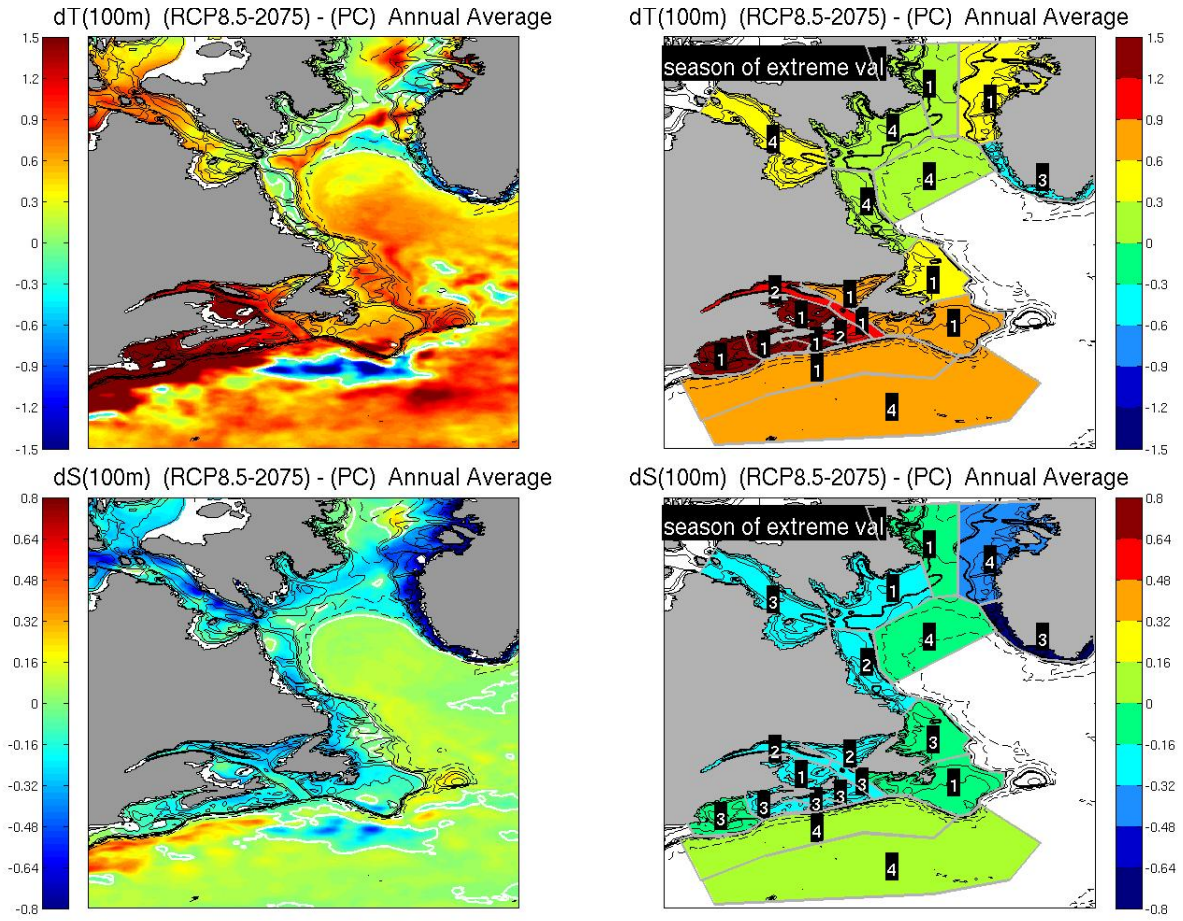

(a) (b)

Figure A7: Predicted annual change in T and S at 100m for RCP8.5-2075. (a) Spatial plot. (b) Region plot. The season of extrema in T and S change is annotated.

Table A7: Predicted changes in 100m T and S, (RCP8.5-2075)-(PC), by region, season, and on an annual basis.

	dT(°C)					**dS(PSU)**				
Region	**winter**	**spring**	**summer**	**fall**	**annual**	**winter**	**spring**	**summer**	**fall**	**annual**
S-Grnlnd-coast	0.120	-0.797	-1.116	-0.383	-0.544	-0.342	-0.443	-1.162	-0.702	-0.662
N-Lab-Sea	0.240	0.247	0.264	0.291	0.261	-0.021	0.001	-0.008	-0.033	-0.015
E-Davis-Str	0.895	0.389	-0.270	0.237	0.313	-0.298	-0.268	-0.453	-0.527	-0.386
W-Davis-Str	0.386	0.101	0.038	0.207	0.183	-0.251	-0.080	0.003	-0.070	-0.099
SW-Davis-Str	0.268	0.215	-0.064	0.330	0.187	-0.314	-0.240	-0.107	-0.121	-0.195
Hudson-Str	0.335	0.308	0.590	0.762	0.499	-0.213	-0.304	-0.336	-0.187	-0.260
Lab-Shelf	0.192	0.077	0.083	0.349	0.175	-0.146	-0.244	-0.220	-0.108	-0.180
N-Nfld-Shelf	0.782	0.409	0.445	0.594	0.557	-0.077	-0.130	-0.168	-0.138	-0.128
S-Nfld-Shelf	0.985	0.681	0.478	0.637	0.695	-0.151	-0.146	-0.130	-0.149	-0.144
L-Channel	1.132	1.113	0.839	0.774	0.964	-0.126	-0.188	-0.246	-0.157	-0.179
E-GSL	0.948	0.814	0.593	0.642	0.749	-0.319	-0.353	-0.291	-0.248	-0.302
SLE	1.249	1.259	1.192	0.958	1.164	-0.249	-0.292	-0.243	-0.152	-0.234
W-GSL	1.737	1.675	1.447	1.214	1.518	-0.232	-0.218	-0.150	-0.125	-0.181
ESS	1.252	1.285	1.014	0.898	1.112	-0.158	-0.213	-0.219	-0.183	-0.193
CSS	1.399	1.341	1.103	1.194	1.259	-0.188	-0.230	-0.256	-0.237	-0.228
WSS-BoF	1.692	1.410	1.230	1.228	1.390	-0.126	-0.205	-0.224	-0.150	-0.176
GoM	1.728	1.682	1.628	1.714	1.688	-0.085	-0.128	-0.155	-0.124	-0.123
Recirc-Zone	1.054	1.020	0.389	0.735	0.799	0.079	0.079	0.004	0.086	0.062
Gulf-Stream	0.585	0.599	0.544	0.700	0.607	0.030	0.041	0.049	0.059	0.045
H-Bay	0.865	0.904	1.119	1.158	1.011	-0.199	-0.216	-0.211	-0.182	-0.202

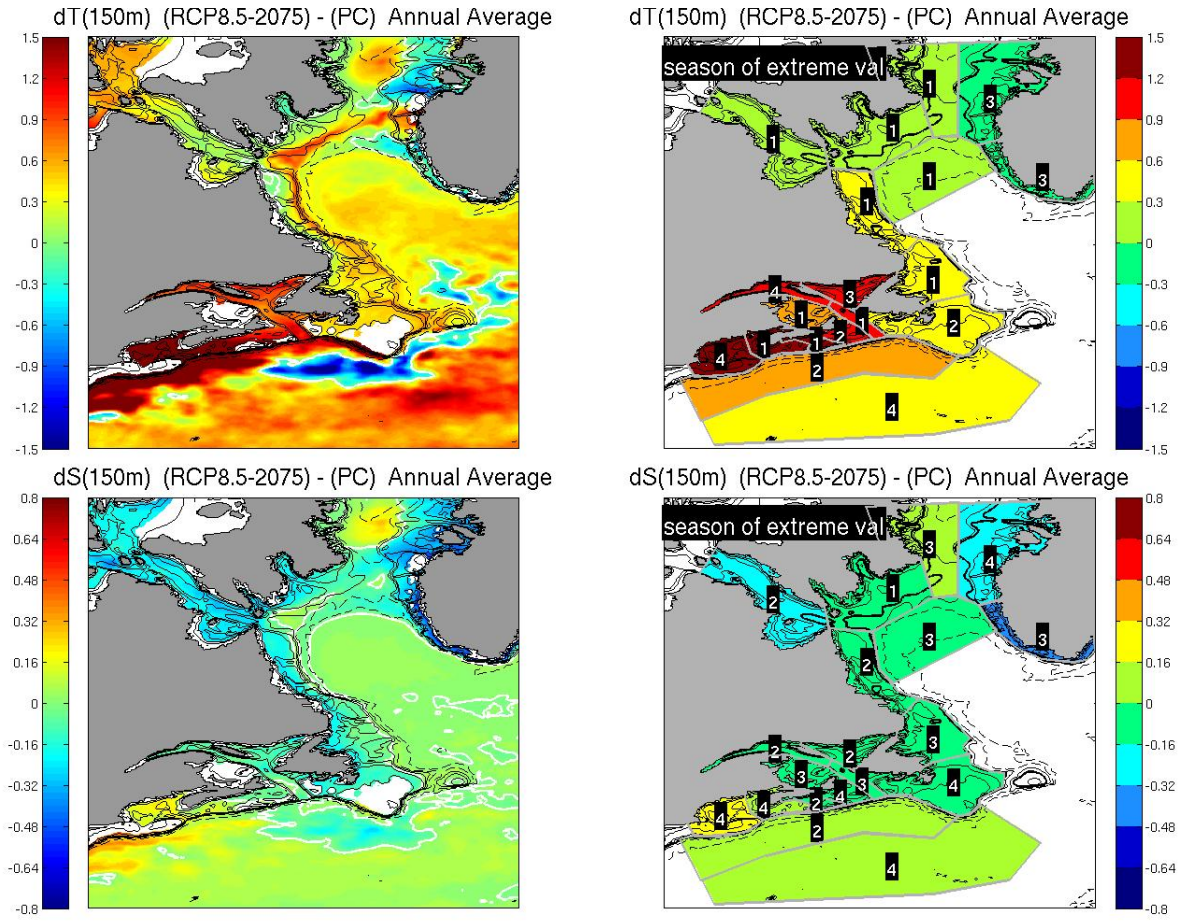

(a) (b)

Figure A8: Predicted annual change in T and S at 150m for RCP8.5-2075. (a) Spatial plot. (b) Region plot. The season of extrema in T and S change is annotated.

Table A8: Predicted changes in 150m T and S, (RCP8.5-2075)-(PC), by region, season, and on an annual basis.

	dT(°C)					**dS(PSU)**				
Region	**winter**	**spring**	**summer**	**fall**	**annual**	**winter**	**spring**	**summer**	**fall**	**annual**
S-Grnlnd-coast	0.073	-0.512	-0.584	0.004	-0.255	-0.271	-0.313	-0.493	-0.411	-0.372
N-Lab-Sea	0.274	0.210	0.171	0.264	0.230	-0.008	-0.009	-0.016	-0.005	-0.009
E-Davis-Str	0.091	-0.031	-0.159	-0.006	-0.026	-0.172	-0.164	-0.230	-0.273	-0.210
W-Davis-Str	0.379	0.274	0.182	0.090	0.231	0.003	0.003	0.031	-0.003	0.009
SW-Davis-Str	0.454	0.413	0.182	0.052	0.275	-0.164	-0.140	-0.069	-0.070	-0.111
Hudson-Str	0.224	0.213	0.198	0.197	0.208	-0.219	-0.252	-0.252	-0.215	-0.234
Lab-Shelf	0.421	0.310	0.273	0.270	0.318	-0.082	-0.206	-0.148	-0.058	-0.124
N-Nfld-Shelf	0.474	0.398	0.399	0.433	0.426	-0.049	-0.083	-0.121	-0.092	-0.086
S-Nfld-Shelf	0.650	0.658	0.483	0.495	0.572	-0.087	-0.068	-0.091	-0.122	-0.092
L-Channel	0.977	0.957	0.869	0.830	0.908	-0.023	-0.044	-0.086	-0.079	-0.058
E-GSL	0.842	0.942	0.997	0.905	0.921	-0.109	-0.142	-0.104	-0.060	-0.104
SLE	0.899	0.887	0.901	0.956	0.911	-0.077	-0.091	-0.073	-0.037	-0.070
W-GSL	0.962	0.815	0.770	0.829	0.844	-0.009	-0.084	-0.105	-0.055	-0.063
ESS	1.072	1.128	1.109	0.957	1.067	-0.029	-0.035	-0.046	-0.054	-0.041
CSS	1.407	1.355	1.393	1.328	1.371	0.009	-0.009	-0.002	-0.005	-0.002
WSS-BoF	1.741	1.637	1.721	1.730	1.707	0.098	0.058	0.108	0.124	0.097
GoM	1.928	1.843	1.897	2.033	1.925	0.181	0.146	0.179	0.216	0.181
Recirc-Zone	0.784	0.959	0.718	0.845	0.826	0.046	0.078	0.049	0.054	0.057
Gulf-Stream	0.581	0.534	0.473	0.582	0.543	0.040	0.040	0.041	0.059	0.045
H-Bay	0.827	0.828	0.845	0.851	0.838	-0.091	-0.088	-0.085	-0.089	-0.088

Results for RCP 4.5 – 2055 Climatology

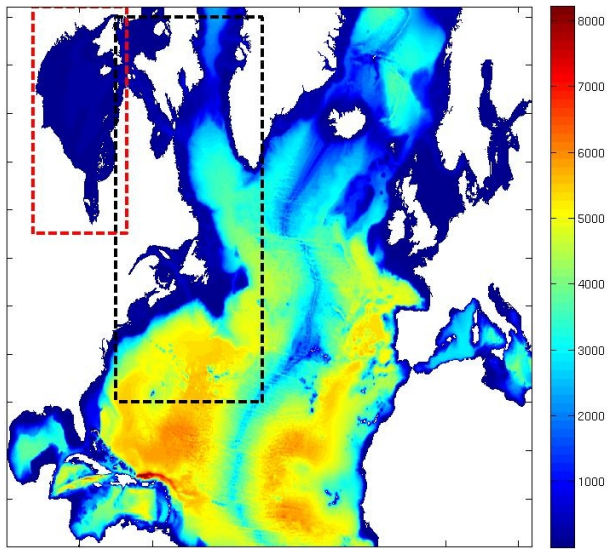

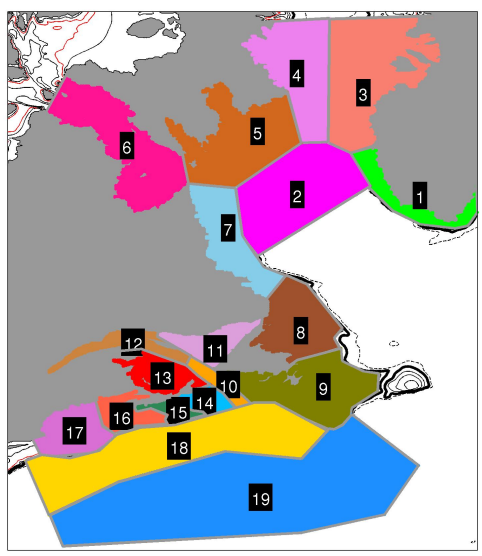

Reminder of model domains and regions used for various analyses.

For region names see table 4

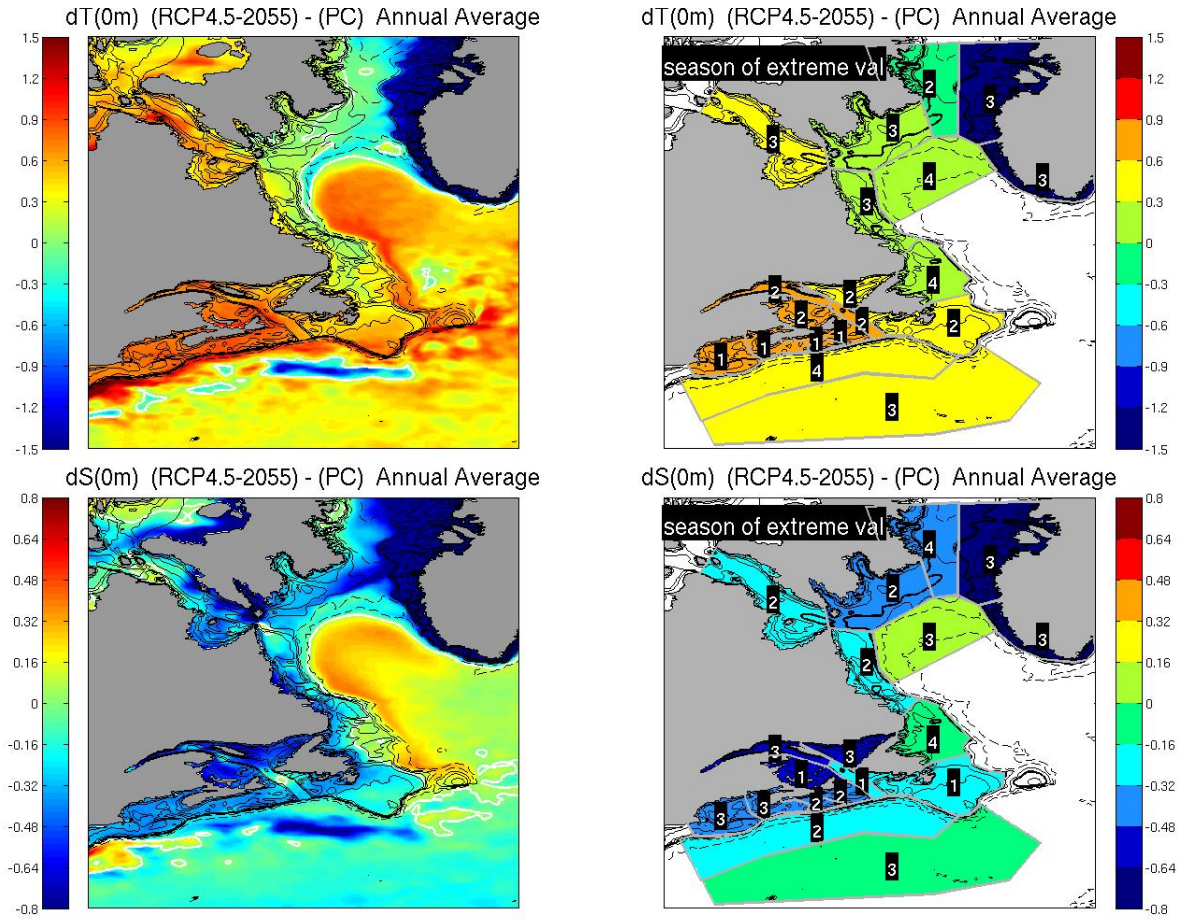

(a) (b)

Figure A9: Predicted annual change in T and S at 0m for RCP4.5-2055. (a) Spatial plot. (b) Region plot. The season of extrema in T and S change is annotated.

Table A9: Predicted changes in 0m T and S, (RCP4.5-2055)-(PC), by region, season, and on an annual basis.

	dT(°C)					**dS(PSU)**				
Region	**winter**	**spring**	**summer**	**fall**	**annual**	**winter**	**spring**	**summer**	**fall**	**annual**
S-Grnlnd-coast	-0.987	-1.538	-2.466	-1.415	-1.601	-0.581	-0.933	-2.469	-1.085	-1.267
N-Lab-Sea	0.100	0.028	0.263	0.485	0.219	-0.045	0.065	0.271	0.114	0.101
E-Davis-Str	-0.029	-1.764	-3.229	-0.940	-1.491	-0.758	-1.447	-3.468	-1.557	-1.807
W-Davis-Str	-0.022	-0.319	0.020	0.009	-0.078	-0.374	-0.261	-0.116	-0.549	-0.325
SW-Davis-Str	-0.059	-0.191	0.245	0.239	0.058	-0.336	-0.521	-0.306	-0.194	-0.339
Hudson-Str	0.025	0.484	1.198	0.564	0.568	-0.261	-0.488	-0.222	-0.257	-0.307
Lab-Shelf	-0.009	0.123	0.430	0.349	0.223	-0.196	-0.388	-0.287	-0.319	-0.298
N-Nfld-Shelf	0.260	0.305	0.140	0.394	0.275	-0.189	-0.114	-0.013	-0.227	-0.136
S-Nfld-Shelf	0.524	0.606	0.499	0.534	0.541	-0.295	-0.216	-0.124	-0.198	-0.208
L-Channel	0.768	0.895	0.529	0.688	0.720	-0.360	-0.213	-0.198	-0.190	-0.240
E-GSL	0.294	0.833	0.492	0.523	0.535	-0.517	-0.546	-0.584	-0.428	-0.519
SLE	0.307	1.018	0.778	0.705	0.702	-0.504	-0.305	-0.677	-0.504	-0.498
W-GSL	0.472	1.190	0.728	0.871	0.815	-0.635	-0.491	-0.358	-0.517	-0.500
ESS	0.952	0.921	0.597	0.784	0.813	-0.344	-0.417	-0.286	-0.326	-0.343
CSS	0.975	0.858	0.629	0.836	0.824	-0.401	-0.408	-0.405	-0.303	-0.379
WSS-BoF	0.938	0.872	0.678	0.734	0.806	-0.381	-0.443	-0.458	-0.268	-0.388
GoM	0.881	0.831	0.655	0.762	0.782	-0.282	-0.384	-0.462	-0.359	-0.372
Recirc-Zone	0.281	0.262	0.385	0.480	0.352	-0.256	-0.265	-0.209	-0.142	-0.218
Gulf-Stream	0.251	0.327	0.411	0.388	0.344	-0.126	-0.122	-0.154	-0.119	-0.130
H-Bay	0.025	0.656	1.020	0.622	0.581	-0.327	-0.386	-0.035	-0.161	-0.227

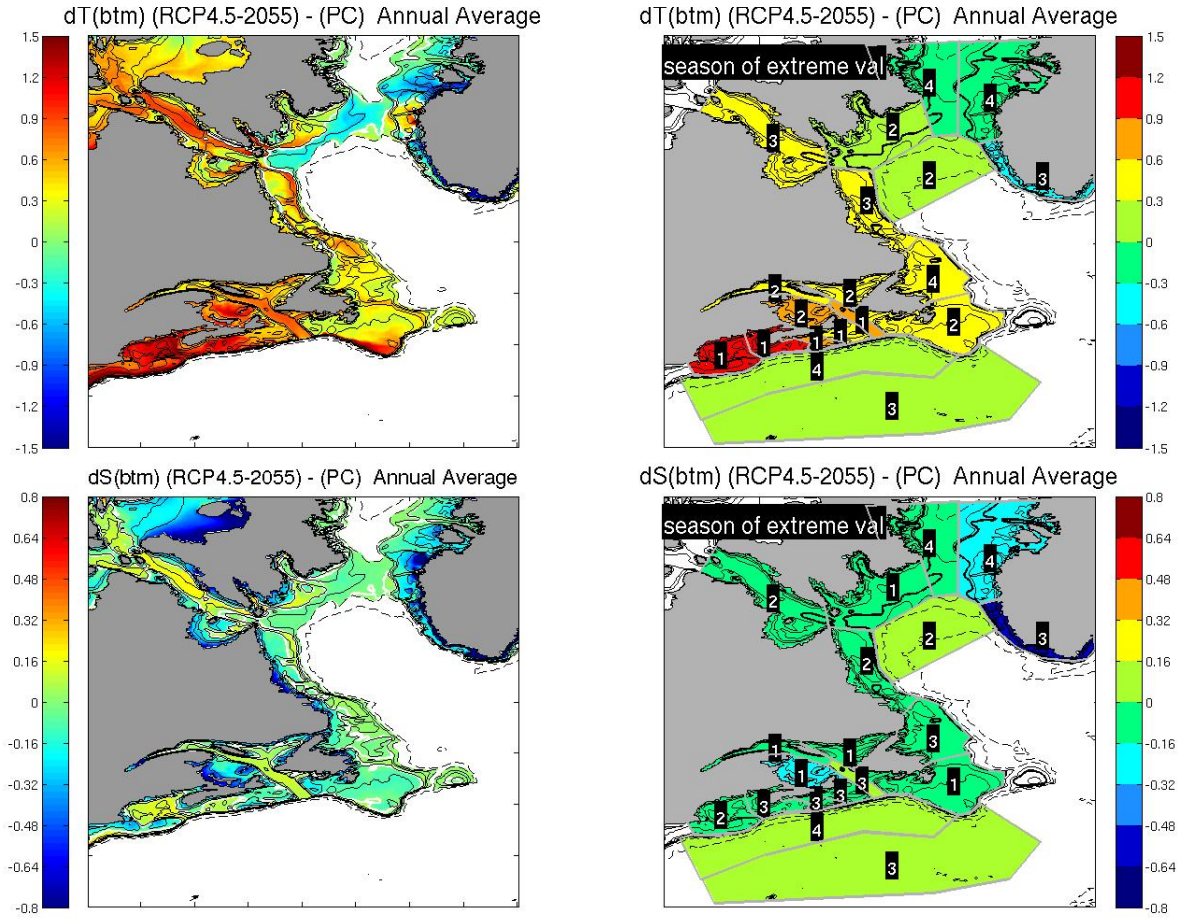

(a) (b)

Figure A10: Predicted annual change in bottom T and S for RCP4.5-2055. (a) Spatial plot. (b) Region plot. The season of extrema in T and S change is annotated. Deep water region is masked out for clarity.

Table A10: Predicted changes in bottom T and S, (RCP4.5-2055)-(PC), by region, season, and on an annual basis.

	dT(°C)					**dS(PSU)**				
Region	**winter**	**spring**	**summer**	**fall**	**annual**	**winter**	**spring**	**summer**	**fall**	**annual**
S-Grnlnd-coast	0.016	-0.516	-1.110	-0.392	-0.500	-0.335	-0.417	-0.945	-0.542	-0.560
N-Lab-Sea	0.077	0.137	0.118	0.093	0.106	0.016	0.026	0.020	0.015	0.019
E-Davis-Str	-0.050	-0.110	-0.274	-0.282	-0.179	-0.127	-0.115	-0.209	-0.243	-0.174
W-Davis-Str	-0.032	-0.039	-0.086	-0.102	-0.065	-0.012	-0.009	-0.012	-0.019	-0.013
SW-Davis-Str	-0.020	0.143	0.040	-0.052	0.028	-0.069	-0.060	-0.063	-0.067	-0.065
Hudson-Str	0.415	0.481	0.568	0.501	0.491	-0.041	-0.076	-0.063	-0.062	-0.061
Lab-Shelf	0.264	0.394	0.463	0.360	0.370	-0.086	-0.139	-0.097	-0.092	-0.103
N-Nfld-Shelf	0.332	0.306	0.311	0.413	0.341	-0.041	-0.048	-0.059	-0.030	-0.045
S-Nfld-Shelf	0.414	0.459	0.424	0.396	0.423	-0.098	-0.051	-0.040	-0.075	-0.066
L-Channel	0.786	0.773	0.761	0.743	0.766	0.081	0.082	0.084	0.084	0.083
E-GSL	0.460	0.528	0.454	0.487	0.482	-0.171	-0.155	-0.086	-0.081	-0.123
SLE	0.428	0.559	0.547	0.537	0.518	-0.153	-0.122	-0.060	-0.048	-0.095
W-GSL	0.725	0.999	0.695	0.700	0.780	-0.407	-0.349	-0.248	-0.234	-0.310
ESS	0.694	0.618	0.339	0.626	0.569	-0.092	-0.115	-0.117	-0.073	-0.099
CSS	1.201	0.872	0.509	0.865	0.862	-0.069	-0.130	-0.139	-0.083	-0.105
WSS-BoF	1.172	1.065	0.862	0.856	0.989	-0.031	-0.088	-0.097	-0.022	-0.059
GoM	1.229	1.074	1.040	1.049	1.098	0.017	-0.045	-0.036	0.011	-0.013
Recirc-Zone	0.059	0.043	0.036	0.061	0.050	0.007	0.004	0.004	0.008	0.006
Gulf-Stream	-0.001	0.001	0.004	0.002	0.002	0.000	0.001	0.001	0.001	0.001
H-Bay	0.430	0.539	0.625	0.572	0.542	-0.130	-0.149	-0.105	-0.125	-0.128

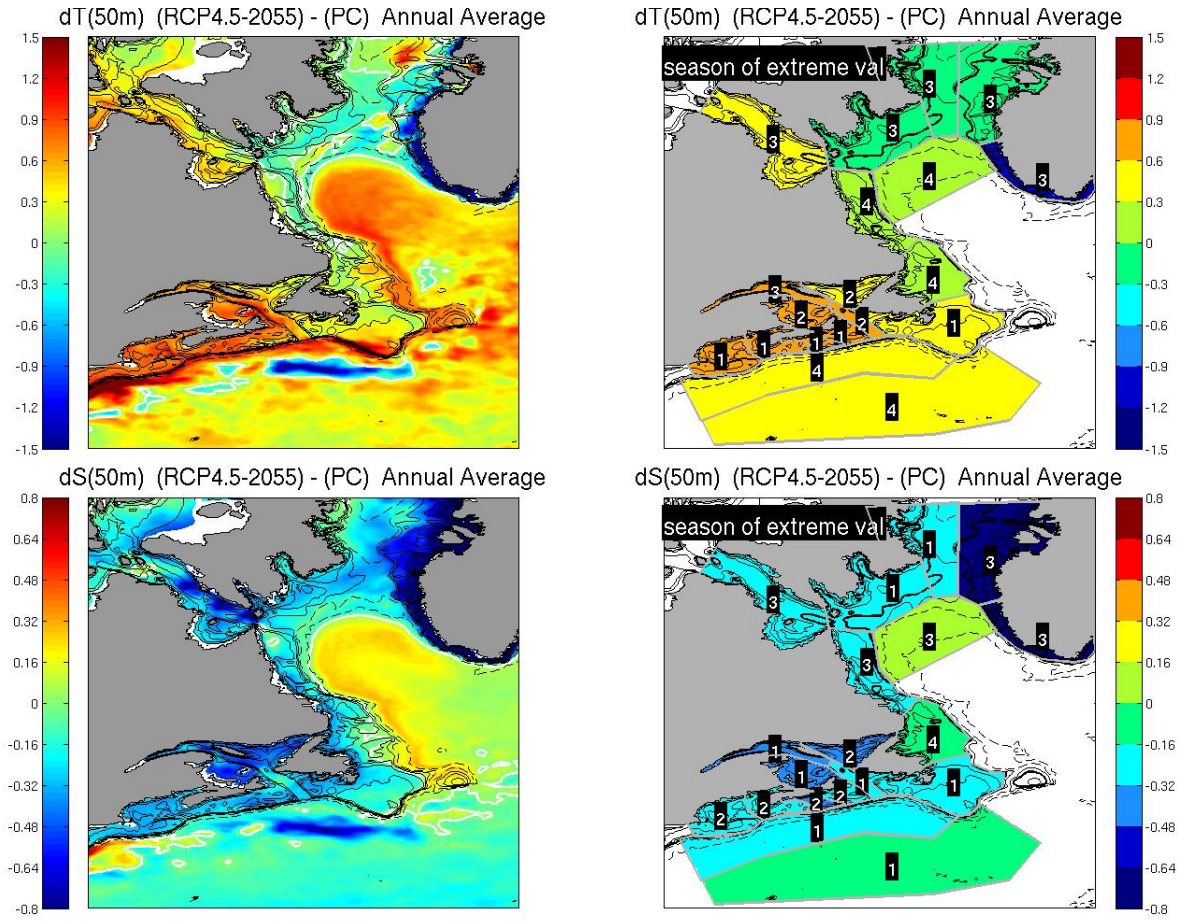

(a) (b)

Figure A11: Predicted annual change in T and S at 50m for RCP4.5-2055. (a) Spatial plot. (b) Region plot. The season of extrema in T and S change is annotated.

Table A11: Predicted changes in 50m T and S, (RCP4.5-2055)-(PC), by region, season, and on an annual basis.

	dT(°C)					**dS(PSU)**				
Region	**winter**	**spring**	**summer**	**fall**	**annual**	**winter**	**spring**	**summer**	**fall**	**annual**
S-Grnlnd-coast	-0.615	-1.084	-1.871	-1.075	-1.161	-0.470	-0.523	-1.663	-0.895	-0.888
N-Lab-Sea	0.256	0.179	0.281	0.436	0.288	-0.005	0.047	0.121	0.114	0.069
E-Davis-Str	0.764	-0.152	-1.168	0.042	-0.129	-0.559	-0.441	-0.957	-0.895	-0.713
W-Davis-Str	0.019	-0.186	-0.188	0.161	-0.048	-0.361	-0.109	-0.030	-0.354	-0.213
SW-Davis-Str	-0.078	-0.212	-0.328	0.228	-0.097	-0.337	-0.305	-0.192	-0.164	-0.250
Hudson-Str	0.078	0.189	0.675	0.565	0.377	-0.273	-0.367	-0.375	-0.246	-0.315
Lab-Shelf	-0.017	-0.095	-0.083	0.288	0.023	-0.141	-0.239	-0.269	-0.181	-0.208
N-Nfld-Shelf	0.314	0.198	0.164	0.372	0.262	-0.143	-0.122	-0.145	-0.189	-0.150
S-Nfld-Shelf	0.527	0.426	0.267	0.435	0.414	-0.270	-0.178	-0.116	-0.163	-0.182
L-Channel	0.758	0.828	0.405	0.652	0.661	-0.351	-0.332	-0.228	-0.157	-0.267
E-GSL	0.376	0.489	0.193	0.408	0.367	-0.480	-0.480	-0.420	-0.395	-0.444
SLE	0.426	0.642	0.711	0.647	0.607	-0.476	-0.451	-0.376	-0.343	-0.411
W-GSL	0.535	0.918	0.721	0.884	0.764	-0.529	-0.470	-0.376	-0.430	-0.451
ESS	0.974	0.789	0.222	0.825	0.702	-0.303	-0.372	-0.267	-0.231	-0.293
CSS	1.032	0.763	0.387	0.791	0.743	-0.373	-0.382	-0.329	-0.229	-0.328
WSS-BoF	1.050	0.719	0.645	0.655	0.767	-0.312	-0.352	-0.314	-0.175	-0.288
GoM	0.910	0.816	0.767	0.752	0.811	-0.267	-0.340	-0.334	-0.312	-0.313
Recirc-Zone	0.357	0.263	0.289	0.574	0.371	-0.214	-0.209	-0.137	-0.102	-0.166
Gulf-Stream	0.252	0.325	0.347	0.378	0.325	-0.124	-0.114	-0.117	-0.115	-0.117
H-Bay	0.261	0.379	0.725	0.651	0.504	-0.236	-0.291	-0.263	-0.166	-0.239

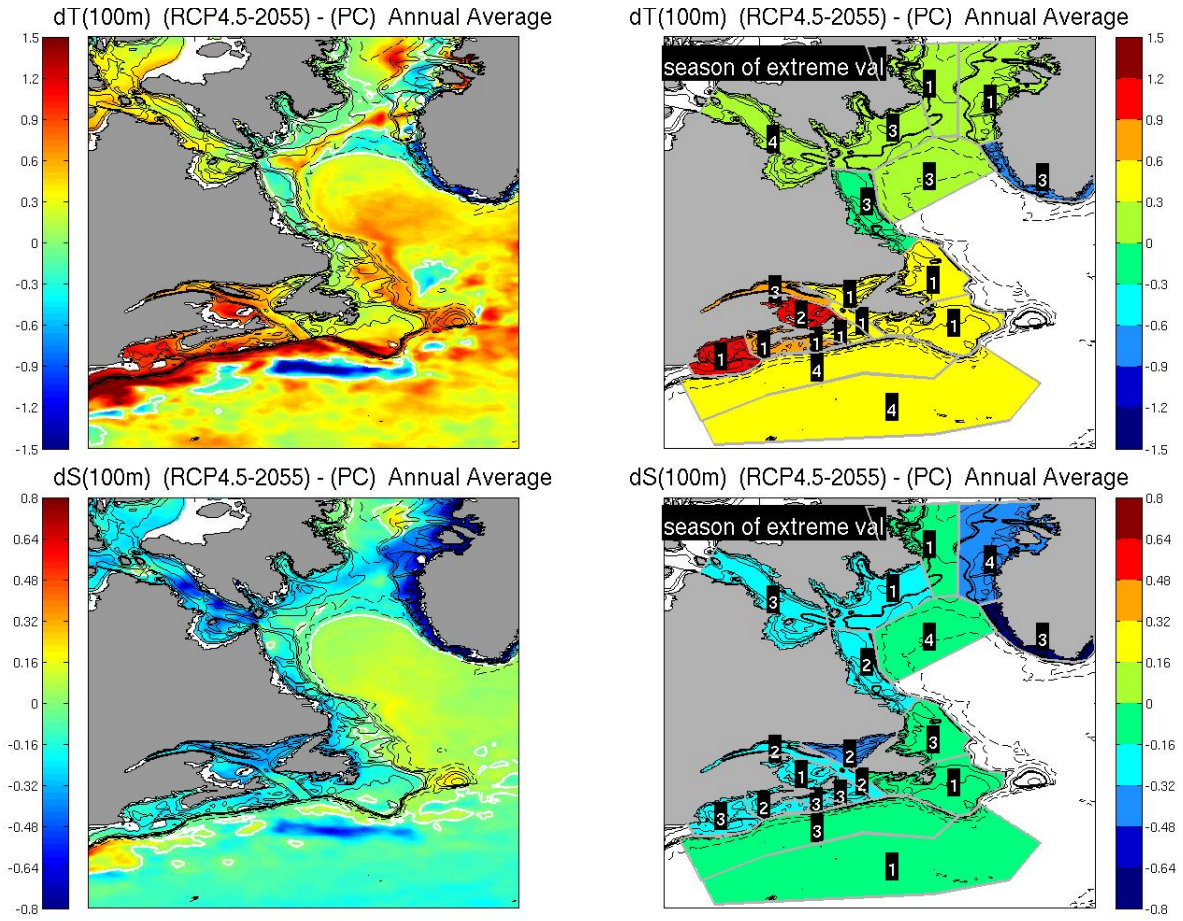

(a) (b)

Figure A12: Predicted annual change in T and S at 100m for RCP4.5-2055. (a) Spatial plot. (b) Region plot. The season of extrema in T and S change is annotated.

Table A12: Predicted changes in 100m T and S, (RCP4.5-2055)-(PC), by region, season, and on an annual basis.

	dT(°C)					**dS(PSU)**				
Region	**winter**	**spring**	**summer**	**fall**	**annual**	**winter**	**spring**	**summer**	**fall**	**annual**
S-Grnlnd-coast	-0.091	-0.883	-1.329	-0.677	-0.745	-0.350	-0.413	-1.160	-0.707	-0.658
N-Lab-Sea	0.191	0.131	0.202	0.116	0.160	-0.002	0.003	-0.001	-0.024	-0.006
E-Davis-Str	0.755	0.254	-0.444	0.070	0.159	-0.293	-0.269	-0.459	-0.527	-0.387
W-Davis-Str	0.296	0.037	-0.035	0.125	0.106	-0.254	-0.075	-0.003	-0.081	-0.103
SW-Davis-Str	0.163	0.101	-0.191	0.130	0.051	-0.290	-0.231	-0.112	-0.124	-0.189
Hudson-Str	0.180	0.174	0.307	0.344	0.251	-0.278	-0.318	-0.348	-0.243	-0.297
Lab-Shelf	0.058	-0.029	-0.128	0.053	-0.012	-0.117	-0.226	-0.207	-0.122	-0.168
N-Nfld-Shelf	0.514	0.198	0.236	0.346	0.323	-0.067	-0.100	-0.164	-0.153	-0.121
S-Nfld-Shelf	0.554	0.424	0.345	0.351	0.418	-0.143	-0.098	-0.093	-0.141	-0.119
L-Channel	0.689	0.492	0.315	0.468	0.491	-0.181	-0.252	-0.217	-0.167	-0.204
E-GSL	0.637	0.519	0.252	0.253	0.415	-0.356	-0.366	-0.318	-0.287	-0.332
SLE	0.661	0.653	0.693	0.546	0.638	-0.348	-0.354	-0.295	-0.216	-0.303
W-GSL	1.022	1.025	0.869	0.737	0.913	-0.298	-0.295	-0.266	-0.229	-0.272
ESS	0.911	0.629	0.087	0.740	0.592	-0.167	-0.226	-0.251	-0.152	-0.199
CSS	1.331	0.755	0.266	0.759	0.778	-0.200	-0.227	-0.250	-0.194	-0.218
WSS-BoF	1.340	0.802	0.594	0.550	0.822	-0.108	-0.242	-0.237	-0.142	-0.182
GoM	1.173	1.010	0.921	0.932	1.009	-0.136	-0.190	-0.210	-0.166	-0.175
Recirc-Zone	0.570	0.399	0.254	0.686	0.477	-0.086	-0.081	-0.087	-0.069	-0.081
Gulf-Stream	0.259	0.333	0.322	0.356	0.317	-0.118	-0.101	-0.092	-0.102	-0.104
H-Bay	0.502	0.515	0.589	0.601	0.552	-0.193	-0.212	-0.214	-0.189	-0.202

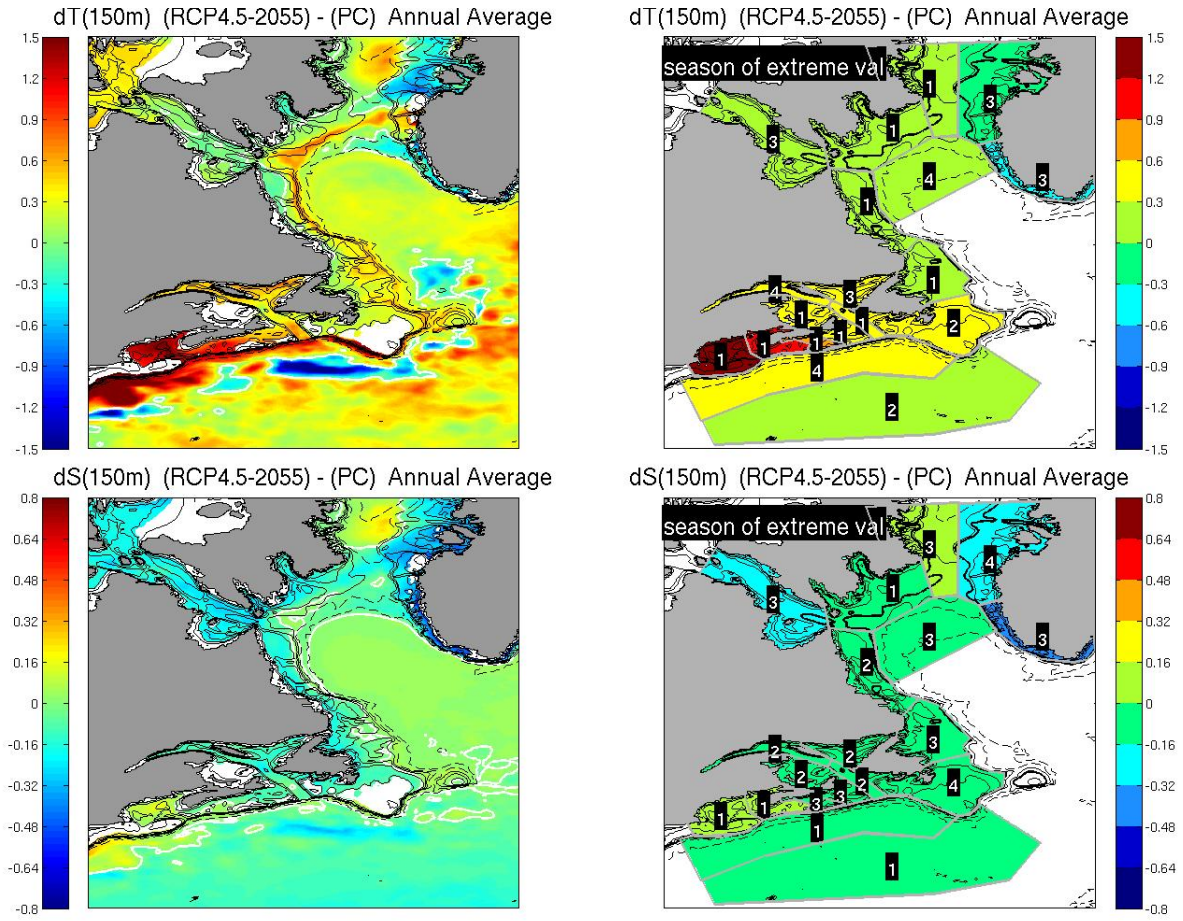

(a) (b)

Figure A13: Predicted annual change in T and S at 150m for RCP4.5-2055. (a) Spatial plot. (b) Region plot. The season of extrema in T and S change is annotated.

Table A13: Predicted changes in 150m T and S, (RCP4.5-2055)-(PC), by region, season, and on an annual basis.

	dT(°C)					**dS(PSU)**				
Region	**winter**	**spring**	**summer**	**fall**	**annual**	**winter**	**spring**	**summer**	**fall**	**annual**
S-Grnlnd-coast	-0.066	-0.523	-0.684	-0.245	-0.380	-0.277	-0.274	-0.465	-0.423	-0.360
N-Lab-Sea	0.134	0.099	0.118	0.139	0.123	-0.007	-0.008	-0.011	-0.005	-0.008
E-Davis-Str	-0.011	-0.102	-0.227	-0.106	-0.111	-0.170	-0.158	-0.221	-0.264	-0.203
W-Davis-Str	0.288	0.223	0.127	0.028	0.166	-0.015	0.003	0.025	-0.012	0.000
SW-Davis-Str	0.342	0.307	0.087	-0.042	0.173	-0.153	-0.144	-0.079	-0.069	-0.111
Hudson-Str	0.029	0.046	0.052	0.017	0.036	-0.193	-0.214	-0.219	-0.194	-0.205
Lab-Shelf	0.282	0.180	0.191	0.123	0.194	-0.062	-0.192	-0.122	-0.049	-0.106
N-Nfld-Shelf	0.344	0.269	0.239	0.308	0.290	-0.030	-0.059	-0.112	-0.089	-0.073
S-Nfld-Shelf	0.391	0.414	0.347	0.289	0.360	-0.087	-0.048	-0.056	-0.105	-0.074
L-Channel	0.498	0.412	0.287	0.393	0.397	-0.086	-0.115	-0.110	-0.079	-0.097
E-GSL	0.444	0.525	0.602	0.463	0.508	-0.133	-0.156	-0.102	-0.077	-0.117
SLE	0.453	0.451	0.487	0.529	0.480	-0.127	-0.129	-0.093	-0.068	-0.104
W-GSL	0.475	0.338	0.346	0.406	0.391	-0.089	-0.121	-0.110	-0.075	-0.099
ESS	0.647	0.575	0.339	0.409	0.493	-0.079	-0.092	-0.113	-0.092	-0.094
CSS	1.031	0.847	0.589	0.680	0.787	-0.016	-0.059	-0.085	-0.042	-0.051
WSS-BoF	1.328	1.081	0.825	0.956	1.047	0.068	-0.028	-0.056	0.032	0.004
GoM	1.469	1.289	1.271	1.321	1.338	0.125	0.067	0.065	0.100	0.089
Recirc-Zone	0.439	0.321	0.324	0.673	0.439	-0.048	-0.045	-0.045	-0.031	-0.042
Gulf-Stream	0.265	0.318	0.284	0.276	0.286	-0.101	-0.090	-0.089	-0.091	-0.093
H-Bay	0.493	0.491	0.502	0.512	0.499	-0.090	-0.086	-0.089	-0.095	-0.090

Results for RCP 4.5 – 2075 Climatology

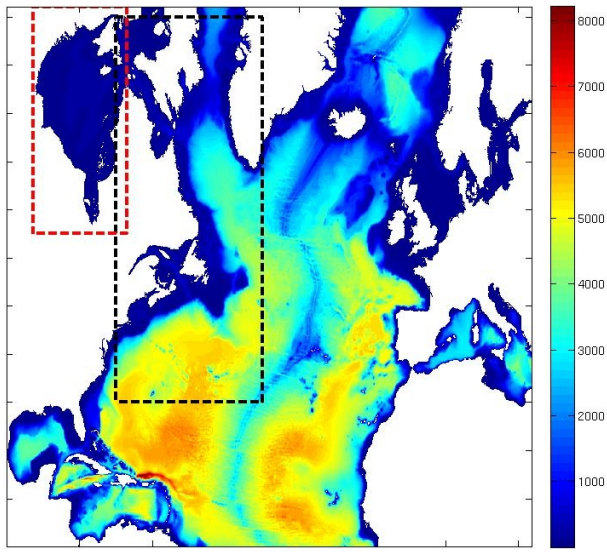

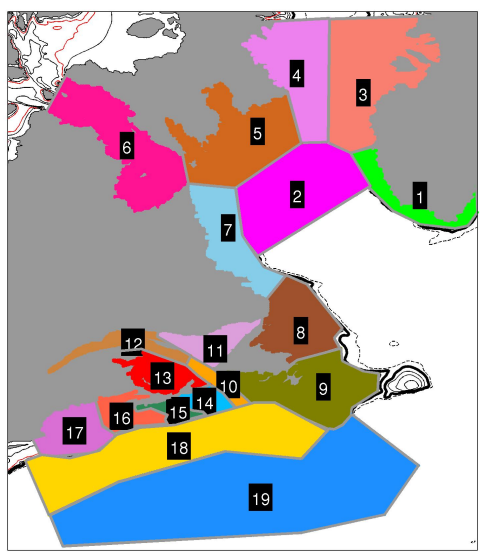

Reminder of model domains and regions used for various analyses.

For region names see table 4

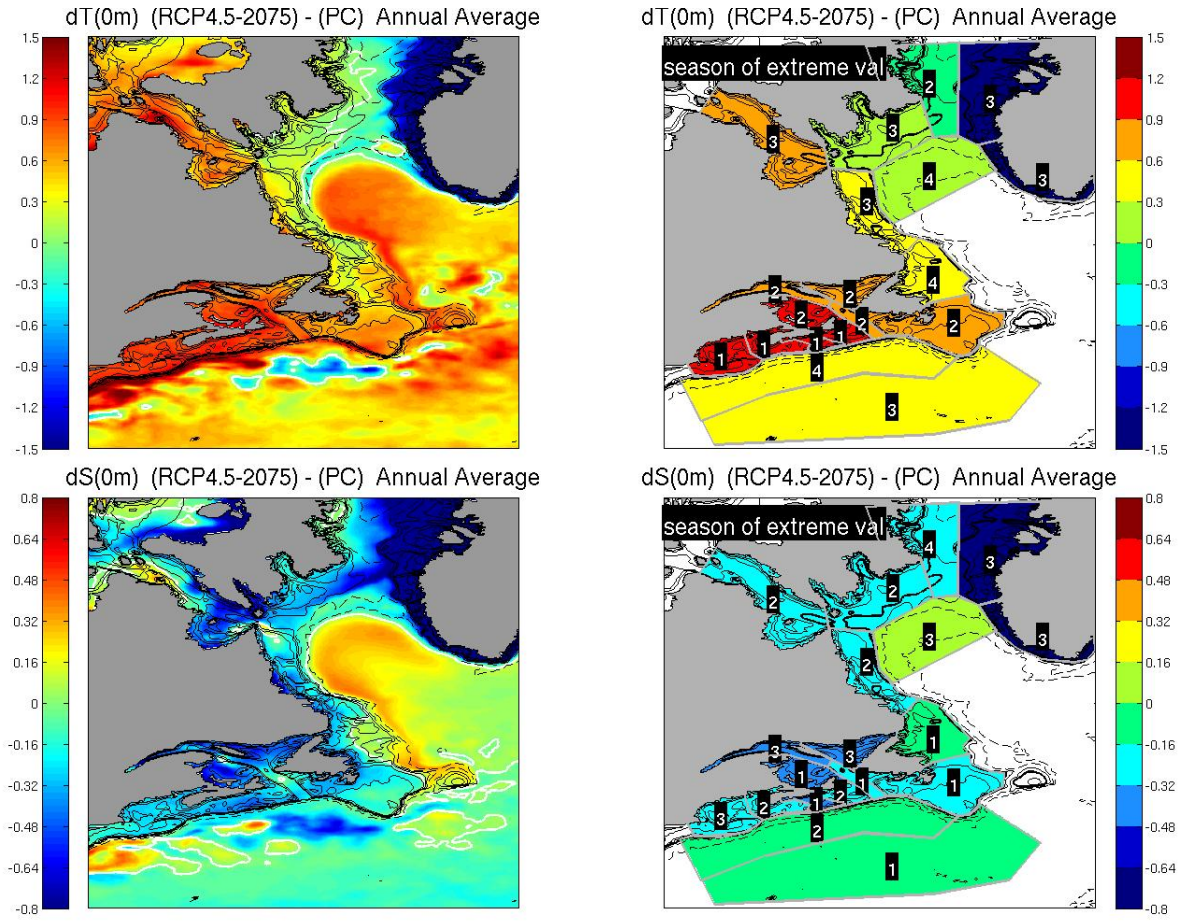

(a) (b)

Figure A14: Predicted annual change in T and S at 0m for RCP4.5-2075. (a) Spatial plot. (b) Region plot. The season of extrema in T and S change is annotated.

Table A14: Predicted changes in 0m T and S, (RCP4.5-2075)-(PC), by region, season, and on an annual basis.

	dT(°C)					**dS(PSU)**				
Region	**winter**	**spring**	**summer**	**fall**	**annual**	**winter**	**spring**	**summer**	**fall**	**annual**
S-Grnlnd-coast	-0.952	-1.468	-2.380	-1.359	-1.540	-0.583	-0.942	-2.462	-1.076	-1.266
N-Lab-Sea	0.162	0.125	0.369	0.531	0.297	-0.036	0.077	0.284	0.110	0.109
E-Davis-Str	-0.023	-1.714	-3.092	-0.890	-1.430	-0.764	-1.462	-3.416	-1.543	-1.796
W-Davis-Str	-0.017	-0.244	0.181	0.043	-0.009	-0.373	-0.272	-0.069	-0.521	-0.309
SW-Davis-Str	-0.052	-0.118	0.380	0.333	0.136	-0.328	-0.502	-0.270	-0.161	-0.315
Hudson-Str	0.029	0.599	1.445	0.728	0.700	-0.261	-0.466	-0.128	-0.235	-0.273
Lab-Shelf	-0.005	0.255	0.547	0.443	0.310	-0.199	-0.370	-0.232	-0.229	-0.258
N-Nfld-Shelf	0.307	0.414	0.239	0.526	0.372	-0.188	-0.121	0.014	-0.185	-0.120
S-Nfld-Shelf	0.612	0.713	0.611	0.615	0.638	-0.257	-0.189	-0.107	-0.169	-0.180
L-Channel	0.961	1.080	0.652	0.787	0.870	-0.288	-0.156	-0.160	-0.195	-0.200
E-GSL	0.387	0.995	0.602	0.673	0.664	-0.442	-0.482	-0.511	-0.360	-0.449
SLE	0.380	1.261	0.885	0.785	0.828	-0.437	-0.179	-0.620	-0.468	-0.426
W-GSL	0.570	1.370	0.827	0.995	0.940	-0.597	-0.423	-0.283	-0.434	-0.434
ESS	1.067	1.060	0.753	0.902	0.946	-0.359	-0.379	-0.179	-0.222	-0.285
CSS	1.110	0.990	0.717	0.983	0.950	-0.483	-0.419	-0.369	-0.223	-0.373
WSS-BoF	1.128	1.067	0.778	0.834	0.952	-0.311	-0.392	-0.389	-0.178	-0.318
GoM	1.102	1.053	0.794	0.912	0.965	-0.140	-0.277	-0.335	-0.223	-0.244
Recirc-Zone	0.666	0.260	0.436	0.820	0.545	-0.096	-0.234	-0.189	-0.002	-0.130
Gulf-Stream	0.322	0.478	0.490	0.429	0.430	-0.098	-0.060	-0.080	-0.070	-0.077
H-Bay	0.029	0.854	1.293	0.781	0.739	-0.334	-0.370	0.016	-0.145	-0.208

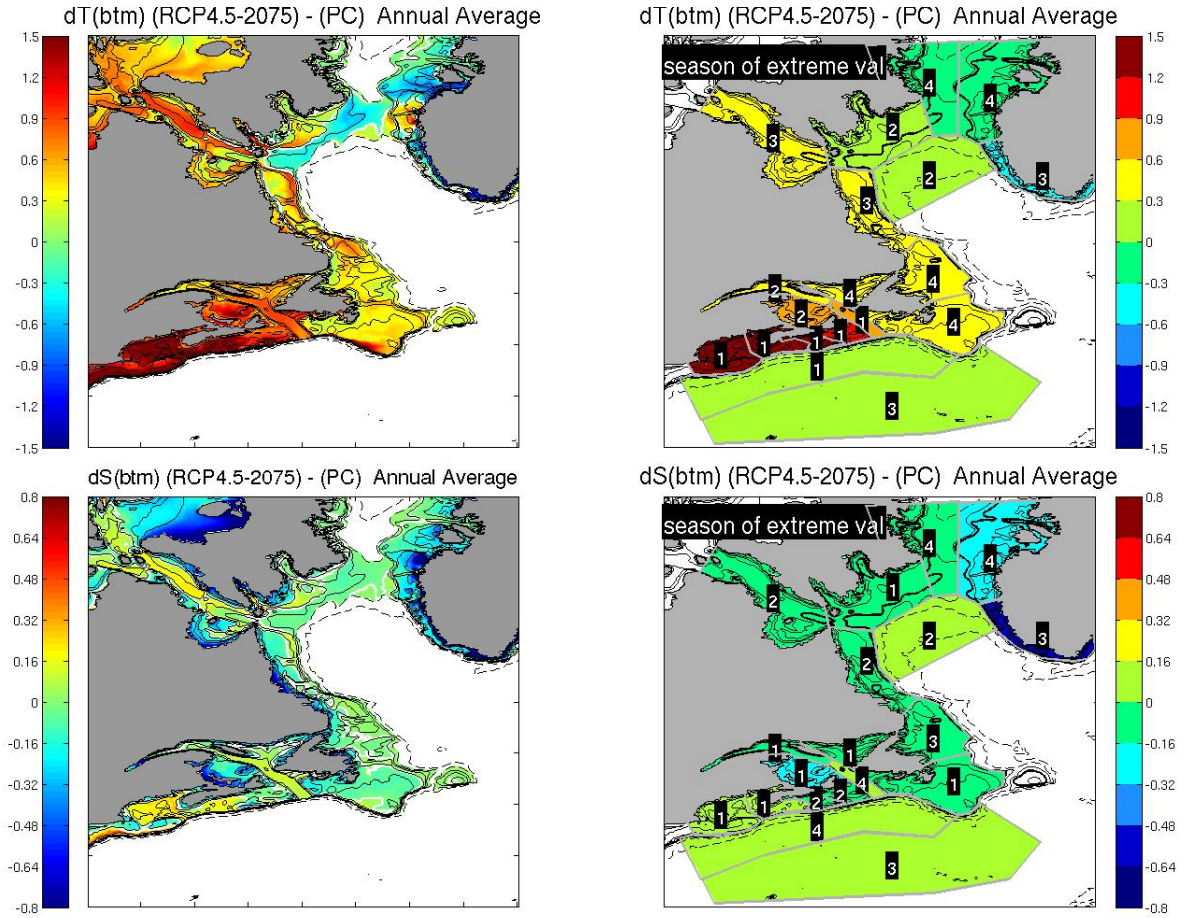

(a) (b)

Figure A15: Predicted annual change in bottom T and S for RCP4.5-2075. (a) Spatial plot. (b) Region plot. The season of extrema in T and S change is annotated. Deep water region is masked out for clarity.

Table A15: Predicted changes in bottom T and S, (RCP4.5-2075)-(PC), by region, season, and on an annual basis.

	dT(°C)					**dS(PSU)**				
Region	**winter**	**spring**	**summer**	**fall**	**annual**	**winter**	**spring**	**summer**	**fall**	**annual**
S-Grnlnd-coast	0.023	-0.503	-1.043	-0.362	-0.471	-0.340	-0.430	-0.942	-0.539	-0.563
N-Lab-Sea	0.085	0.139	0.123	0.100	0.112	0.018	0.028	0.022	0.017	0.021
E-Davis-Str	-0.026	-0.091	-0.252	-0.262	-0.158	-0.125	-0.115	-0.208	-0.243	-0.173
W-Davis-Str	-0.030	-0.028	-0.074	-0.103	-0.059	-0.013	-0.009	-0.009	-0.019	-0.013
SW-Davis-Str	-0.041	0.163	0.061	-0.039	0.036	-0.073	-0.054	-0.057	-0.066	-0.062
Hudson-Str	0.436	0.518	0.613	0.538	0.526	-0.055	-0.081	-0.053	-0.067	-0.064
Lab-Shelf	0.242	0.460	0.494	0.376	0.393	-0.104	-0.146	-0.076	-0.079	-0.101
N-Nfld-Shelf	0.345	0.326	0.350	0.450	0.368	-0.044	-0.051	-0.053	-0.023	-0.043
S-Nfld-Shelf	0.450	0.445	0.452	0.462	0.452	-0.086	-0.036	-0.027	-0.064	-0.053
L-Channel	0.880	0.827	0.814	0.829	0.837	0.091	0.087	0.092	0.094	0.091
E-GSL	0.515	0.575	0.530	0.602	0.556	-0.161	-0.149	-0.071	-0.053	-0.108
SLE	0.439	0.588	0.577	0.574	0.544	-0.153	-0.119	-0.048	-0.032	-0.088
W-GSL	0.801	1.149	0.819	0.829	0.900	-0.387	-0.305	-0.201	-0.175	-0.267
ESS	1.067	0.847	0.738	0.973	0.906	-0.052	-0.076	-0.045	-0.007	-0.045
CSS	1.588	1.169	0.840	1.262	1.215	-0.075	-0.093	-0.053	0.011	-0.052
WSS-BoF	1.641	1.536	1.242	1.206	1.406	0.083	0.008	-0.013	0.071	0.037
GoM	1.642	1.525	1.471	1.398	1.509	0.119	0.052	0.056	0.102	0.082
Recirc-Zone	0.072	0.051	0.047	0.070	0.060	0.009	0.006	0.006	0.009	0.007
Gulf-Stream	0.001	0.002	0.006	0.005	0.004	0.001	0.001	0.001	0.001	0.001
H-Bay	0.481	0.617	0.719	0.659	0.619	-0.135	-0.157	-0.102	-0.127	-0.130

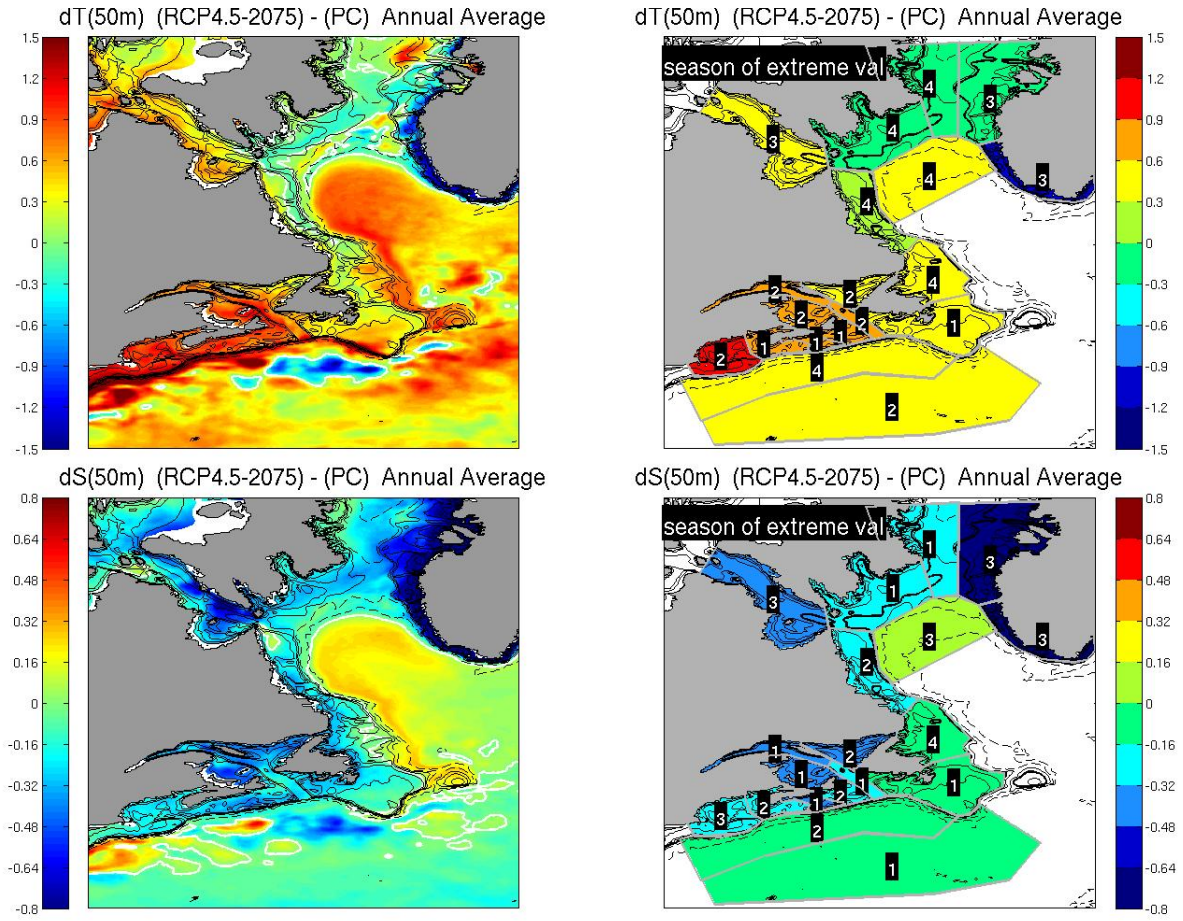

(a) (b)

Figure A16: Predicted annual change in T and S at 50m for RCP4.5-2075. (a) Spatial plot. (b) Region plot. The season of extrema in T and S change is annotated.

Table A16: Predicted changes in 50m T and S, (RCP4.5-2075)-(PC), by region, season, and on an annual basis.

	dT(°C)					**dS(PSU)**				
Region	**winter**	**spring**	**summer**	**fall**	**annual**	**winter**	**spring**	**summer**	**fall**	**annual**
S-Grnlnd-coast	-0.577	-1.024	-1.785	-1.029	-1.104	-0.469	-0.530	-1.659	-0.886	-0.886
N-Lab-Sea	0.306	0.261	0.367	0.478	0.353	0.003	0.055	0.130	0.109	0.074
E-Davis-Str	0.790	-0.091	-1.092	0.063	-0.083	-0.564	-0.439	-0.946	-0.901	-0.713
W-Davis-Str	0.034	-0.157	-0.132	0.174	-0.020	-0.359	-0.120	-0.040	-0.338	-0.214
SW-Davis-Str	-0.071	-0.184	-0.226	0.317	-0.041	-0.331	-0.302	-0.178	-0.139	-0.237
Hudson-Str	0.074	0.208	0.830	0.692	0.451	-0.290	-0.381	-0.388	-0.280	-0.335
Lab-Shelf	-0.009	-0.054	0.021	0.359	0.079	-0.143	-0.248	-0.236	-0.131	-0.190
N-Nfld-Shelf	0.367	0.248	0.237	0.491	0.336	-0.140	-0.131	-0.129	-0.152	-0.138
S-Nfld-Shelf	0.606	0.450	0.294	0.500	0.462	-0.232	-0.148	-0.095	-0.137	-0.153
L-Channel	0.931	0.999	0.548	0.743	0.805	-0.287	-0.269	-0.208	-0.175	-0.235
E-GSL	0.480	0.602	0.262	0.552	0.474	-0.402	-0.410	-0.345	-0.326	-0.371
SLE	0.486	0.763	0.752	0.692	0.673	-0.407	-0.407	-0.316	-0.291	-0.355
W-GSL	0.628	1.055	0.836	0.994	0.878	-0.494	-0.392	-0.299	-0.363	-0.387
ESS	1.063	0.891	0.635	0.914	0.876	-0.336	-0.343	-0.147	-0.167	-0.248
CSS	1.105	0.868	0.468	0.974	0.854	-0.500	-0.401	-0.276	-0.166	-0.336
WSS-BoF	1.189	0.983	0.694	0.702	0.892	-0.285	-0.329	-0.315	-0.120	-0.262
GoM	1.116	1.120	1.022	0.918	1.044	-0.141	-0.244	-0.266	-0.194	-0.211
Recirc-Zone	0.794	0.252	0.182	0.909	0.534	-0.032	-0.132	-0.108	0.027	-0.061
Gulf-Stream	0.325	0.476	0.434	0.415	0.412	-0.095	-0.053	-0.051	-0.066	-0.066
H-Bay	0.297	0.466	0.913	0.800	0.619	-0.240	-0.301	-0.261	-0.163	-0.241

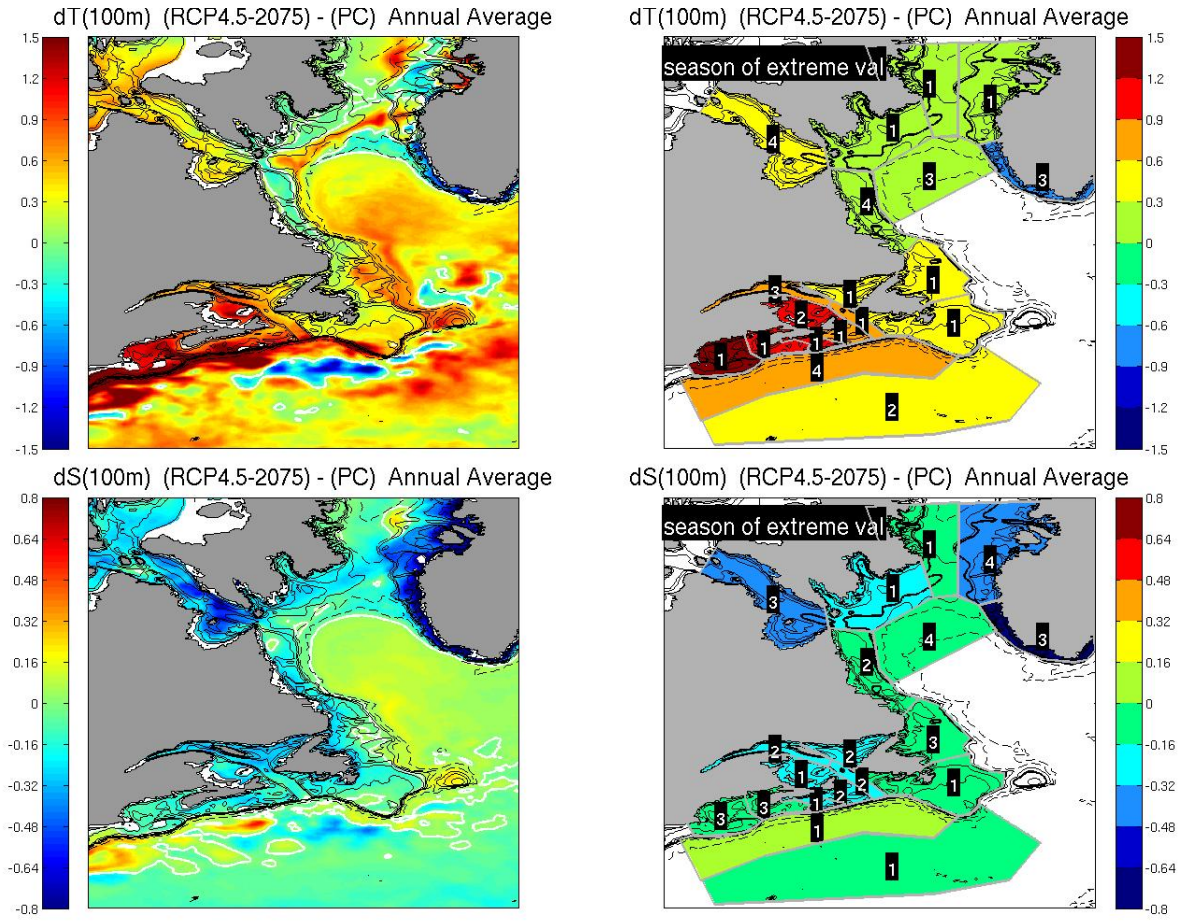

(a) (b)

Figure A17: Predicted annual change in T and S at 100m for RCP4.5-2075. (a) Spatial plot. (b) Region plot. The season of extrema in T and S change is annotated.

Table A17: Predicted changes in 100m T and S, (RCP4.5-2075)-(PC), by region, season, and on an annual basis.

	dT(°C)					**dS(PSU)**				
Region	**winter**	**spring**	**summer**	**fall**	**annual**	**winter**	**spring**	**summer**	**fall**	**annual**
S-Grnlnd-coast	-0.068	-0.860	-1.248	-0.644	-0.705	-0.350	-0.423	-1.159	-0.702	-0.658
N-Lab-Sea	0.209	0.176	0.256	0.156	0.199	0.001	0.007	0.005	-0.027	-0.003
E-Davis-Str	0.791	0.292	-0.401	0.074	0.189	-0.294	-0.267	-0.457	-0.542	-0.390
W-Davis-Str	0.316	0.051	-0.030	0.136	0.118	-0.256	-0.084	-0.019	-0.092	-0.113
SW-Davis-Str	0.214	0.156	-0.134	0.198	0.108	-0.278	-0.216	-0.103	-0.107	-0.176
Hudson-Str	0.244	0.229	0.405	0.489	0.342	-0.313	-0.363	-0.404	-0.310	-0.347
Lab-Shelf	0.073	0.006	-0.072	0.115	0.030	-0.123	-0.233	-0.186	-0.093	-0.159
N-Nfld-Shelf	0.583	0.230	0.294	0.425	0.383	-0.058	-0.111	-0.155	-0.126	-0.112
S-Nfld-Shelf	0.571	0.404	0.349	0.403	0.432	-0.127	-0.075	-0.074	-0.126	-0.100
L-Channel	0.784	0.618	0.546	0.639	0.647	-0.150	-0.209	-0.202	-0.171	-0.183
E-GSL	0.612	0.520	0.283	0.327	0.436	-0.319	-0.332	-0.283	-0.242	-0.294
SLE	0.652	0.665	0.718	0.555	0.648	-0.305	-0.327	-0.263	-0.176	-0.268
W-GSL	1.115	1.138	0.979	0.815	1.012	-0.250	-0.229	-0.207	-0.178	-0.216
ESS	1.105	0.733	0.504	0.842	0.796	-0.195	-0.213	-0.143	-0.092	-0.161
CSS	1.617	0.874	0.481	1.106	1.019	-0.315	-0.268	-0.183	-0.089	-0.214
WSS-BoF	1.671	1.192	0.759	0.665	1.072	-0.071	-0.207	-0.229	-0.107	-0.153
GoM	1.443	1.378	1.252	1.225	1.325	-0.064	-0.108	-0.146	-0.085	-0.101
Recirc-Zone	0.949	0.458	0.305	1.106	0.704	0.075	0.010	-0.032	0.018	0.018
Gulf-Stream	0.344	0.473	0.379	0.362	0.389	-0.083	-0.050	-0.033	-0.052	-0.054
H-Bay	0.583	0.595	0.698	0.721	0.649	-0.199	-0.218	-0.221	-0.196	-0.208

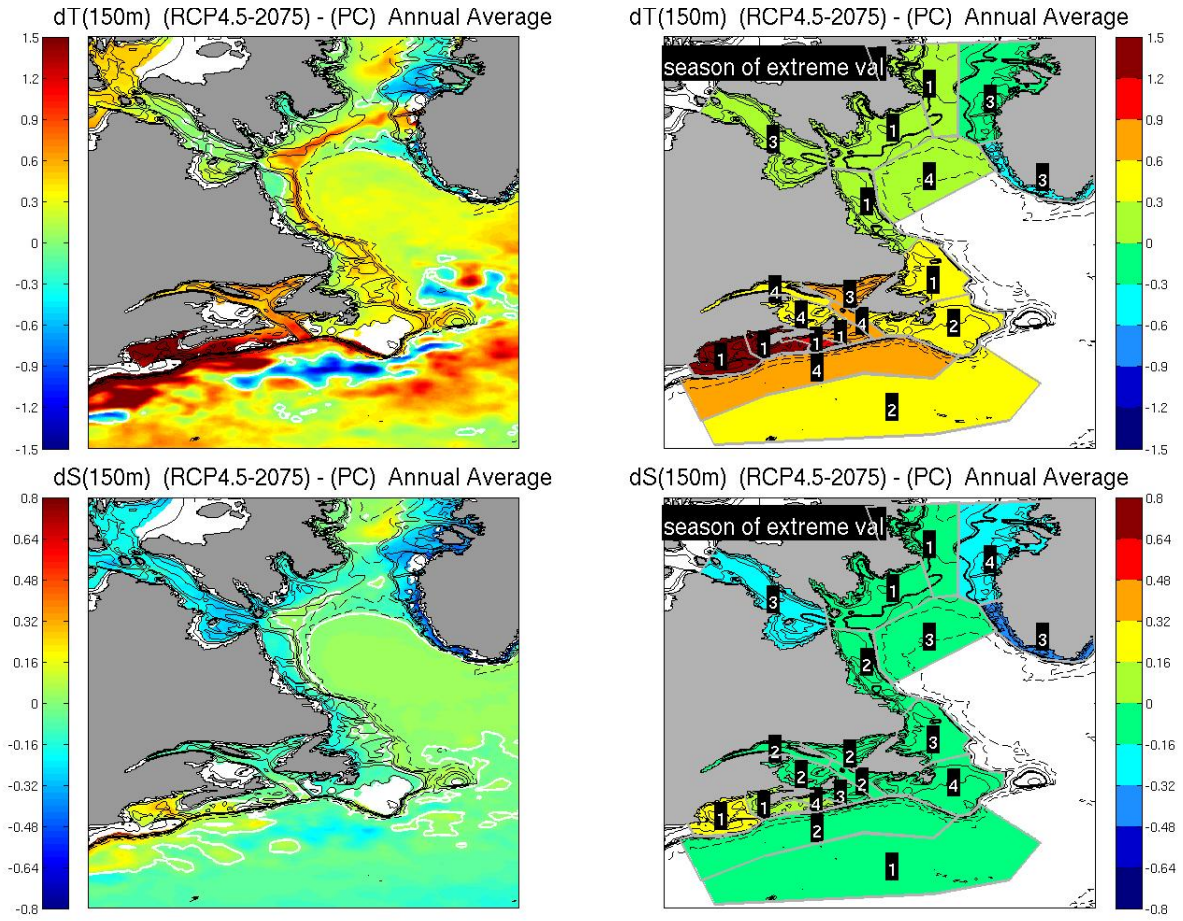

(a) (b)

Figure A18: Predicted annual change in T and S at 150m for RCP4.5-2075. (a) Spatial plot. (b) Region plot. The season of extrema in T and S change is annotated.

Table A18: Predicted changes in 150m T and S, (RCP4.5-2075)-(PC), by region, season, and on an annual basis.

	dT(°C)					**dS(PSU)**				
Region	**winter**	**spring**	**summer**	**fall**	**annual**	**winter**	**spring**	**summer**	**fall**	**annual**
S-Grnlnd-coast	-0.054	-0.522	-0.615	-0.222	-0.353	-0.278	-0.285	-0.465	-0.418	-0.361
N-Lab-Sea	0.157	0.132	0.154	0.196	0.160	-0.002	-0.005	-0.007	-0.002	-0.004
E-Davis-Str	0.023	-0.080	-0.205	-0.092	-0.089	-0.171	-0.160	-0.224	-0.276	-0.208
W-Davis-Str	0.297	0.203	0.100	0.036	0.159	-0.029	-0.019	0.004	-0.025	-0.017
SW-Davis-Str	0.396	0.359	0.114	-0.014	0.214	-0.141	-0.129	-0.069	-0.066	-0.101
Hudson-Str	0.082	0.094	0.101	0.084	0.090	-0.216	-0.234	-0.240	-0.226	-0.229
Lab-Shelf	0.292	0.243	0.223	0.147	0.226	-0.072	-0.186	-0.115	-0.046	-0.105
N-Nfld-Shelf	0.359	0.271	0.292	0.358	0.320	-0.033	-0.071	-0.106	-0.076	-0.071
S-Nfld-Shelf	0.427	0.431	0.397	0.395	0.412	-0.079	-0.042	-0.055	-0.092	-0.067
L-Channel	0.738	0.626	0.775	0.811	0.737	-0.032	-0.084	-0.046	-0.017	-0.045
E-GSL	0.582	0.592	0.658	0.628	0.615	-0.108	-0.153	-0.105	-0.052	-0.105
SLE	0.498	0.500	0.539	0.593	0.533	-0.110	-0.124	-0.084	-0.052	-0.093
W-GSL	0.587	0.487	0.529	0.644	0.562	-0.042	-0.099	-0.097	-0.033	-0.068
ESS	1.037	0.802	0.665	0.871	0.844	-0.021	-0.049	-0.052	-0.001	-0.031
CSS	1.402	1.122	0.932	1.148	1.151	0.022	-0.033	-0.025	0.050	0.004
WSS-BoF	1.965	1.720	1.340	1.396	1.605	0.199	0.089	0.034	0.121	0.111
GoM	2.017	1.876	1.800	1.767	1.865	0.241	0.194	0.182	0.203	0.205
Recirc-Zone	0.746	0.362	0.492	1.128	0.682	-0.014	-0.037	-0.019	0.037	-0.008
Gulf-Stream	0.330	0.414	0.325	0.286	0.339	-0.071	-0.054	-0.054	-0.056	-0.059
H-Bay	0.559	0.557	0.570	0.580	0.566	-0.095	-0.091	-0.092	-0.099	-0.094

Results for Stratification changes

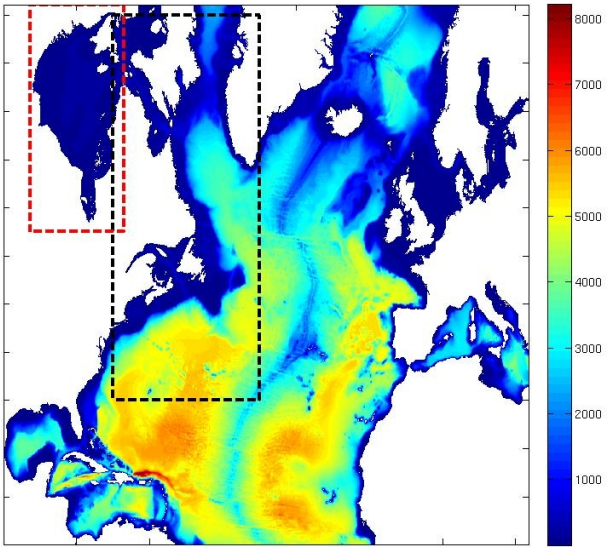

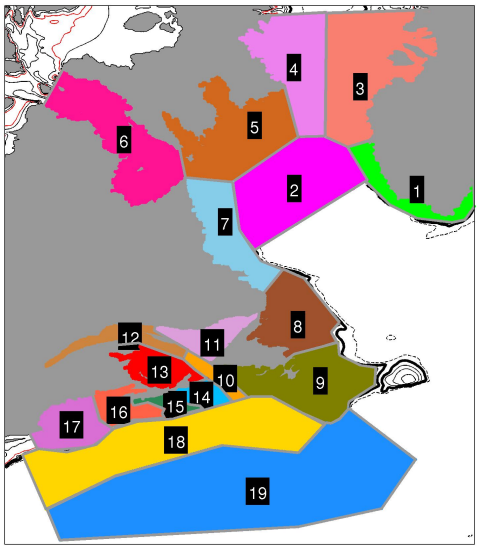

Reminder of model domains and regions used for various analyses.

For region names see table 4

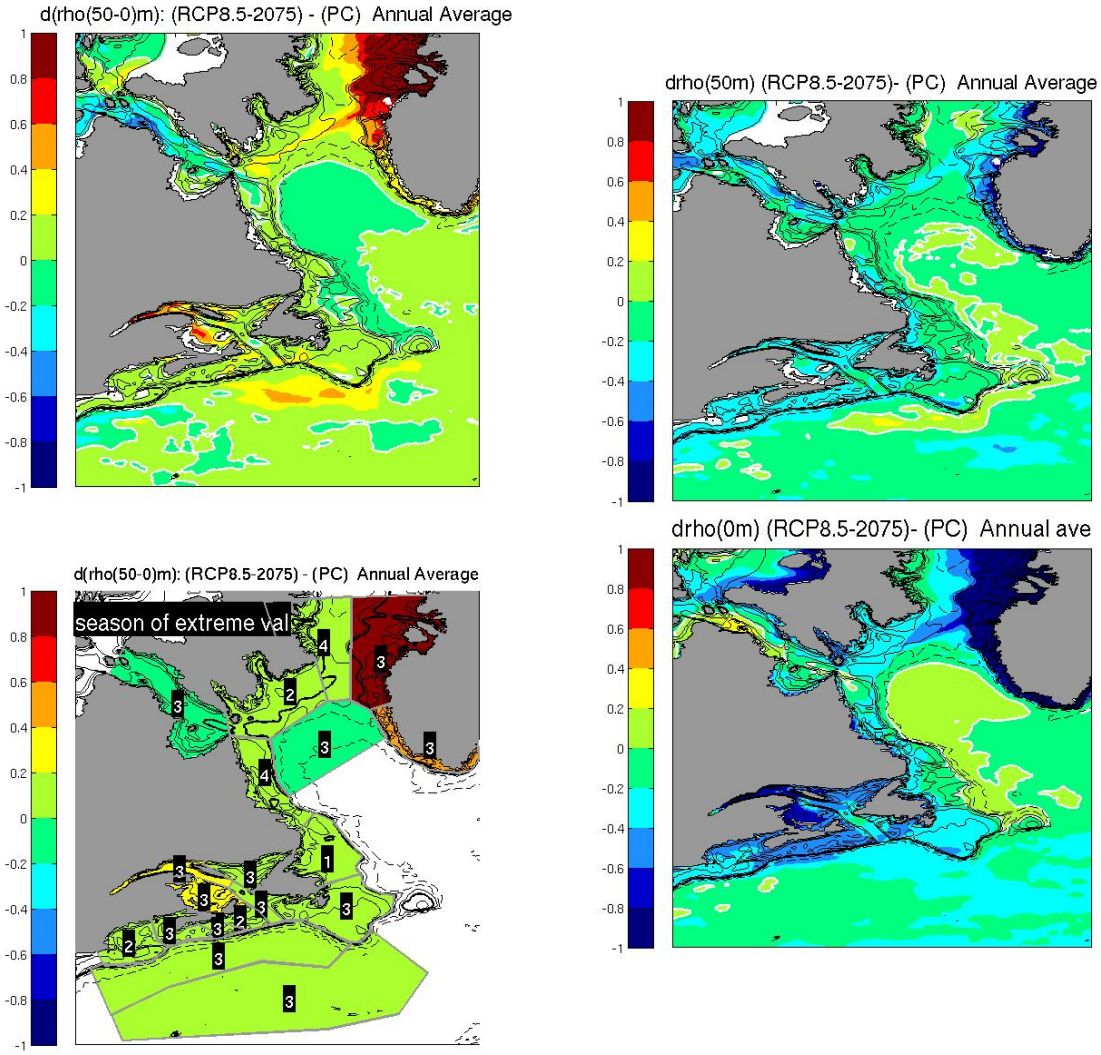

(b)

(a)

Figure A19: (a) Predicted annual change in 50m-0m stratification for RCP8.5-2075 – spatial and regional plots. The season of extrema in stratification change is annotated. (b) Predicted annual change in 50m and 0m density for RCP8.5-2075.

Table A19: Predicted changes in 50m-0m stratification, (RCP8.5-2075)-(PC), by region, season, and on an annual basis. The units are kg·m^{-3}.

Region	**winter**	**spring**	**summer**	**fall**	**annual**
S-Grnlnd-coast	0.153	0.366	0.877	0.243	0.410
N-Lab-Sea	0.019	-0.027	-0.134	-0.044	-0.046
E-Davis-Str	0.323	0.925	2.099	0.741	1.022
W-Davis-Str	0.094	0.162	0.106	0.361	0.181
SW-Davis-Str	0.033	0.243	0.192	0.060	0.132
Hudson-Str	-0.130	0.033	-0.193	-0.142	-0.108
Lab-Shelf	0.080	0.038	0.072	0.117	0.077
N-Nfld-Shelf	0.111	0.038	-0.088	0.066	0.032
S-Nfld-Shelf	0.098	0.157	0.158	0.082	0.124
L-Channel	0.106	0.055	0.109	0.087	0.089
E-GSL	0.091	0.183	0.312	0.164	0.188
SLE	0.269	0.170	0.604	0.388	0.358
W-GSL	0.282	0.361	0.400	0.354	0.349
ESS	0.107	0.250	0.220	0.181	0.189
CSS	0.109	0.208	0.249	0.119	0.171
WSS-BoF	0.105	0.246	0.256	0.094	0.175
GoM	-0.007	0.160	0.156	0.038	0.087
Recirc-Zone	0.074	0.088	0.186	0.104	0.113
Gulf-Stream	0.005	0.032	0.111	0.024	0.043
H-Bay	0.022	0.035	-0.171	-0.149	-0.066

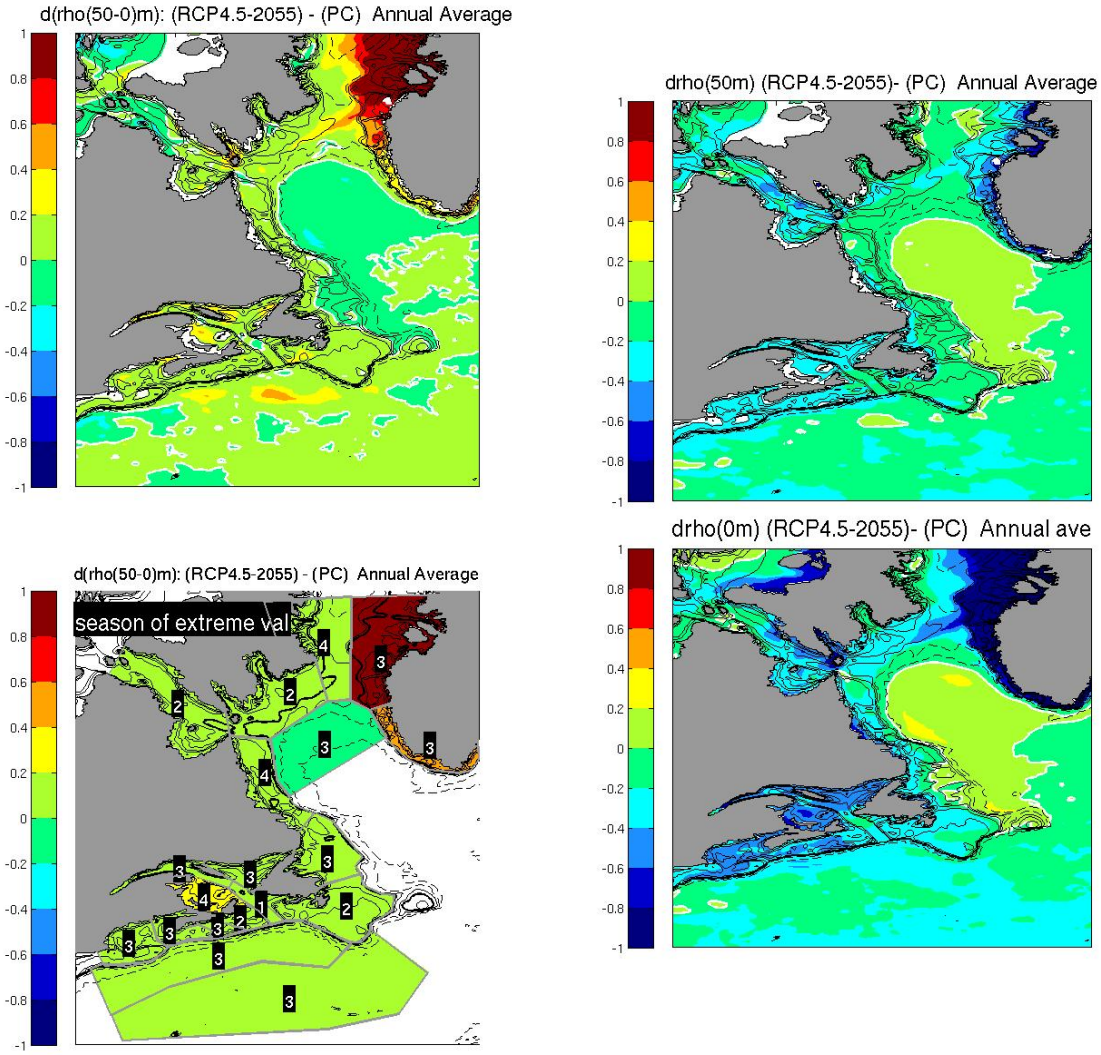

(b)

(a)

Figure A20: (a) Predicted annual change in 50m-0m stratification for RCP4.5-2055 – spatial and regional plots. The season of extrema in stratification change is annotated. (b) Predicted annual change in 50m and 0m density for RCP4.5-2055.

Table A20: Predicted changes in 50m-0m stratification, (RCP4.5-2055)-(PC), by region, season, and on an annual basis. The units are kg·m^{-3}.

Region	**winter**	**spring**	**summer**	**fall**	**annual**
S-Grnlnd-coast	0.142	0.360	0.901	0.249	0.413
N-Lab-Sea	0.027	-0.051	-0.200	-0.078	-0.075
E-Davis-Str	0.329	0.846	2.186	0.777	1.034
W-Davis-Str	0.083	0.131	0.094	0.377	0.171
SW-Davis-Str	0.028	0.219	0.186	0.065	0.125
Hudson-Str	-0.020	0.149	0.001	0.017	0.037
Lab-Shelf	0.062	0.139	0.116	0.176	0.123
N-Nfld-Shelf	0.085	0.023	-0.116	0.065	0.014
S-Nfld-Shelf	0.117	0.123	0.091	0.086	0.104
L-Channel	0.133	0.017	0.064	0.064	0.070
E-GSL	0.106	0.187	0.270	0.145	0.177
SLE	0.093	-0.093	0.345	0.232	0.144
W-GSL	0.231	0.205	0.144	0.255	0.209
ESS	0.119	0.197	0.143	0.160	0.155
CSS	0.087	0.174	0.228	0.106	0.149
WSS-BoF	0.130	0.194	0.256	0.139	0.180
GoM	0.056	0.162	0.237	0.157	0.153
Recirc-Zone	0.075	0.118	0.156	0.024	0.093
Gulf-Stream	0.004	0.017	0.081	0.021	0.031
H-Bay	0.068	0.133	-0.087	-0.064	0.013

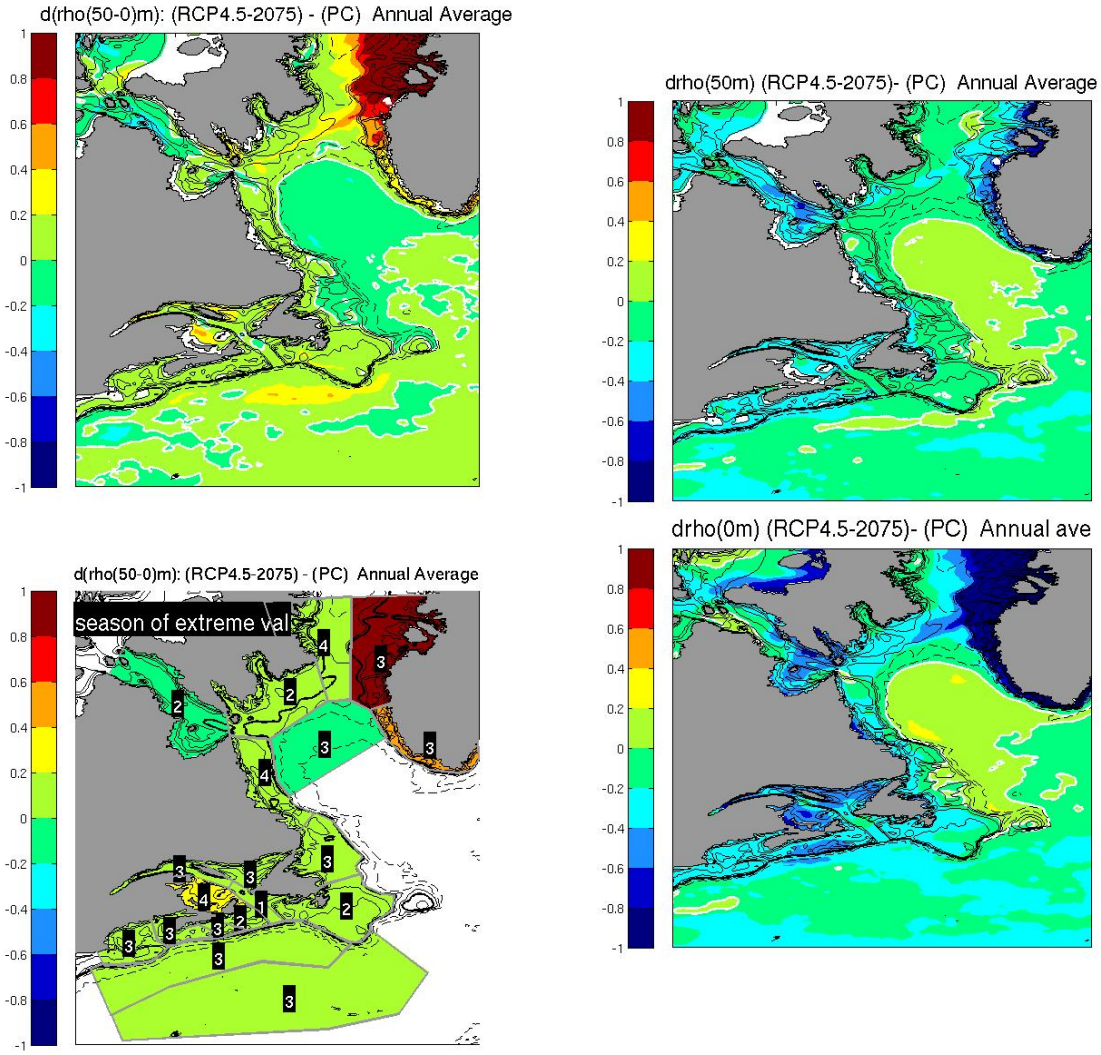

(b)

(a)

Figure A21: (a) Predicted annual change in 50m-0m stratification for RCP4.5-2075 – spatial and regional plots. The season of extrema in stratification change is annotated. (b) Predicted annual change in 50m and 0m density for RCP4.5-2075.

Table A21: Predicted changes in 50m-0m stratification, (RCP4.5-2075)-(PC), by region, season, and on an annual basis. The units are kg·m^{-3}.

Region	**winter**	**spring**	**summer**	**fall**	**annual**
S-Grnlnd-coast	0.144	0.361	0.896	0.247	0.412
N-Lab-Sea	0.026	-0.053	-0.196	-0.077	-0.075
E-Davis-Str	0.331	0.859	2.151	0.755	1.024
W-Davis-Str	0.079	0.135	0.057	0.346	0.154
SW-Davis-Str	0.029	0.218	0.177	0.053	0.119
Hudson-Str	-0.050	0.097	-0.095	-0.055	-0.026
Lab-Shelf	0.059	0.125	0.100	0.128	0.103
N-Nfld-Shelf	0.091	0.027	-0.118	0.059	0.015
S-Nfld-Shelf	0.103	0.133	0.118	0.083	0.109
L-Channel	0.103	0.016	0.052	0.062	0.059
E-GSL	0.081	0.177	0.260	0.136	0.163
SLE	0.076	-0.109	0.354	0.242	0.141
W-GSL	0.237	0.216	0.145	0.238	0.209
ESS	0.098	0.184	0.139	0.135	0.139
CSS	0.037	0.154	0.250	0.107	0.137
WSS-BoF	0.077	0.168	0.215	0.099	0.140
GoM	-0.016	0.132	0.183	0.099	0.099
Recirc-Zone	0.071	0.154	0.177	-0.028	0.093
Gulf-Stream	0.008	0.012	0.080	0.031	0.033
H-Bay	0.062	0.121	-0.105	-0.083	-0.001

Results for Hudson Bay

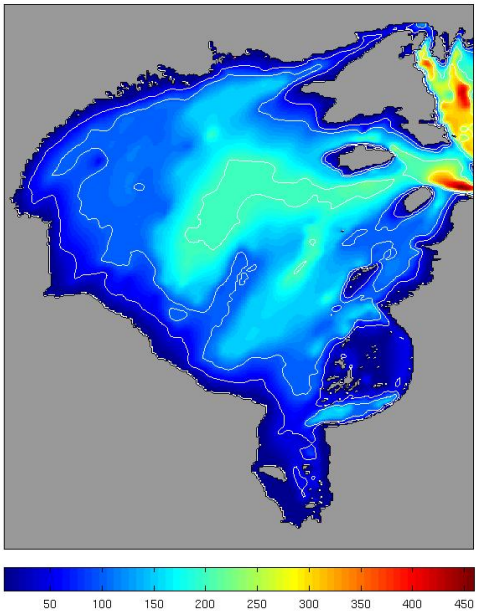

Hudson Bay subdomain

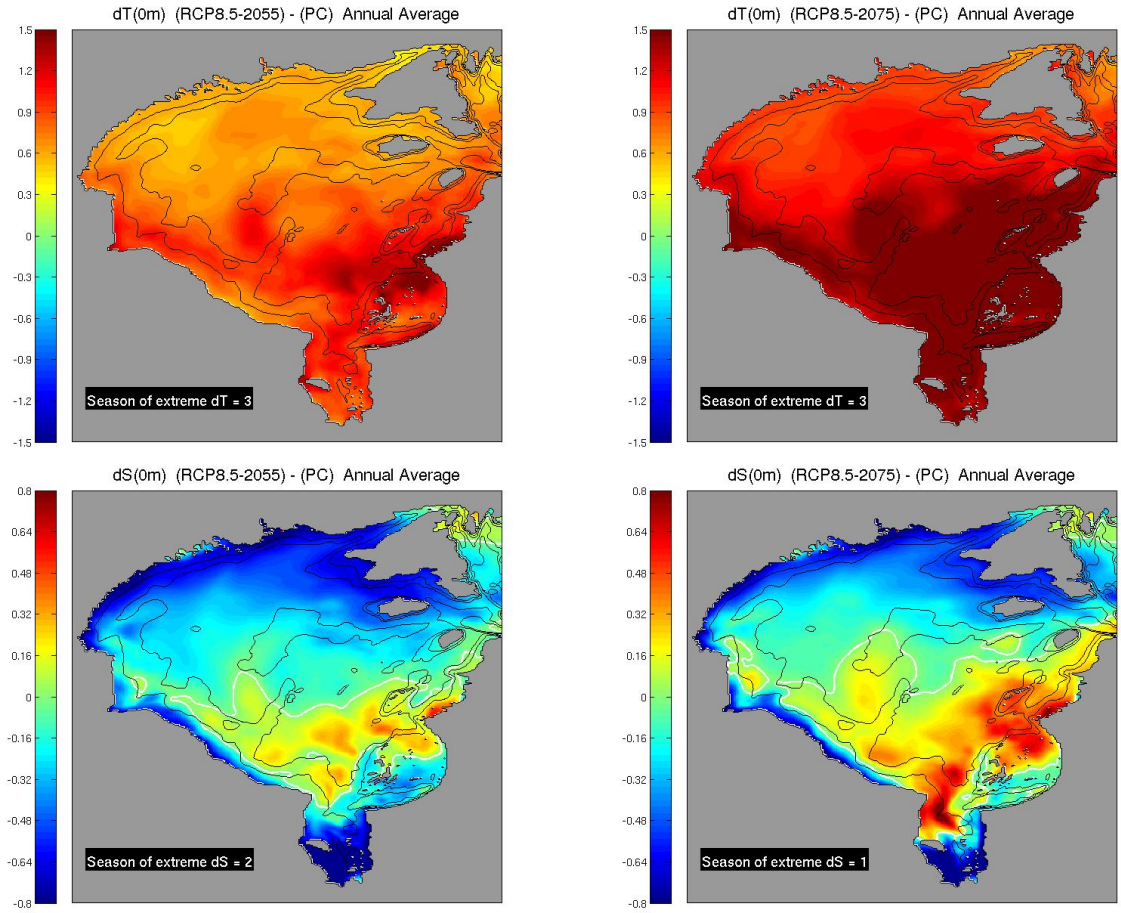

(a) (b)

Figure A22: Hudson Bay: (a) Predicted annual change in T and S at 0m for RCP8.5-2055. (b) Predicted annual change in T and S at 0m for RCP8.5-2075. The seasons of extrema in T and S change are annotated.

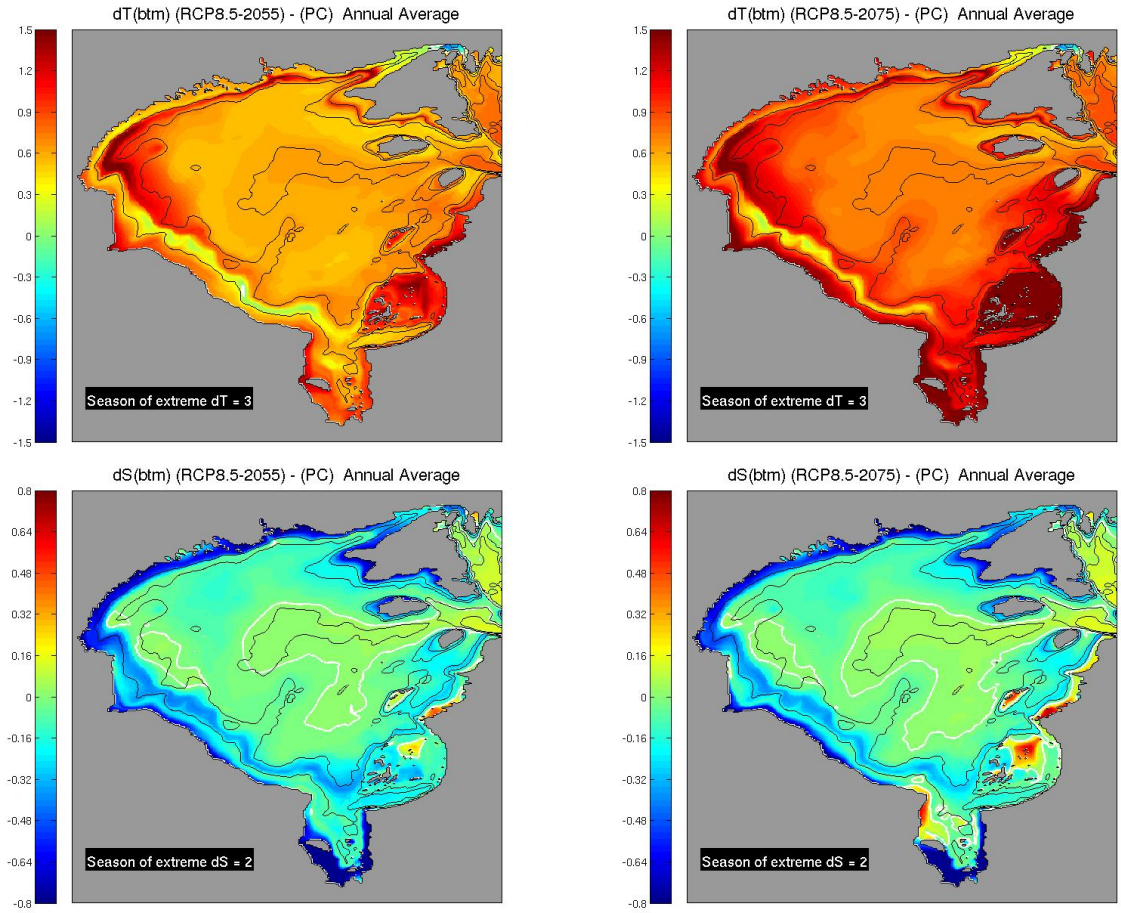

(a) (b)

Figure A23: Hudson Bay: (a) Predicted annual change in bottom T and S for RCP8.5-2055. (b) Predicted annual change in bottom T and S for RCP8.5-2075. The seasons of extrema in T and S change are annotated.

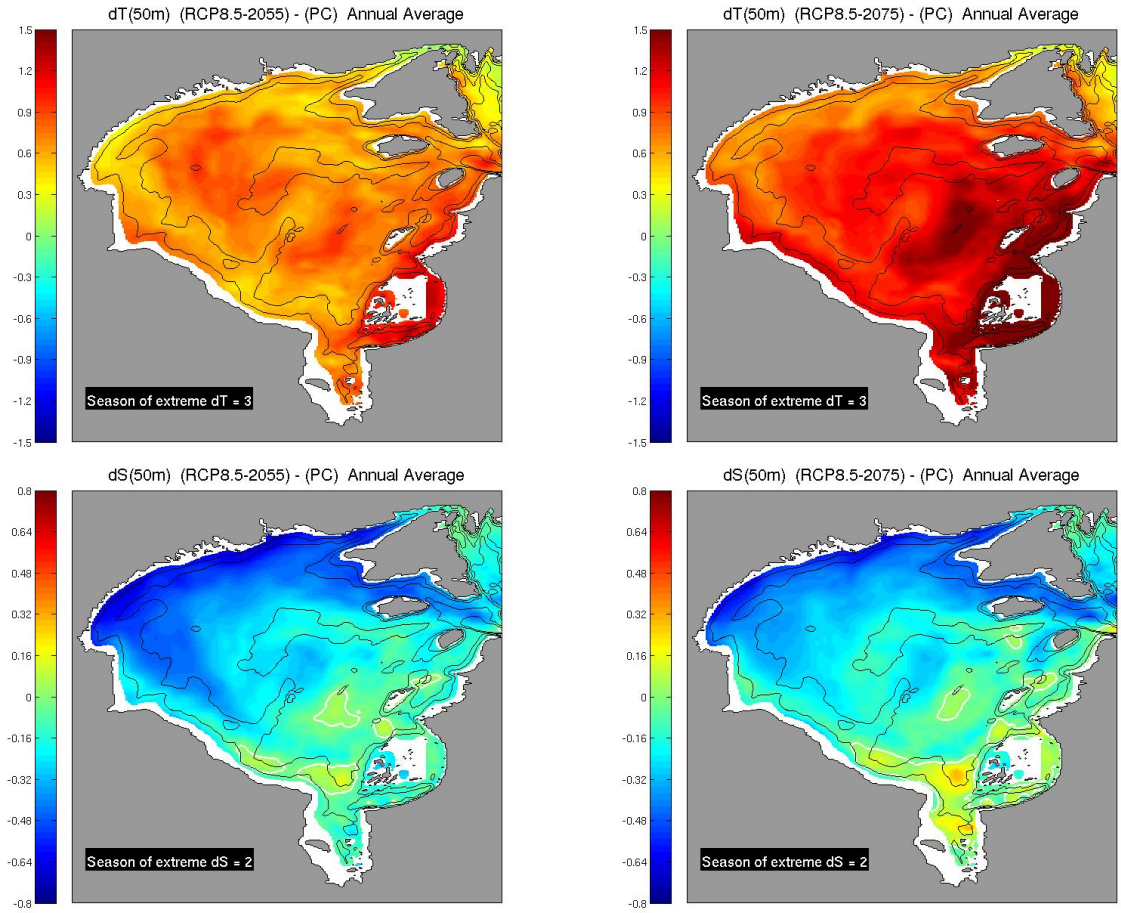

(a) (b)

Figure A24: Hudson Bay: (a) Predicted annual change in T and S at 50m for RCP8.5-2055. (b) Predicted annual change in T and S at 50m for RCP8.5-2075. The seasons of extrema in T and S change are annotated.

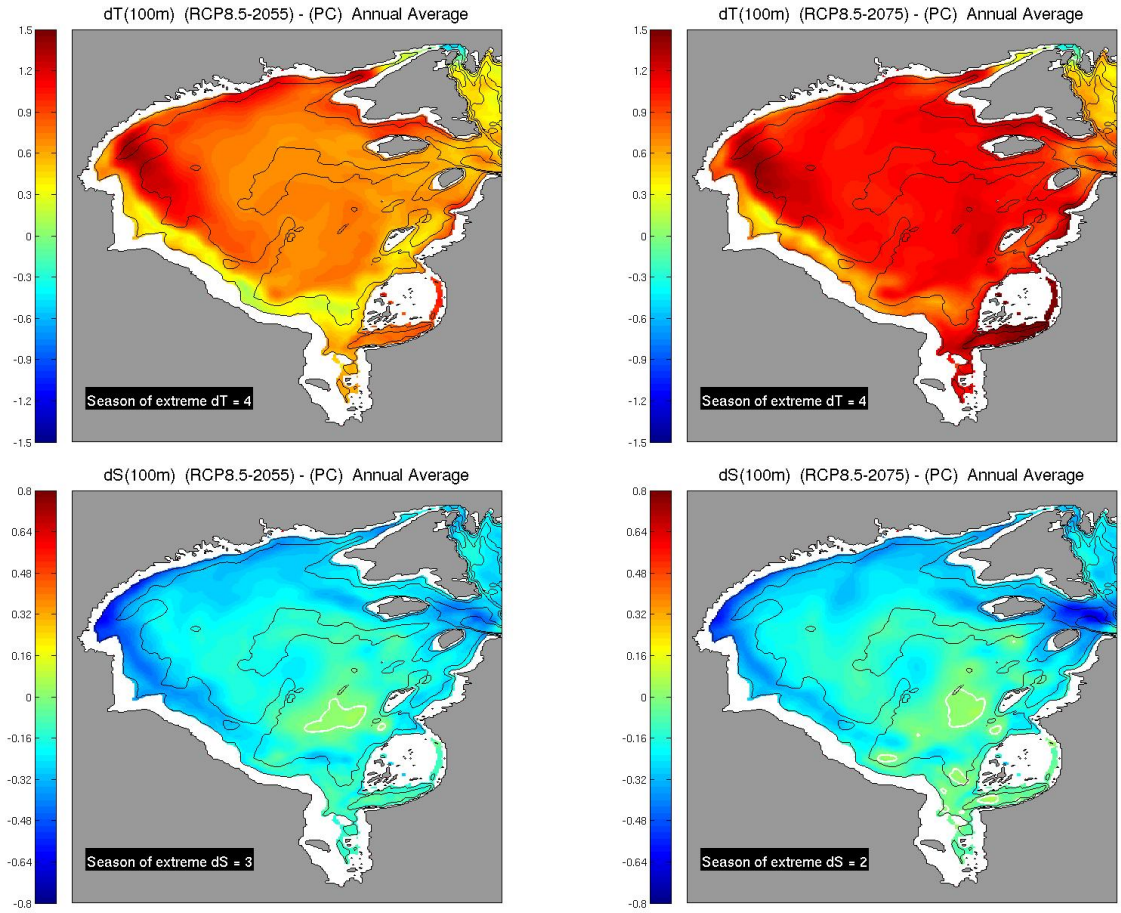

(a) (b)

Figure A25: Hudson Bay: (a) Predicted annual change in T and S at 100m for RCP8.5-2055. (b) Predicted annual change in T and S at 100m for RCP8.5-2075. The seasons of extrema in T and S change are annotated.

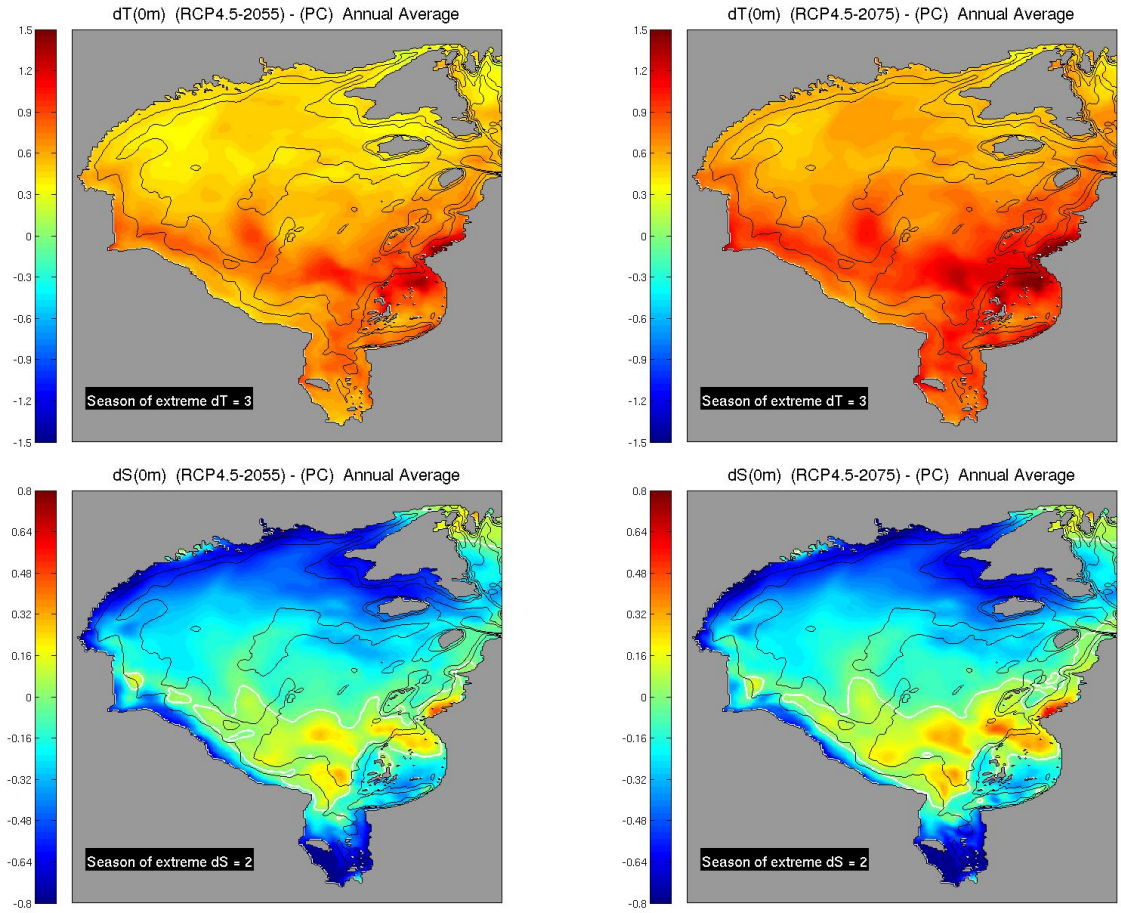

(a) (b)

Figure A26: Hudson Bay: (a) Predicted annual change in T and S at 0m for RCP4.5-2055. (b) Predicted annual change in T and S at 0m for RCP4.5-2075. The seasons of extrema in T and S change are annotated.

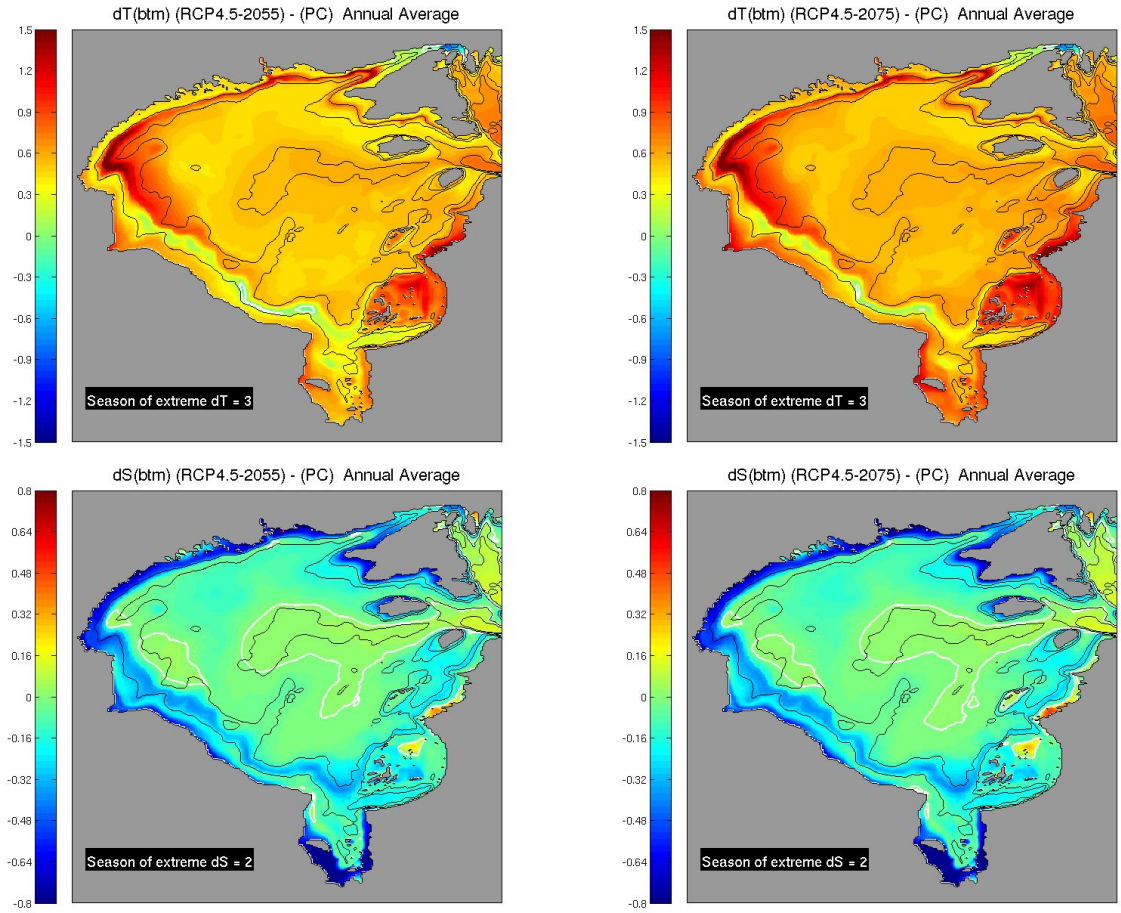

(a) (b)

Figure A27: Hudson Bay: (a) Predicted annual change in bottom T and S for RCP4.5-2055. (b) Predicted annual change in bottom T and S for RCP4.5-2075. The seasons of extrema in T and S change are annotated.

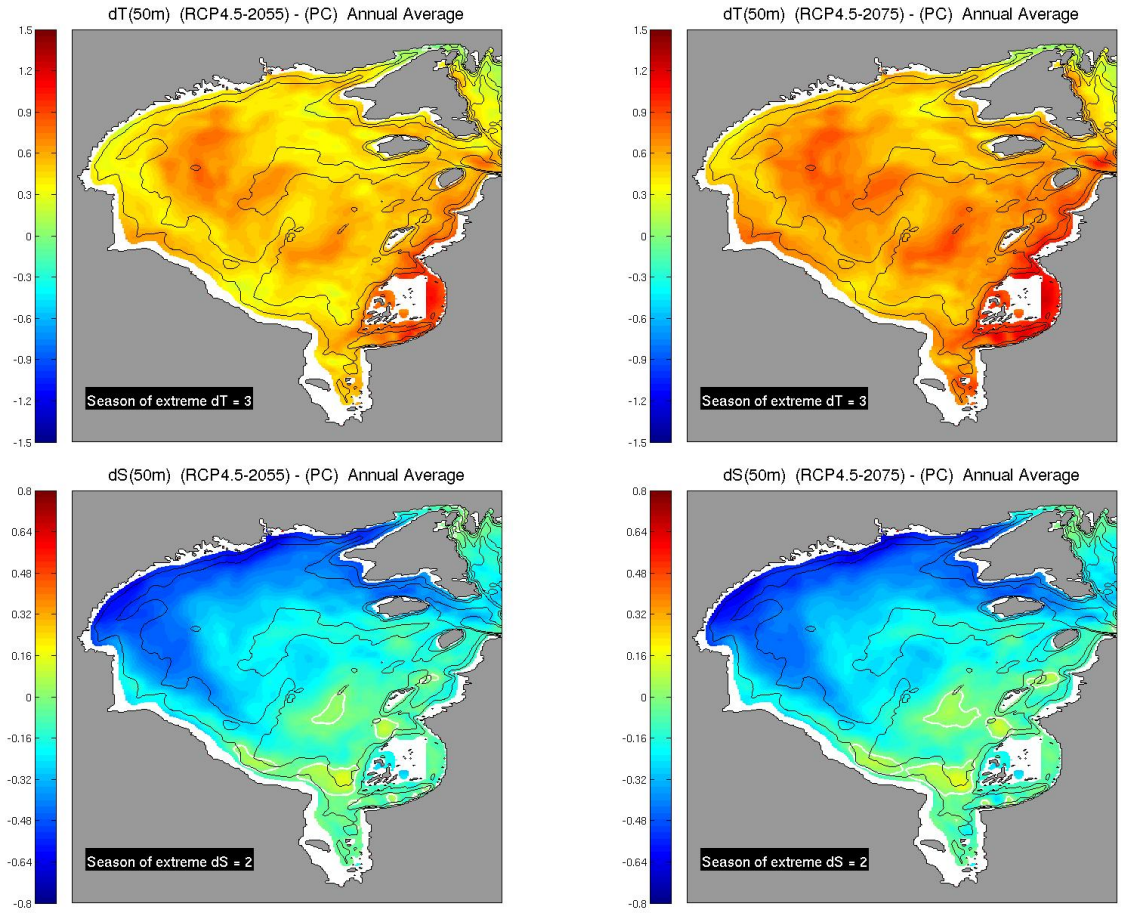

(a) (b)

Figure A28: Hudson Bay: (a) Predicted annual change in T and S at 50m for RCP4.5-2055. (b) Predicted annual change in T and S at 50m for RCP4.5-2075. The seasons of extrema in T and S change are annotated.

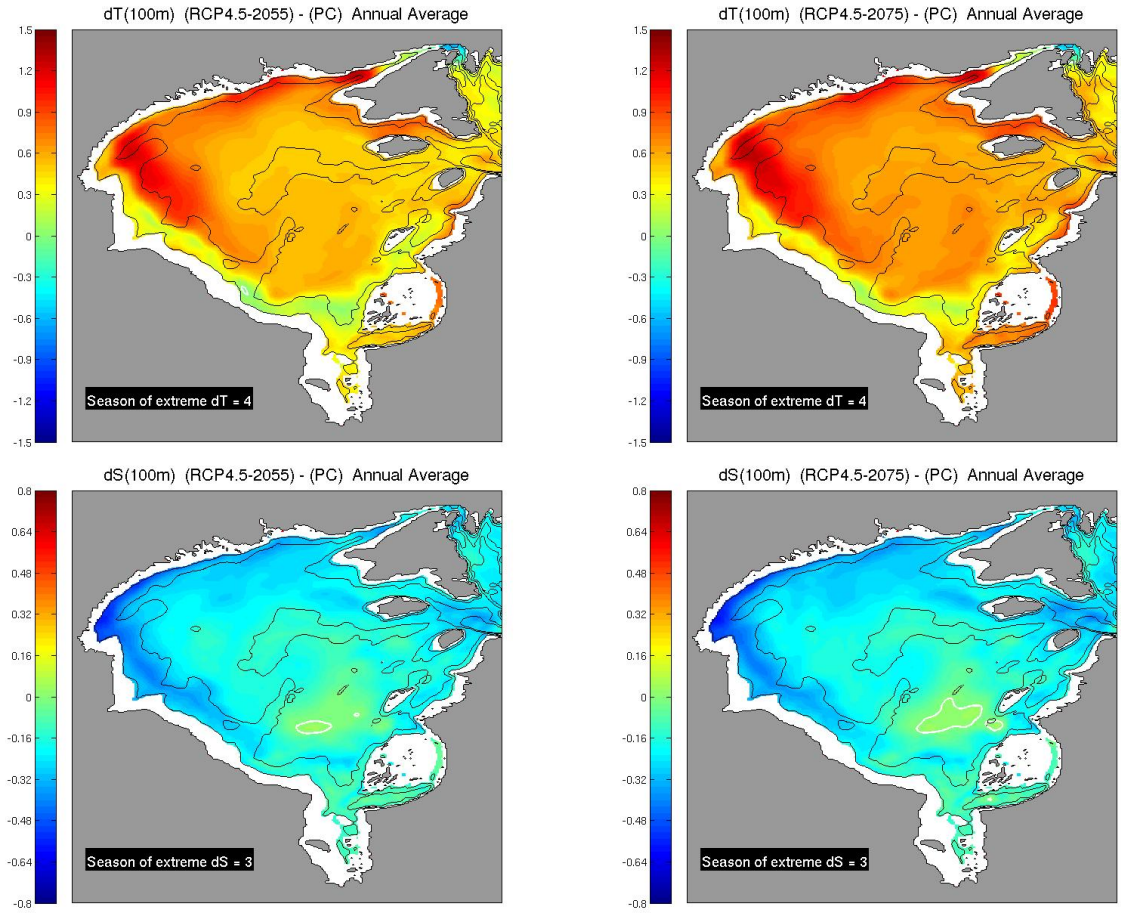

(a) (b)

Figure A29: Hudson Bay: (a) Predicted annual change in T and S at 100m for RCP4.5-2055. (b) Predicted annual change in T and S at 100m for RCP4.5-2075. The seasons of extrema in T and S change are annotated.

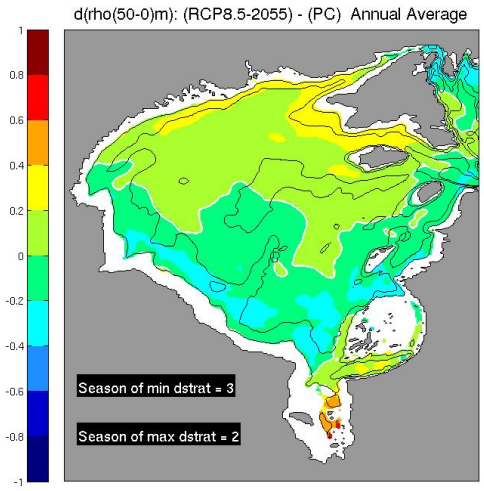

(a)

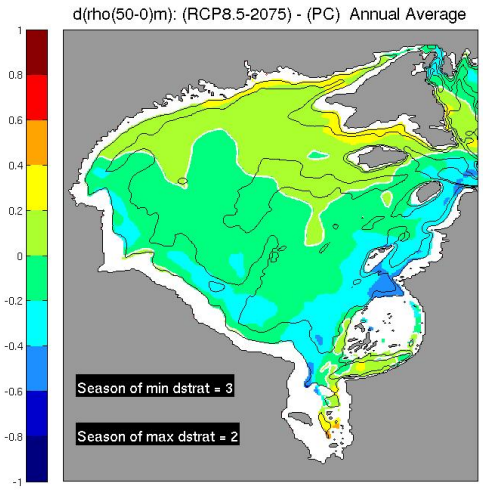

(b)

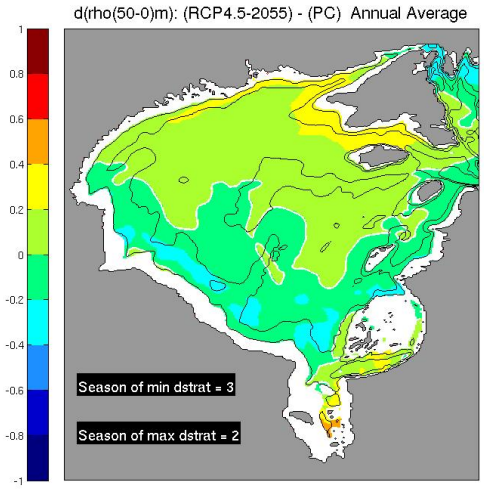

(c)

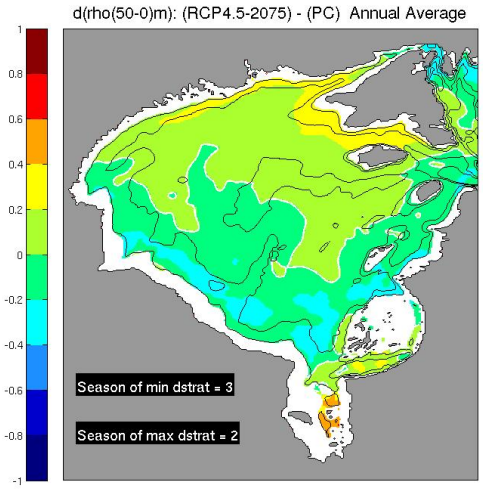

(d)

Figure A30: Hudson Bay: Predicted annual change in 50m-0m stratification for (a) RCP8.5-2055, (b) RCP8.5-2075, (c) RCP4.5-2055 and (d) RCP4.5-2075.

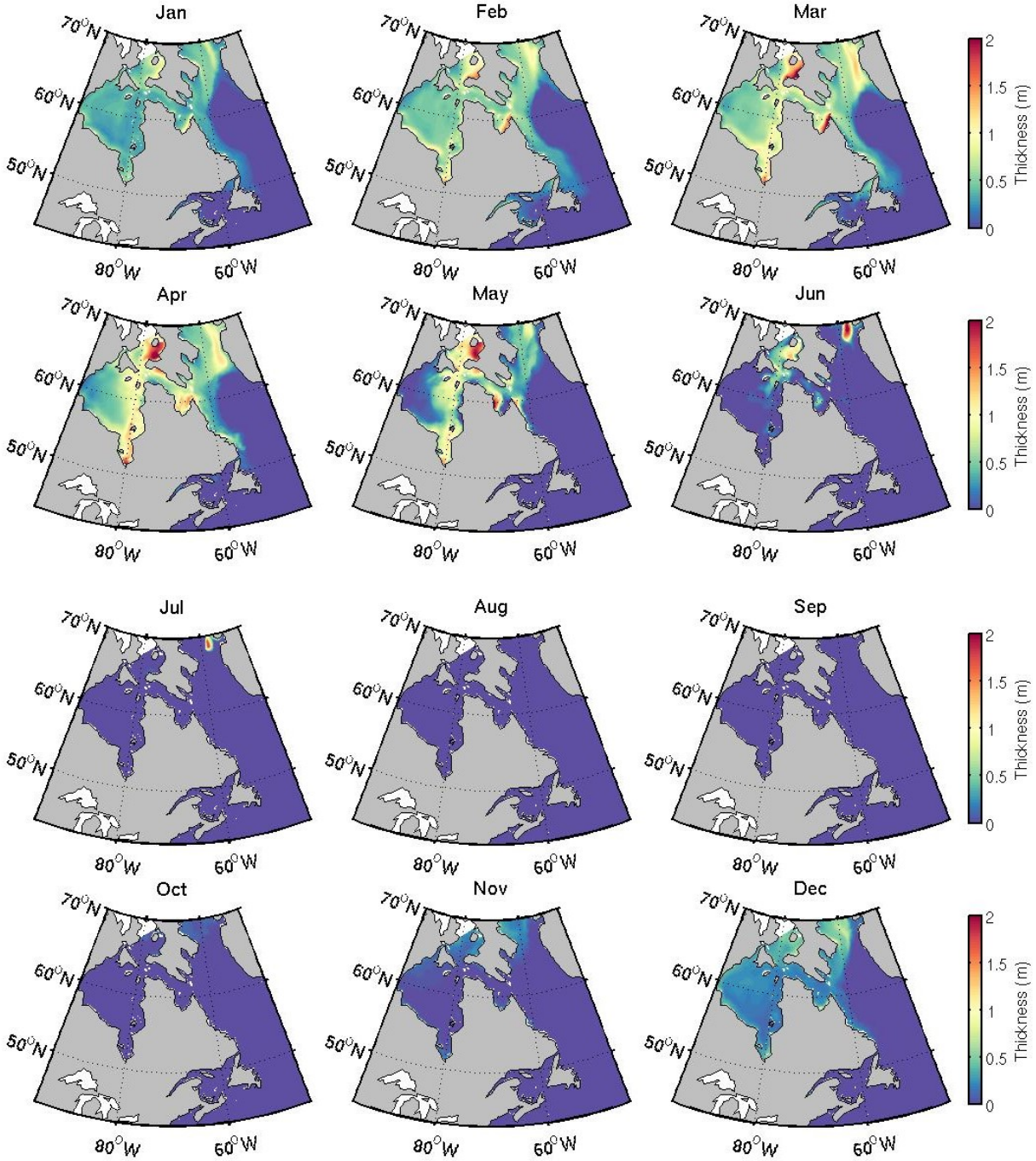

Figure A31: RCP8.5-2055 ice thickness.

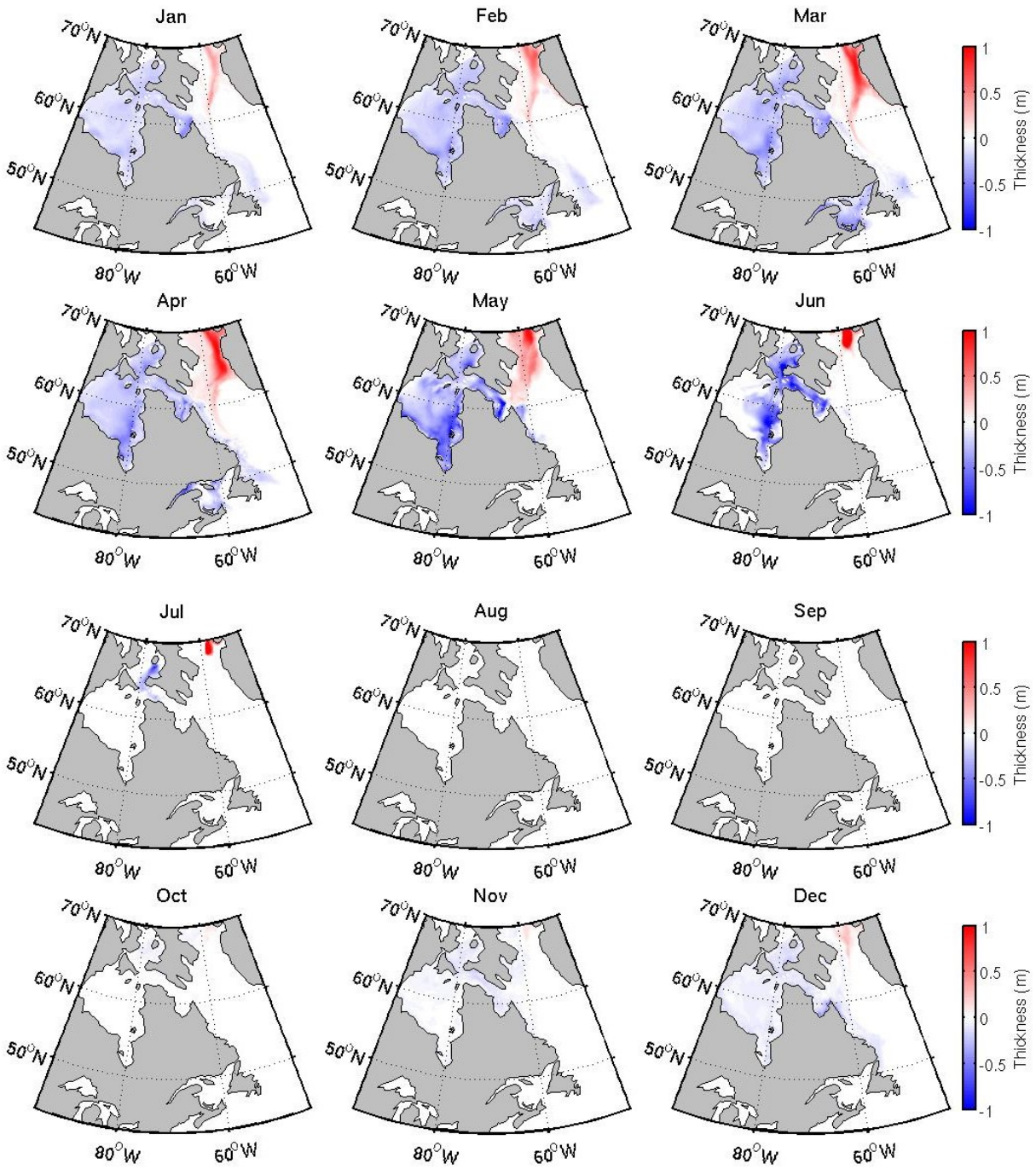

Figure A32: Difference between RCP8.5-2055 and PC ice thickness.

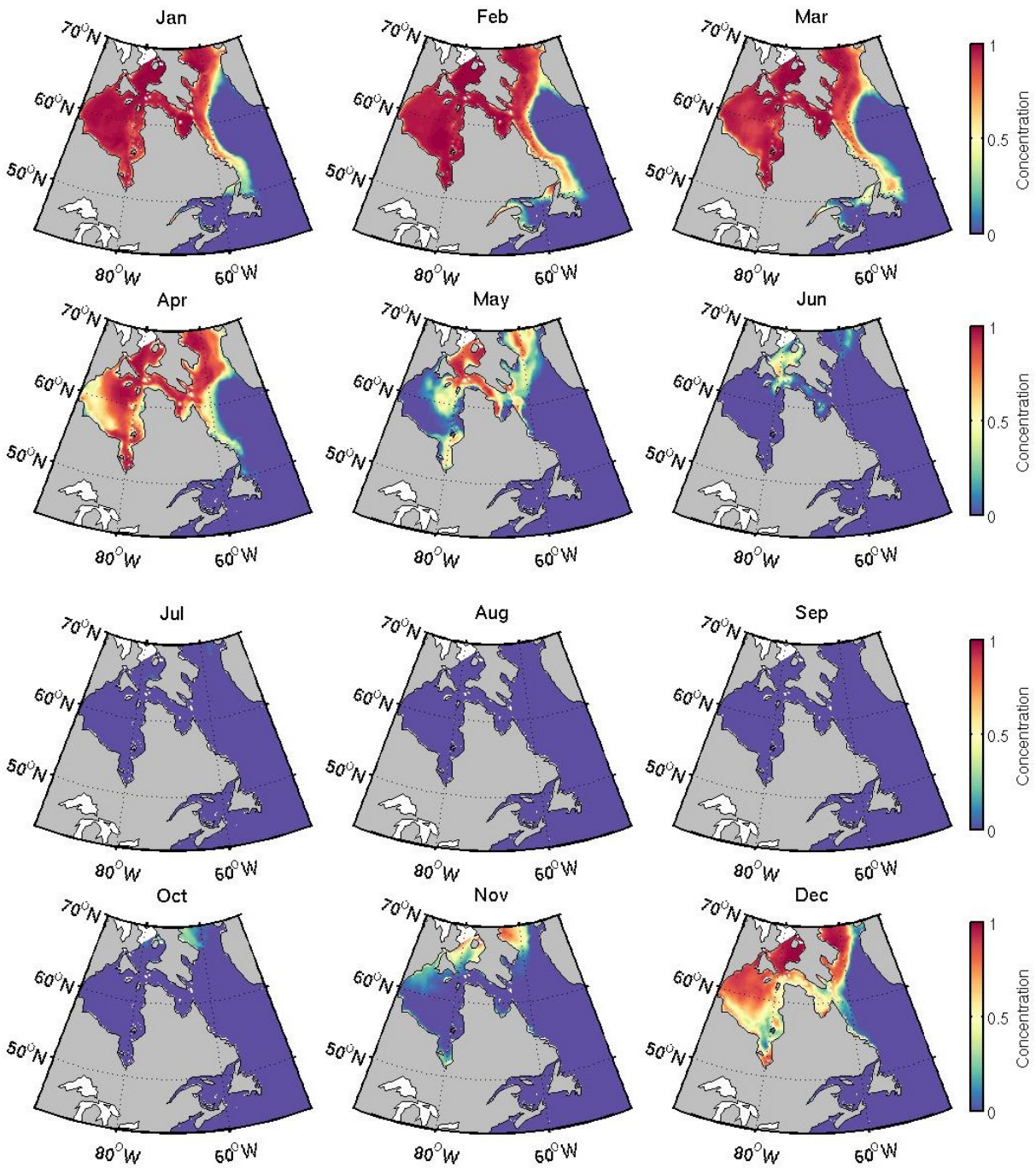

Figure A33: RCP8.5-2075 ice concentration.

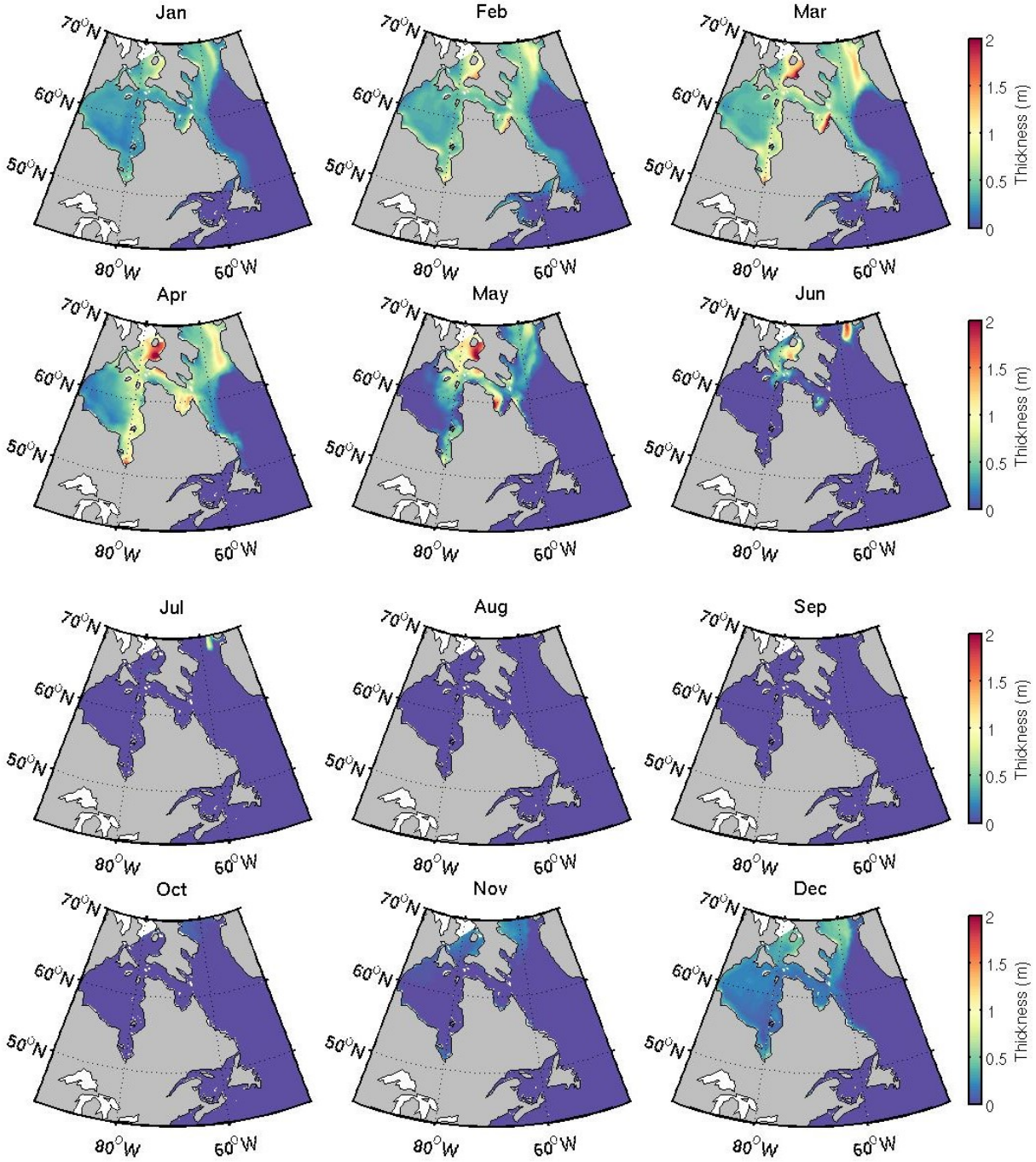

Figure A34: RCP8.5-2075 ice thickness.

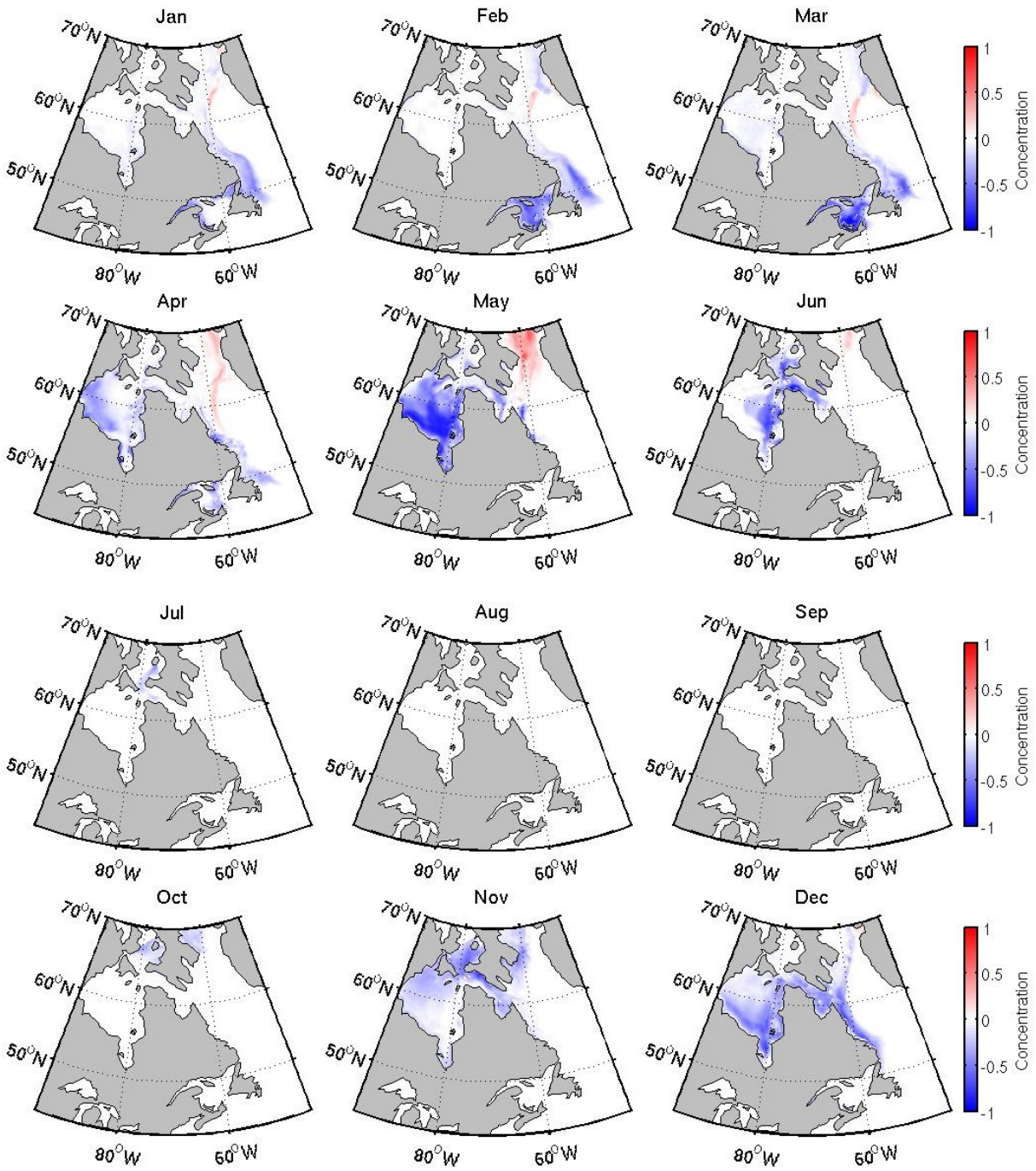

Figure A35: Difference between RCP8.5-2075 and PC ice concentration.

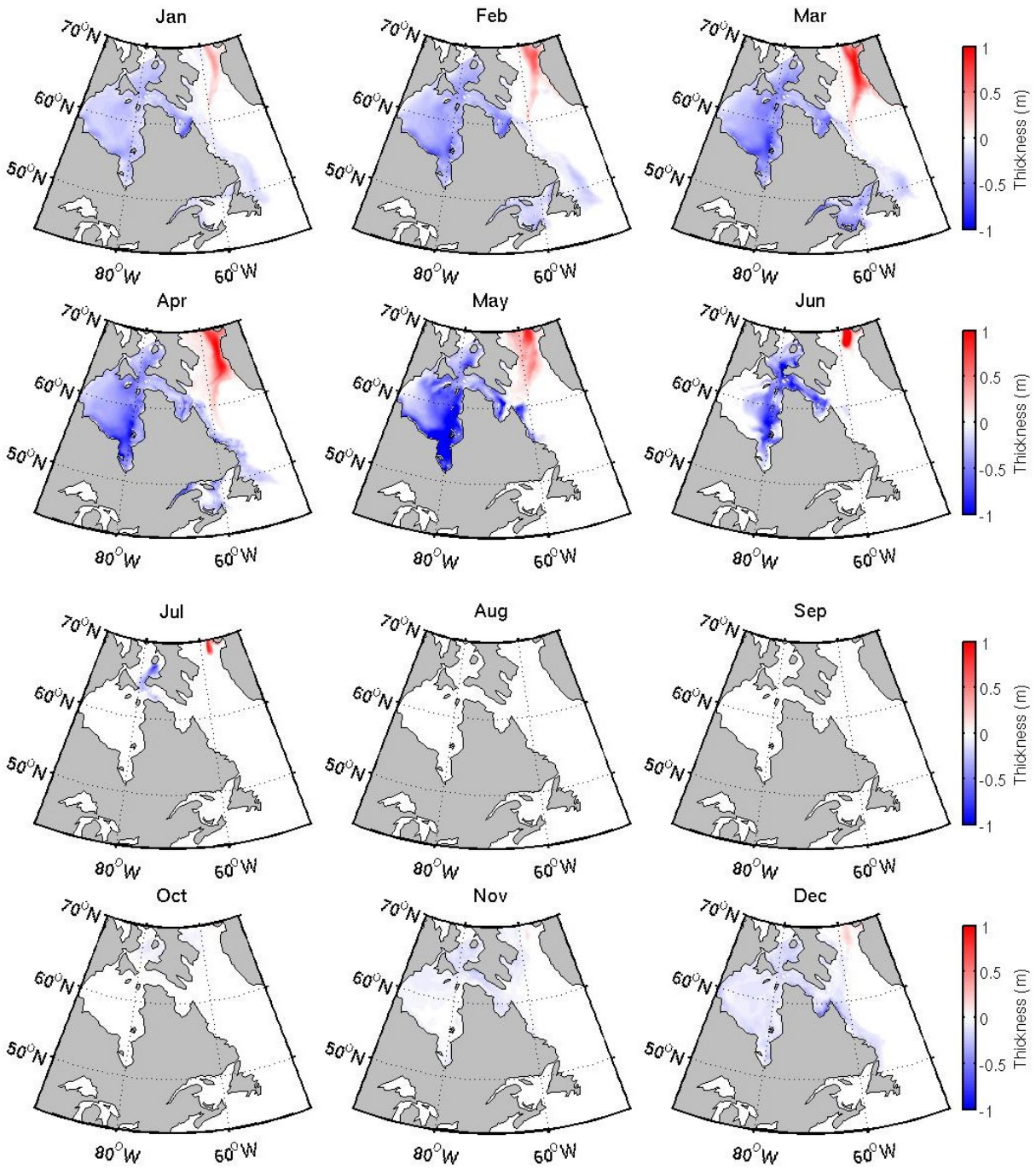

Figure A36: Difference between RCP8.5-2075 and PC ice thickness.

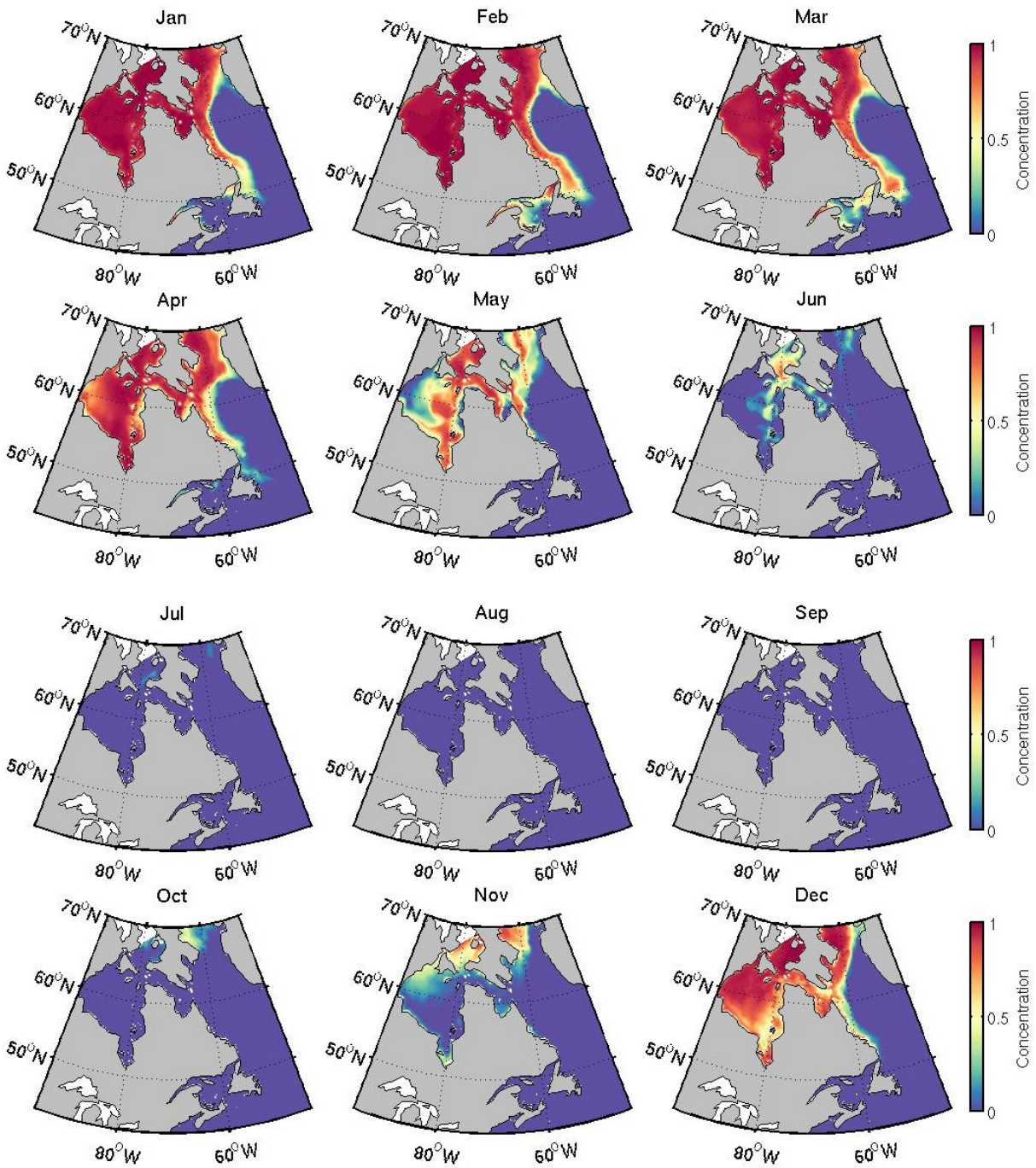

Figure A37: RCP4.5-2055 ice concentration.

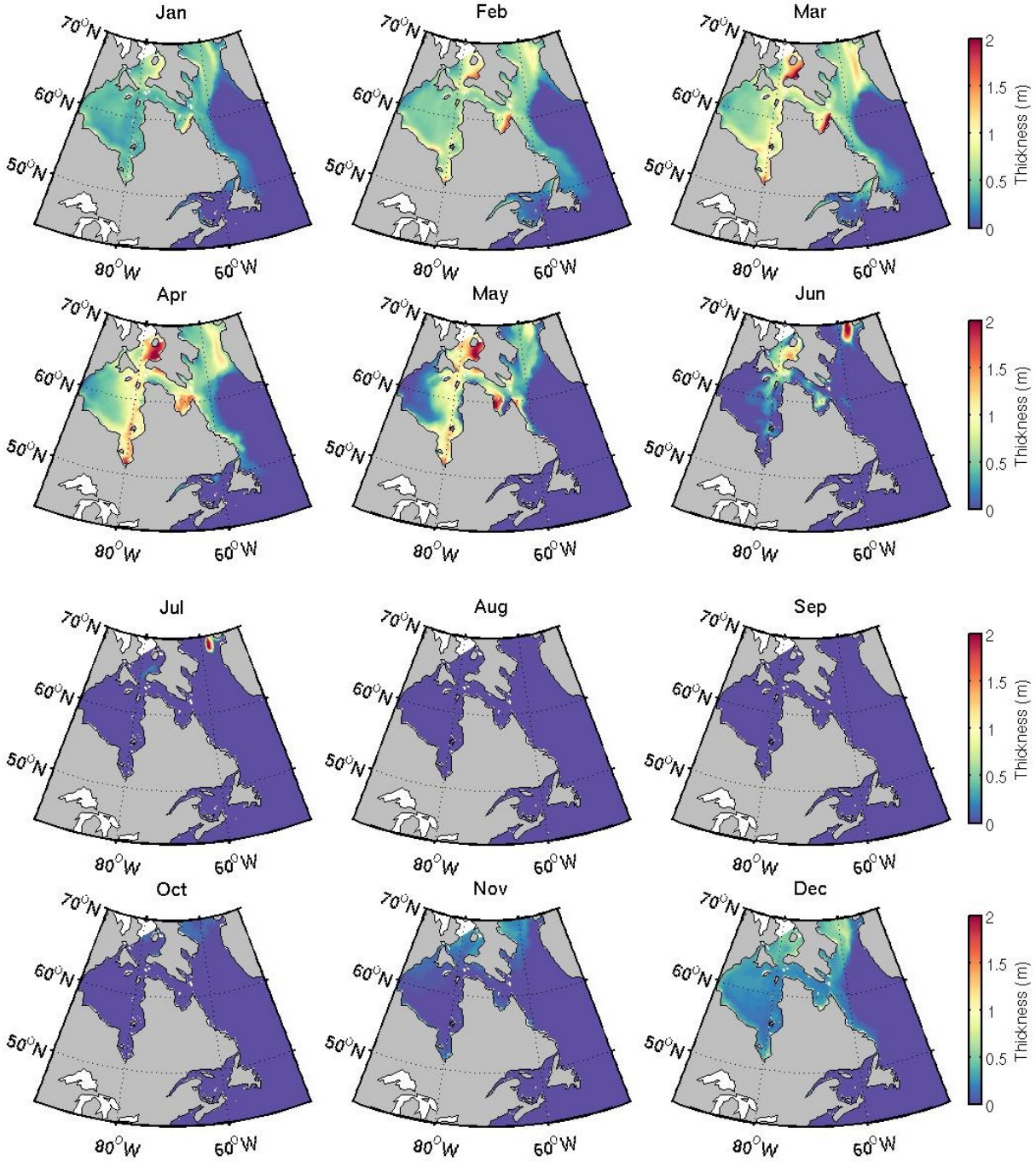

Figure A38: RCP4.5-2055 ice thickness.

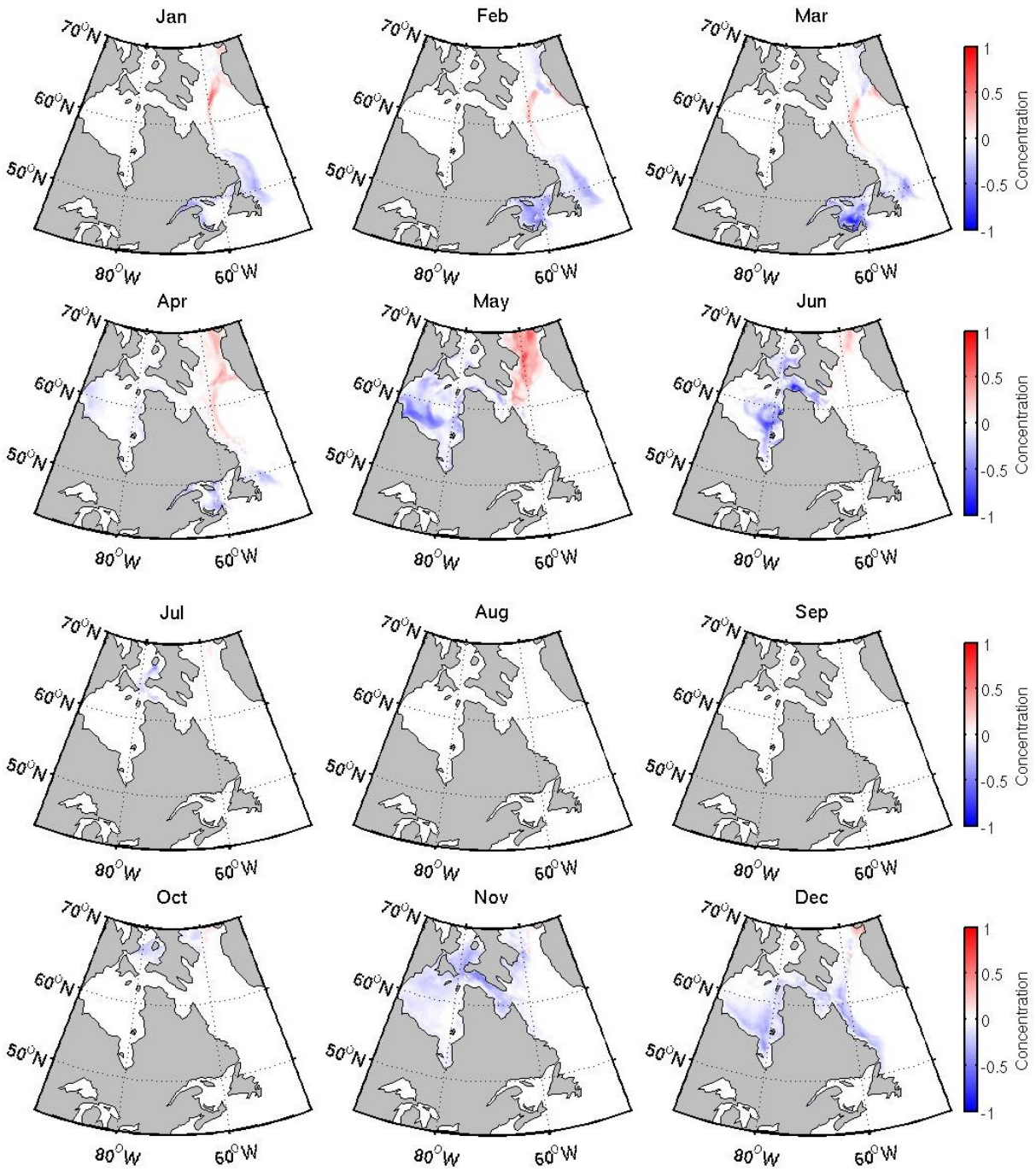

Figure A39: Difference between RCP4.5-2055 and PC ice concentration.

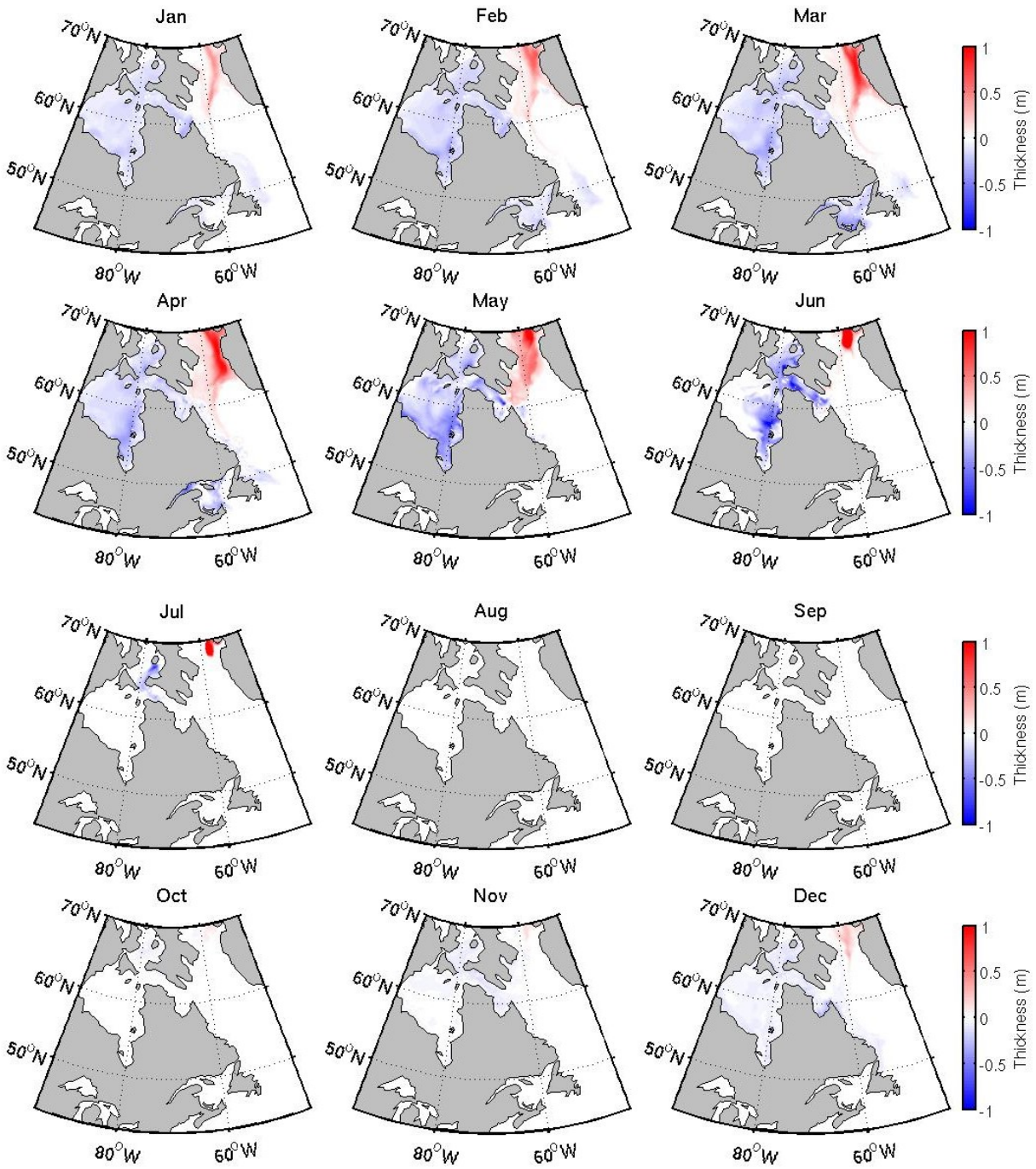

Figure A40: Difference between RCP4.5-2055 and PC ice thickness.

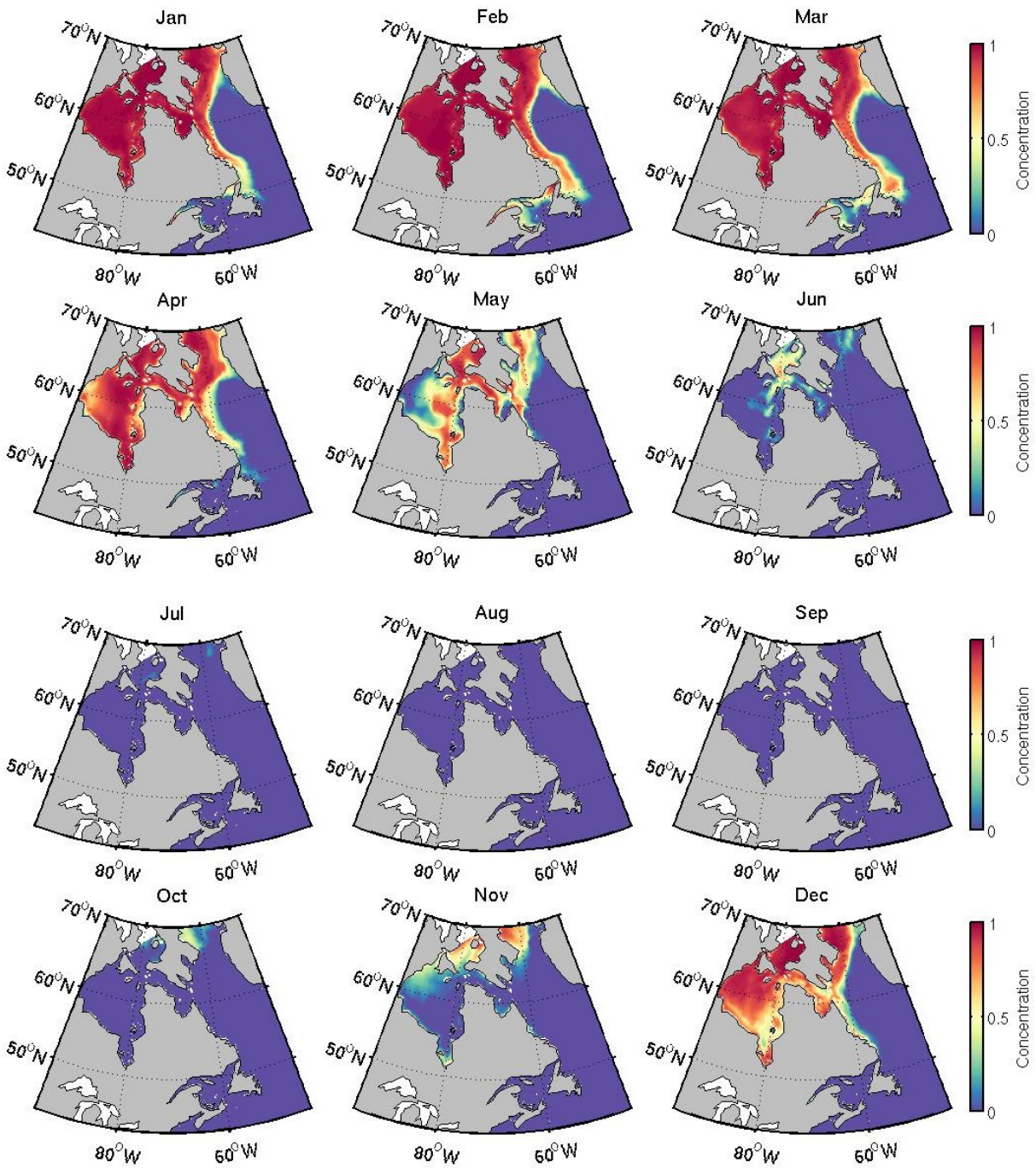

Figure A41: RCP4.5-2075 ice concentration.

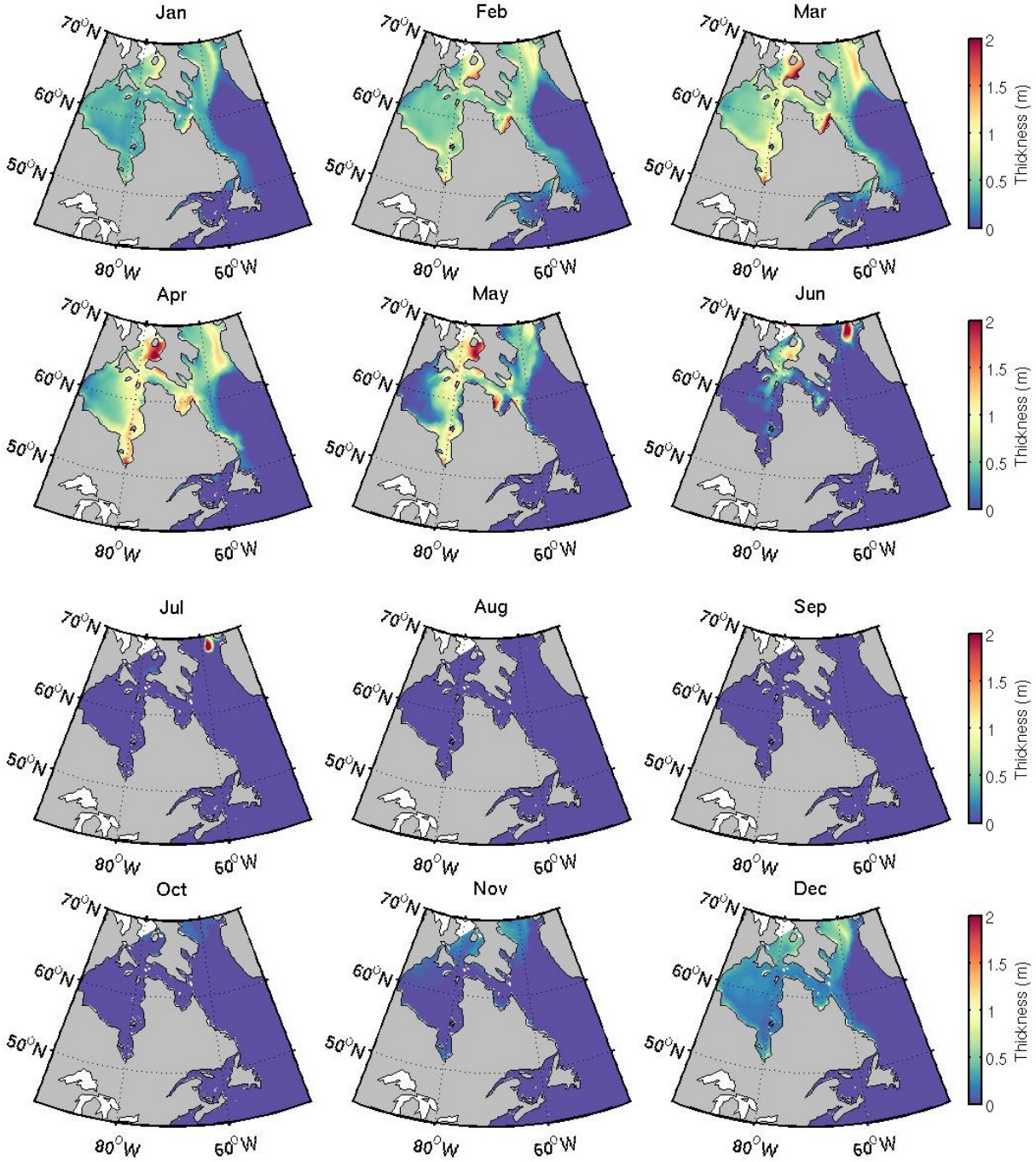

Figure A42: RCP4.5-2075 ice thickness.

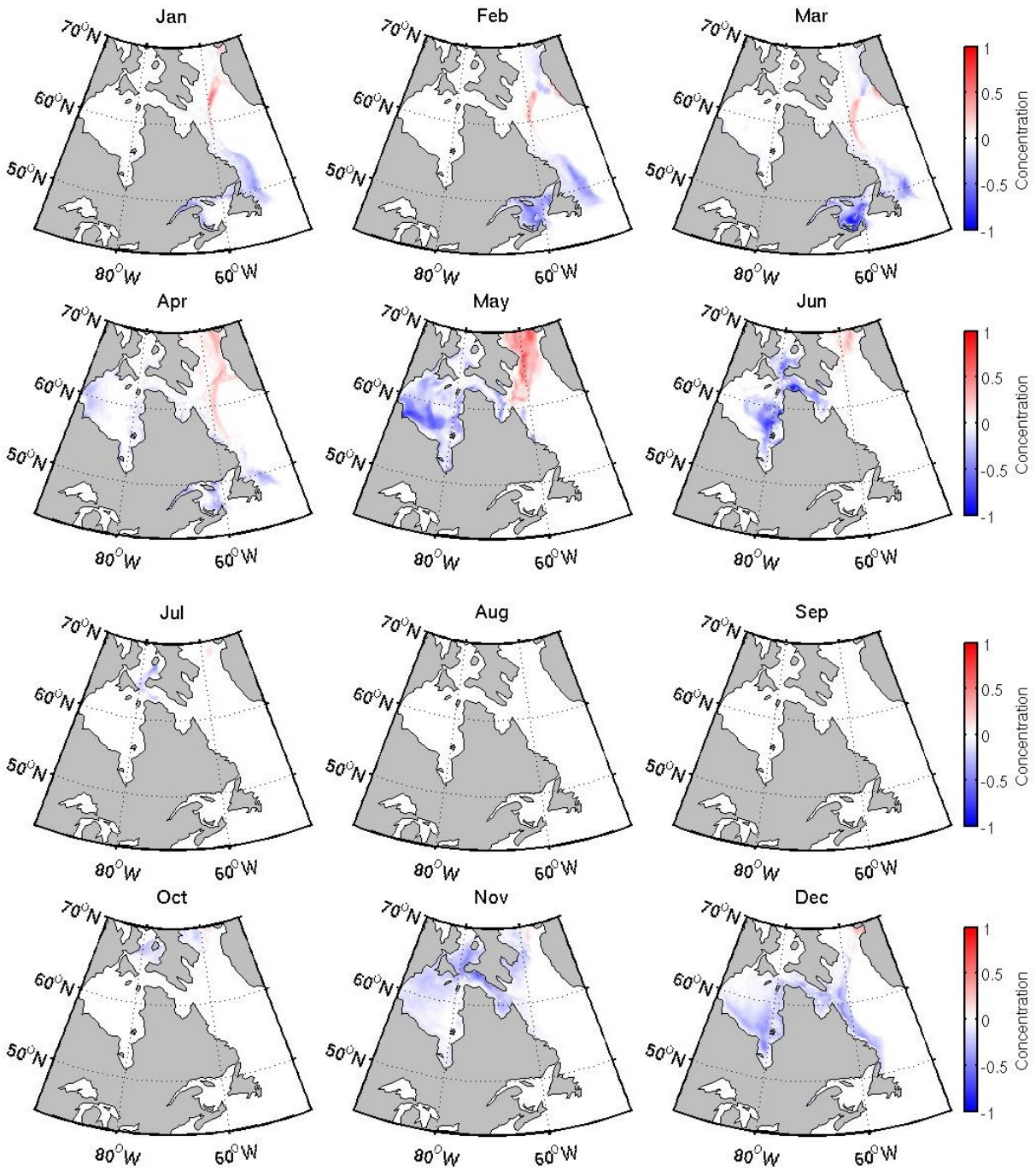

Figure A43: Difference between RCP4.5-2075 and PC ice concentration.

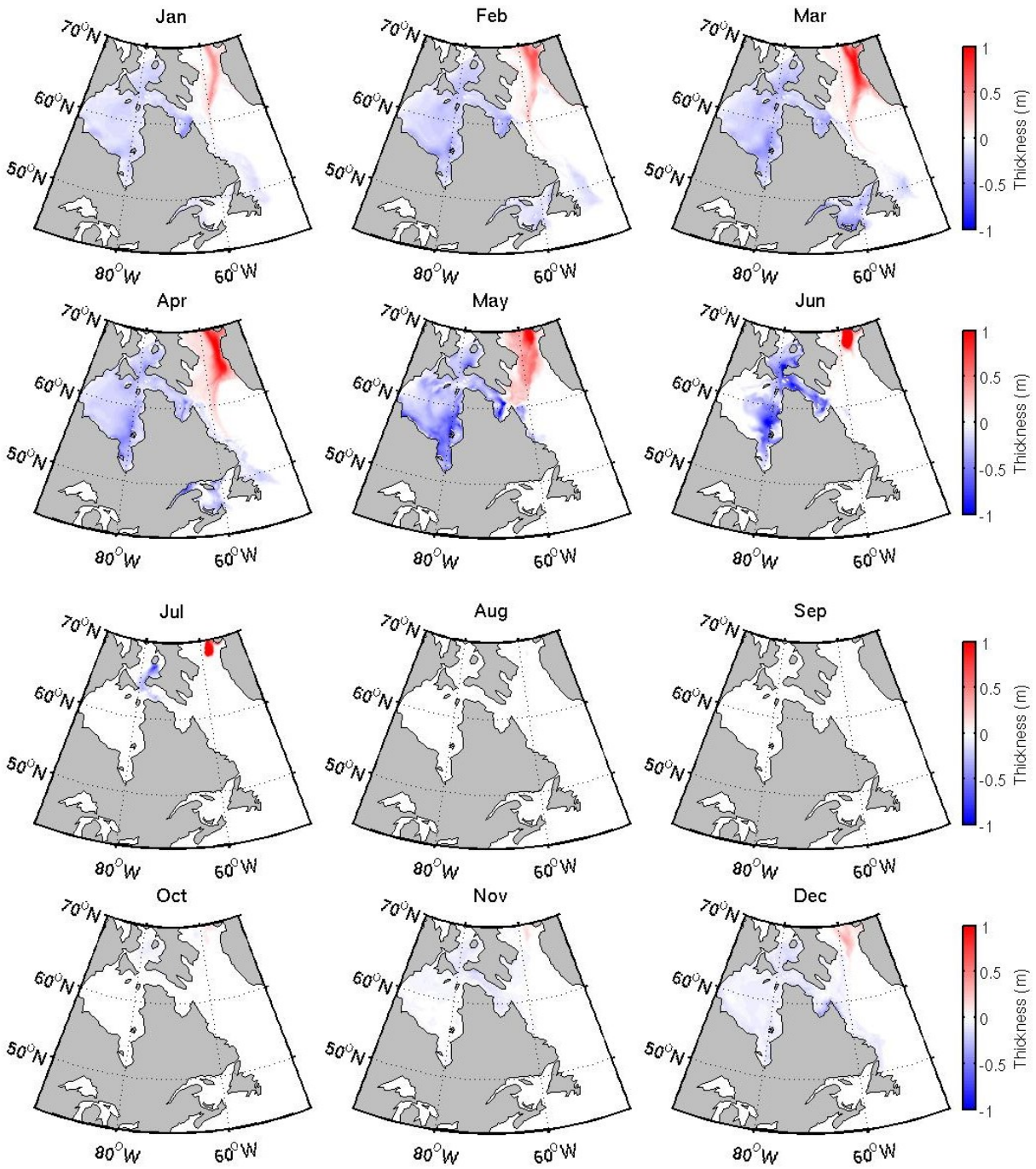

Figure A44: Difference between RCP4.5-2075 and PC ice thickness.

Table A22: Annual mean percentage change from PC, for ice area, volume and extent. Ice box abbreviations are: HB=Hudson Bay; HS=Hudson Strait; DS=Davis Strait; NLS= Northern Labrador Sea; SLS=Southern Labrador Sea; ENW=East Newfoundland Waters; GSL=Gulf of St.Lawrence/Scotian Shelf.

	RCP4.5						RCP8.5					
	Area		Volume		Extent		Area		Volume		Extent	
	2055	2075	2055	2075	2055	2075	2055	2075	2055	2075	2055	2075
HB	-9	-12	-26	-32	-8	-10	-13	-23	-35	-55	-11	-19
HS	-11	-14	-23	-31	-13	-17	-16	-20	-35	-42	-18	-19
DS	6	4	34	31	6	4	3	-4	26	11	4	-1
NLS	-1	-5	-4	-14	6	4	-7	-19	-17	-36	3	-7
SLS	-16	-23	-17	-28	-11	-16	-25	-40	-32	-52	-17	-28
ENW	-39	-48	-46	-56	-36	-45	-51	-65	-60	-74	-47	-58
GSL	-47	-55	-61	-68	-35	-45	-59	-73	-71	-83	-49	-66
Total	-10	-13	-20	-26	-9	-12	-15	-24	-30	-47	-13	-21

Table A23: Annual mean percentage change from PC, for maximum ice area, volume and extent. Abbreviations as in table A22.

	RCP4.5						RCP8.5					
	Area		Volume		Extent		Area		Volume		Extent	
	2055	2075	2055	2075	2055	2075	2055	2075	2055	2075	2055	2075
HB	-1	-1	-21	-25	0	0	-2	-3	-28	-45	0	0
HS	-1	-2	-14	-21	0	0	-2	-3	-24	-32	0	0
DS	1	1	32	30	4	8	2	-1	30	21	5	7
NLS	7	5	2	-5	11	18	5	-4	-5	-21	14	11
SLS	-14	-20	-11	-21	-6	-9	-21	-31	-25	-41	-9	-19
ENW	-29	-37	-38	-48	-30	-40	-40	-54	-53	-69	-38	-50
GSL	-39	-46	-61	-66	-21	-29	-50	-66	-69	-80	-35	-57
Total	-6	-8	-15	-20	-4	-6	-8	-13	-23	-37	-7	-11

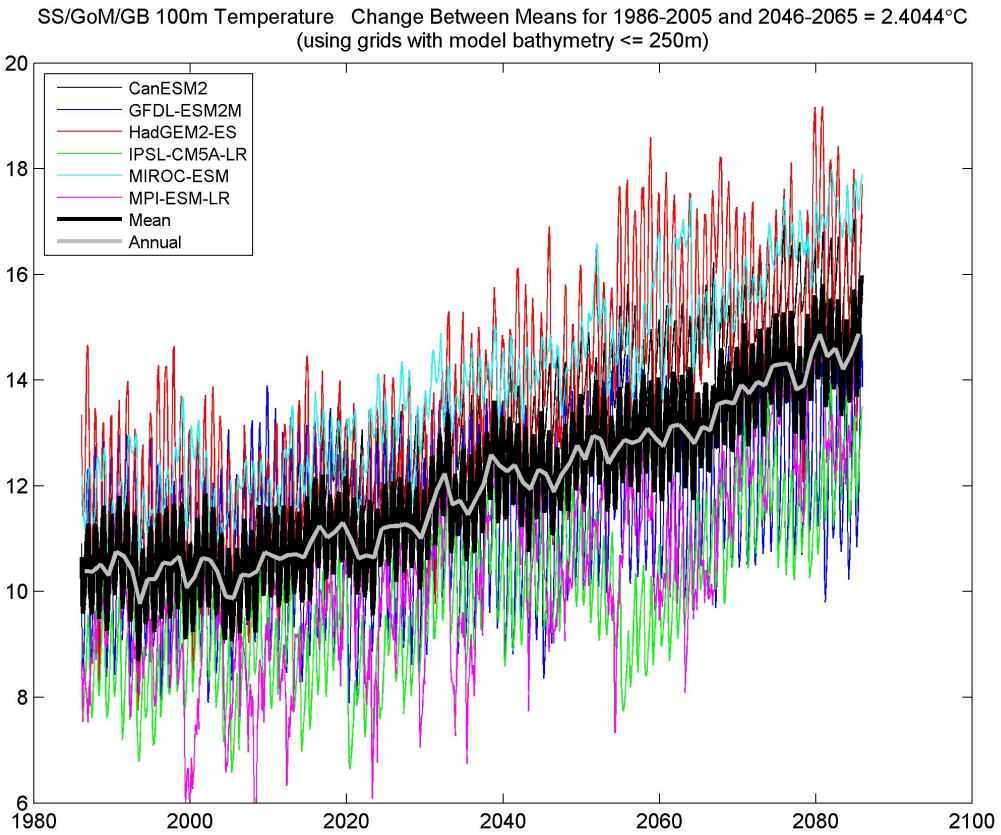

Figure A45: Average temperature at 100m for the Scotian Shelf/GoM from the 6 AOGCMs listed in table 1. Because bottom temperature is not standard model output, the 100m temperature was chosen as representative of this depth.